

**Investigating the Role of Heat Shock Proteins (Hsps)  
40, 70 and 90 in the Life Cycle of Theiler's Murine  
Encephalomyelitis Virus (TMEV)**

Dissertation submitted in fulfilment of the requirements for the degree of

**Masters of Science in Microbiology**

**At**

**Rhodes University**

**By**

**Lorraine Zvichapera Mutsvunguma**

January 2011

## Abstract

**Introduction:** Picornaviruses are a family of RNA viruses which are economically and clinically significant. Like many other viruses, picornaviruses utilise host cell machinery to facilitate their replication and assembly, including heat shock proteins (Hsps). The aim of this research was to investigate the role of Hsp40, Hsp70 and Hsp90 during picornavirus infection using the cardiovirus, Theiler's murine encephalomyelitis virus (TMEV), as a study model. **Methodology:** Picornavirus VP1 capsid proteins were analysed by multiple sequence alignment and multiple structural comparisons. Protein domain architecture was used to analyse Hsp90 cellular and viral client proteins. Effects of Hsp90 inhibitors, novobiocin and geldanamycin, on TMEV growth in BHK-21 cells was observed over a 48hr period. Localisation of Hsp40, Hsp90 and Hsp70 in TMEV-infected BHK-21 cells was investigated by indirect immunofluorescence and confocal microscopy. **Results and Discussion:** VP1 proteins of picornaviruses are highly divergent within the family at the amino acid level, which might be linked to the protein's function in determining virus tropism and antibody neutralisation. An eight-stranded anti-parallel beta-barrel structure was found conserved in the VP1 protein structures which might be linked to the highly conserved picornavirus capsid assembly process. Absence of a common protein domain between Hsp90 viral and cellular client proteins that might be functionally connected to Hsp90, suggests that Hsp90 most likely recognises surface features rather than sequence motifs/patterns. The Hsp90 inhibitors, novobiocin and geldanamycin, had a negative effect on virus growth as virus-induced cytopathic effect was not observed in treated cell after 48hrs. TMEV 2C protein was detected by Western analysis in infected cell lysates treated with geldanamycin but not novobiocin, suggesting novobiocin affects the translation or processing of TMEV 2C. Immunofluorescence analysis of TMEV-infected cells showed a relocalisation of Hsp40 into the nucleus during infection. Overlap of Hsp40 and TMEV P1 was observed in the perinuclear region, suggesting colocalisation between these proteins. Hsp70 converged around the replication complex during infection but did not overlap with TMEV 2C. Hsp90 concentrated in the region of the replication complex where it overlapped with TMEV 2C and this redistribution was found to be dependent on the stage of infection. The overlap between Hsp90 and TMEV 2C signals observed, suggested colocalisation between the two proteins **Conclusion:** This study identified Hsp90, Hsp70 and Hsp40 as possible host factors required in TMEV replication.

## **Declaration**

I, Lorraine Zvichapera Mutsvunguma, hereby declare that this MSc dissertation is my own unaided work completed in fulfilment of the requirements for the degree Masters of Science at Rhodes University.

Signature:.....

Date:.....

# Table of Contents

<b>Abstract</b>	<b>i</b>
<b>Declaration</b>	<b>ii</b>
<b>Table of Contents</b>	<b>iii</b>
<b>List of Figures</b>	<b>vi</b>
<b>List of Tables</b>	<b>viii</b>
<b>List of Abbreviations</b>	<b>ix</b>
<b>List of Outputs</b>	<b>xii</b>
<b>Acknowledgements</b>	<b>xiii</b>
<b><u>Chapter 1: Literature Review</u></b>	<b>1</b>
<b><u>1.1 Introduction</u></b>	<b>1</b>
<b><u>1.2 Picornaviridae</u></b>	<b>1</b>
1.2.1 Picornavirus Classification	1
1.2.2 Clinical and Economical Significance of Picornaviruses	2
<b><u>1.3 TMEV as a Study Model</u></b>	<b>4</b>
1.3.1 Recent Discovery of Human Cardioviruses	5
1.3.2 Picornavirus Genomic Organisation	6
1.3.4 Polyprotein Processing	6
1.3.3 Replication	8
1.3.4 Assembly	10
<b><u>1.4 Molecular Chaperones</u></b>	<b>12</b>
1.4.1 Function of molecular chaperones	12
1.4.2 Heat shock protein 90 (Hsp90)	15
1.4.3 Heat shock protein 70 (Hsp70)	16
1.4.4 Heat shock protein 40 (Hsp40)	18
<b><u>1.5 Virus-Chaperone Interaction</u></b>	<b>20</b>
1.5.1 General viral-chaperone interactions	20
a) Viral entry	21
b) Chaperone regulation by viruses	21
c) Replication and gene expression	21
d) Chaperone-mediated viral assembly	24
e) Chaperone-like viral proteins	24
d) Negative effects of chaperone-virus interactions	25

<b><u>1.6 Picornaviruses and Chaperones</u></b>	<b>27</b>
<b><u>1.7 Project Motivation</u></b>	<b>27</b>
<b><u>1.8 Hypothesis</u></b>	<b>28</b>
<b><u>1.9 Aims and Objectives</u></b>	<b>28</b>
Overall Aim	28
Objectives	28
<b><u>Chapter 2: <i>In Silico</i> Analysis of Picornavirus Capsid Proteins and Hsp90 Client Proteins</u></b>	<b>29</b>
<b><u>2.1 Introduction</u></b>	<b>29</b>
<b><u>2.2 Methods and Materials</u></b>	<b>30</b>
2.2.1 Multiple sequence alignment	30
2.2.2 Modelling of the VP1 Subunit of the TMEV GDVII P1 protein	30
2.2.3 Protein domain architecture	31
<b><u>2.3 Results</u></b>	<b>31</b>
2.3.1 Identification of conserved amino acid residues in the capsid protein of picornaviruses	31
2.3.2 Three dimensional structural modelling and comparison analysis of picornavirus VP1 proteins	33
2.3.3. Protein domain comparison of cellular and viral Hsp90 client proteins	34
<b><u>2.4 Discussion</u></b>	<b>37</b>
<b><u>2.5 Conclusion</u></b>	<b>39</b>
<b><u>Chapter 3: Effects of Hsp90 Inhibitors, Geldanamycin and Novobiocin on TMEV Growth in BHK-21 Cells</u></b>	<b>41</b>
<b><u>3.1: Introduction</u></b>	<b>41</b>
<b><u>3.2 Methods and Materials</u></b>	<b>43</b>
3.2.1 Mammalian cell lines and culture conditions	43
3.2.2 Reagents and antibodies	43
3.2.3 Maintaining a BHK-21 cell line	44
3.2.3.1 Subculturing cells	44
3.2.3.2 Cryopreservation of BHK-21 cells	44
3.2.4 Preparation of TMEV stock	44
3.2.5 Plaque assay for TMEV stock titration	44
3.2.6 Nov and GA treatments	45

3.2.7 SDS-PAGE and Western analysis.	46
<b>3.3 Results</b>	<b>47</b>
3.3.1 Titration of TMEV stock by plaque assay	47
3.3.2 Determining the effects of Nov and GA on TMEV growth by monitoring the development of CPE	47
a) 24hrs post-treatment	47
b) 36hrs post-treatment	49
c) 48hrs post treatment	51
3.3.3 Detection of virally-expressed non-structural TMEV 2C protein in treated cells, 48hrs post-treatment	52
<b>3.4 Discussion</b>	<b>53</b>
<b>3.4 Conclusion</b>	<b>57</b>
<b>Chapter 4: Distribution of Hsp40, Hsp70 and Hsp90 in TMEV-Infected BHK-21 Cells</b>	<b>58</b>
<b>4.1 Introduction</b>	<b>58</b>
<b>4.2 Methods and Materials</b>	<b>60</b>
4.2.1 Preparation of BHK-21 cells for immunofluorescence	60
4.2.2 Indirect immunofluorescence staining of BHK-21 cells	60
4.2.3 Confocal microscopy and image acquisition	62
4.2.4 Preparation of cell lysates and Western analysis	62
<b>4.3 Results</b>	<b>62</b>
4.3.1 Distribution of Hsp40, Hsp70 and Hsp90 in TMEV-infected and mock-infected BHK-21 cells	62
a) Distribution of Hsp40	63
b) Distribution of Hsp70	65
c) Distribution of Hsp90	67
d) Distribution of Hsp90 over time	69
4.3.2 Time course of Hsp expression	70
<b>4.4 Discussion</b>	<b>72</b>
<b>4.5 Conclusion</b>	<b>75</b>
<b>Chapter 5: General Conclusions and Future Work</b>	<b>77</b>
<b>Chapter 6: References</b>	<b>81</b>

## List of Figures

- Figure 1.1:** Schematic representation of the PV genome organisation.
- Figure 1.2:** Schematic diagram of picornavirus genomic organisation and polyprotein processing.
- Figure 1.3:** Overview of picornavirus life cycle.
- Figure 1.4:** Processing and assembly of the picornavirus capsid.
- Figure 1.5:** Schematic diagram illustrating how different classes of molecular chaperones function in the cycle to produce a folded and functional protein using the Hsp90 pathway.
- Figure 1.6:** Schematic diagram of the three functional domains of Hsp90.
- Figure 1.7:** Schematic representation of Hsp70 domains.
- Figure 1.8:** Schematic diagram of the three different types of Hsp40s.
- Figure 1.9:** Systematic diagram illustrating the functions of Hsp40 as a co-chaperone to Hsp70.
- Figure 2.1:** Multiple sequence alignment of picornavirus VP1 protein sequences using ClustalW.
- Figure 2.2:** Structural model of TMEV GDVII and resolved structures of various picornavirus VP1 proteins.
- Figure 2.3:** Schematic representation of the protein domains of cellular and viral Hsp90 client proteins.
- Figure 3.1:** Effects of novobiocin (Nov) and geldanamycin (GA) on the development of CPE in TMEV-infected BHK-21 cells 24hrs post-treatment.
- Figure 3.2:** Effects of novobiocin (Nov) and geldanamycin (GA) on the development of CPE

in TMEV-infected BHK-21 cells 36hrs post-treatment.

**Figure 3.3:** Effects of novobiocin (Nov) and geldanamycin (GA) on the development of CPE in TMEV-infected BHK-21 cells 48hrs post-treatment.

**Figure 3.4:** Western analysis of BHK-21 cells infected with TMEV in the presence and absence of Nov and GA using anti-TMEV 2C antibodies.

**Figure 4.1:** Distribution of Hsp40 in mock-infected and TMEV-infected BHK-21 cells.

**Figure 4.2:** Distribution of Hsp70 in mock-infected and TMEV-infected BHK-21 cells.

**Figure 4.3:** Distribution of Hsp90 in mock-infected and TMEV-infected BHK-21 cells.

**Figure 4.4:** Distribution of Hsp90 in TMEV-infected BHK-21 cells during different stages of infection.

**Figure 4.5:** Western analysis of TMEV-infected cell lysates.

## List of Tables

- Table 1.1:** Genera of the *Picornaviridae* and examples of viruses and resulting diseases.
- Table 1.2:** Picornavirus precursor and mature proteins and the functions they perform.
- Table 1.3:** Hsp families, their members, localisation and functions.
- Table 1.4:** Summary of selected virus-chaperone interactions.
- Table 3.1:** Treatment of mock-infected and TMEV-infected BHK-21 cell using Nov and GA.
- Table 4.1:** Detailed information of primary antibodies utilised in Western analysis and IF.

## List of Abbreviations

### Viruses

<b>CV:</b>	Coxsackievirus
<b>EMCV:</b>	Encephalomyocarditis virus
<b>FHV:</b>	Flock House virus
<b>FMDV:</b>	Foot-and-mouth disease virus
<b>HAV:</b>	Hepatitis A virus
<b>HBV:</b>	Hepatitis B virus
<b>HCV:</b>	Hepatitis C virus
<b>HIV-1:</b>	Human immunodeficiency virus-1
<b>HPV:</b>	Human parechovirus
<b>HRV:</b>	Human Rhinovirus
<b>HSV:</b>	Herpes simplex virus
<b>MHV:</b>	Murine hepatitis virus
<b>PTV:</b>	Porcine teschovirus
<b>PV:</b>	Poliovirus
<b>SAFV:</b>	Saffold virus
<b>SV40:</b>	Simian virus 40
<b>TMEV:</b>	Theiler's murine encephalomyelitis virus
<b>VSV:</b>	Vesicular stomatitis virus

### General

<b>17AGG:</b>	17-allylamino-17-demethoxygeldanamycin
<b>BHK:</b>	Baby hamster kidney
<b>CNS:</b>	Central nervous system
<b>CPE:</b>	Cytopathic effect
<b>DAPI:</b>	4', 6- Diamino-2, phenylindole dihydrochloride
<b>DMEM:</b>	Dulbecco modified Eagle's medium
<b>DMSO:</b>	Dimethyl sulfoxide

<b>DNA:</b>	Deoxyribonucleic acid
<b>ER:</b>	Endoplasmic reticulum
<b>FCS:</b>	Fetal calf serum
<b>GA:</b>	Geldanamycin
<b>h.p.i:</b>	Hours post-infection
<b>HOP:</b>	Hsp70/Hsp90-organising protein
<b>Hsc70:</b>	Heat-shock cognate 70
<b>Hsp40:</b>	Heat shock protein 40
<b>Hsp70:</b>	Heat Shock protein 70
<b>Hsp90:</b>	Heat shock protein 90
<b>Hsps:</b>	Heat shock proteins
<b>ICTV:</b>	The International Committee on Taxonomy of Viruses
<b>IF:</b>	Immunofluorescence
<b>IPV:</b>	Inactivated poliovirus vaccine
<b>LD:</b>	Lid domain
<b>MOI:</b>	Multiplicity of infection
<b>Nov:</b>	Novobiocin
<b>NS:</b>	Non-structural
<b>OPV:</b>	Oral poliovirus vaccine
<b>ORF:</b>	Open reading frame
<b>PBS:</b>	Phosphate buffered saline
<b>Pfu:</b>	Plaque forming units
<b>PIC:</b>	Pre-integration complex
<b>Poly-A:</b>	Polyadenalated
<b>PSF:</b>	Penicillin, streptomycin and fungizone
<b>RdRp:</b>	RNA-dependent RNA polymerase
<b>RNA:</b>	Ribonucleic acid
<b>RNP:</b>	Ribonucleoprotein
<b>RT:</b>	Reverse transcriptase
<b>S:</b>	Structural
<b>SBD:</b>	Substrate binding domain

<b>SMART:</b>	Simple Molecular Architecture Research Tool
<b>TBS:</b>	Tris buffered saline
<b>TPRs:</b>	Tetratricopeptide repeats
<b>UK:</b>	United Kingdom
<b>USA:</b>	United States of America
<b>UTR:</b>	Untranslated region
<b>VPg:</b>	Virus protein of the genome
<b>WHO:</b>	World Health Organisation

## List of Outputs

### Local Conferences Proceedings:

**Lorraine Z. Mutsvunguma**, Gregory L. Blatch and Caroline Knox. Investigating the role of Heat shock protein 40 (Hsp40) in the life cycle of Theiler's murine encephalomyelitis virus (TMEV). SASBMB 2010 Conference, Bloemfontein, Ilanga Estate 18-20 January.

### Research Articles:

Jauka TI, **Mutsvuguma L**, Boshoff A, Edkins AL, Knox C (2010) Localisation of Theiler's Murine Encephalomyelitis virus protein 2C to the Golgi apparatus using antibodies generated against a peptide region. J Virol Methods 168:162-169.

**Lorraine Z. Mutsvunguma**, Boitumelo Moethloa, Adrienne L. Edkins, Garry A. Luke, Gregory L. Blatch and Caroline Knox. Theiler's Murine Encephalomyelitis virus infection induces a redistribution of heat shock proteins 70 and 90 in BHK-21 cells, and is inhibited by novobiocin and geldanamycin. (Cell Stress and Chaperones, Accepted).

## Acknowledgements

**I would like to take this moment to express my gratitude the following people:**

- Firstly, I would like to extend my sincere gratitude to my supervisor Dr Caroline Knox for all the support, inspiration and guidance. I have learnt a great deal from you and I will always cherish all the memories I have of the 'Picornavirus research group'.
- My co-supervisor Prof Greg Blatch, I would like to thank you for the assistance and motivation.
- Dr Edkins, thank you for all the help you gave me when it came to acquiring confocal images and analysing the data. Mrs Val Hodgson, thank you for all the help you gave me in the tissue culture lab.
- Special thanks to my closest friends (Buhle, Fiki, Ingrid, Mpho, Jane, Leanne, Thembi, Rita, Tumi and Nosi) for being there, in and out of the lab, for always encouraging me when times got tough and for letting me cry on your shoulders when I thought all was lost.
- I would like to thank my family for the love, support and encouragement I received, not only these past two years but through out my academic career. Mommy, without you I wouldn't have gotten this far, thank you for always believing in me and always being there when I needed you and also at times when I thought I did not.
- For funding, I would like to extend my gratitude to the NRF for the research grant.
- Finally, I would like to give praise to God for giving me the strength to accomplish all my dreams.

# Chapter 1: Literature Review

## 1.1 Introduction

The term “virus” was derived from the Latin word, ‘poison’. The terminology “virus” was only used to describe these minute disease causing agents starting in the 20<sup>th</sup> century. Before this, they were referred to as ‘*contagium vivum fluidum*’ (contagious living liquid) or ‘filterable agents’ due to their ability to cause disease even after being passed through filtration devices such as the Chamberland candle filter (Levine 1996; Cann, 1997). Since then, the study of viruses has grown extensively and has even given rise to a new science, Virology and with that a definition of viruses; submicroscopic obligate intracellular parasites (Cann, 1997). The definition though simple, is useful for the distinction of viruses from other particles. The study of viruses is of great importance because of the many diseases they cause in humans, which range from less severe (common cold) to more lethal (haemorrhagic fever). Viruses affect a wide variety of organisms such as animals, bacteria, plants and fungi. More than 4000 viruses have been identified and a classification developed. Numerous properties are taken into account when classifying viruses such as, virion size and symmetry, type of nucleic acid (RNA or DNA), size of genome, strandedness (double or single), sense (positive, negative or ambisense), natural host range, pathogenicity and mode of transmission in nature (Levine, 1996). The classification system is monitored by an international body, The International Committee on Taxonomy of Viruses (ICTV).

## 1.2 Picornaviridae

### 1.2.1 Picornavirus Classification

*Picornaviridae* is a virus family that consists of both human and animal viruses. The word *pico* is Italian for “small”, which is one characteristic feature of all viruses within the family. The average size of the non-enveloped capsid is between 28-30 nm in diameter and composed of 60 capsid protein subunits which are arranged in an icosahedral symmetry. Enclosed within the viral capsid, is a single-stranded, positive-sense RNA molecule of about 7.2- 8.4 kb in size. Currently the viruses are sub-classified into twelve genera; *Enterovirus*, *Cardiovirus*, *Aphthovirus*,

*Hepatovirus, Parechovirus, Erbovirus, Kobuvirus, Teschovirus, Sapelovirus, Senecavirus, Tremovirus and Avihepatovirus* (ICTV, 2009). Listed in Table 1.1 are some of the significant viruses within the family and examples of diseases they cause in their hosts.

Table 1.1: Genera of the *Picornaviridae* and examples of viruses and resulting diseases (adapted from ICTV, 2009).

Genus	Virus Example	Disease Causes
<b>Aphthovirus</b>	Foot and mouth disease virus (FMDV)	Foot and mouth disease in cloven hooved animals
<b>Cardiovirus</b>	Theiler's murine encephalomyelitis virus (TMEV)	Mouse encephalomyelitis
	Encephalomyocarditis virus (EMCV)	Encephalomyelitis
<b>Enterovirus</b>	Poliovirus (PV)	Poliomyelitis
	Human Rhinovirus (HRV)	Common cold
<b>Hepatovirus</b>	Hepatitis A virus (HAV)	Liver disease
<b>Parechovirus</b>	Human parechovirus (HPV)	Neonatal carditis
<b>Teschovirus</b>	Porcine teschovirus (PTV)	Teschen-Talfan neurological disease

### 1.2.2 Clinical and Economical Significance of Picornaviruses

As mentioned in the above section, *Picornaviridae* consist of viruses which are of economical and clinical importance. This section will focus on three of those viruses namely; FMDV, HRV and PV.

FMDV belongs to the *Aphthovirus* and causes foot and mouth disease in cloven-hoofed animals. Outbreaks of the FMDV usually cause economical disasters because infected animals and “at risk” animals are slaughtered in order to eliminate any traces of the virus. Animals that do not die from FMDV infection have reduced productivity in terms of milk and the amount of meat. Due to the highly contagious nature of the virus, FMD-free nations have instituted stringent laws to ensure that they remain virus-free and this includes banning any type of livestock and livestock product trades with any nation that is known to have the virus. The FMDV outbreak of 2001 in the United Kingdom (UK) resulted in the loss of billions of pounds for the national economy

because it mostly affected the livestock industry. The livestock industry was not the only industry to suffer, the tourism and other industries lost revenue, totalling ~ £11.9 billion (Thompson *et al.*, 2002). In recent years countries such as the United States of America (USA) and the UK which have \$/£100 billion per year livestock industries, respectively, have began fearing terrorist attacks using FMDV to devastate their economies. This has resulted in scientists renewing their studies in trying to understand the viral agent that causes FMD (as reviewed by Grubman and Baxt, 2004).

Another virus of economical importance is HRV, a virus recently classified within the *Enterovirus* after the *Rhinovirus* was eliminated. According to a study published in 2003, approximately 500 million cases of the common cold are reported each year in the USA and this translates to about \$40 billion lost annually. Losses are due to employees taking leave of absence from work because of viral infection or to attend to sick children or spouses (Fendrick *et al.*, 2003).

PV belongs to the *Enterovirus*. The virus was one of the first recorded infections to plague men as seen on an Egyptian tomb carving of a man with a foot-drop deformity, which is a feature usually found in victims suffering from paralytic poliomyelitis (Levy *et al.*, 1994). Like most enteroviruses, PV is transmitted through the faecal-oral route. Most of the people infected by a virulent strain of the virus will experience paralysis and sometimes death if paralysis of the intercostals and diaphragm occurs. In order to control poliomyelitis, two highly efficient vaccines were created. The first vaccine was developed in the 1950s and it was an inactivated poliovirus vaccine (IPV), a mixture of three wild type poliovirus strains inactivated by treating with formalin to destroy infectivity of the virus without affecting the antigenic properties of the capsid. The second vaccine, meant for the vaccination of underdeveloped countries, was a live attenuated oral poliovirus vaccine (OPV) created in the 1960s. The success of OPV led to the elimination of the virus from entire continents by the 1980s. Due to this success, the World Health Organisation (WHO) aimed to eradicate the virus completely by the year 2000. Even though several countries have been polio free for numerous years, still in 2010, worldwide eradication has not yet been achieved. In several countries such as Nigeria, Pakistan, Afghanistan and India, the virus has never been eradicated and re-emergence of the virus is occurring, in countries such as Haiti, Dominican Republic, Egypt, Philippines and Madagascar. Re-emergence

of the virus is most likely due to the failed vaccination programmes and reduced amount of vaccinations being performed throughout the world as most countries have reduced immunisation (as reviewed by Racaniello, 2001).

With numerous economically and clinically important viruses within a single family, extensive research has been conducted to understand the replication, viral-host interactions and pathogenesis of picornaviruses. Alternative approaches into the study of picornaviruses have been developed because of stringent safety regulations implemented when studying highly virulent viruses and also the inability to successfully culture some of the viruses within the laboratory. One of the alternative methods used to study picornaviruses is usage of viruses not pathogenic to humans or live-stock and in this study a member of the *Cardiovirus* was selected as a study model. Another reason cardioviruses can be used as study models is because genomic organisation and replication strategies are highly conserved among picornaviruses (discussed in-depth in following sections).

### ***1.3 TMEV as a Study Model***

Until recently, only two species were present within the *Cardiovirus*, the EMCV-like viruses (ECMV, Mengo, Columbia-SK and Maus-Elberfeld) and the Theiler's-like viruses (BeAn, DA and GDVII strains) which infect rodents (reviewed by Racaniello, 2001). TMEV GDVII was chosen as the study model for this research.

TMEV, a murine virus, was first described in 1937 by Theiler (Theiler, 1937). The virus causes neurological and enteric diseases in some strains of mice. TMEV has been subdivided into two groups based on the different antigenicity, neurovirulence and growth in culture. The strains in the first group (GDVII and FA) cause rapid and fatal encephalitis in mice (Theiler & Gard, 1940). Mice infected with the second group (BeAn and DA), survive initial large dose infections from the strains but eventually develop progressive demyelinating disease, which results in inflammatory lesions within the central nervous system (CNS) (Lehrich *et al.*, 1976; Lipton, 1975, 1980; Lipton and Dal Canto, 1976; 1979). Due to the fact that TMEV only infects mice, it is a suitable picornavirus study model because it can be cultured in a Type 2 Biosafety environment without the risk of infecting humans and other animals. Another reason why TMEV is a perfect study model in this research is because it infects and replicates within Baby Hamster

kidney 21 (BHK-21) cells (Friedmann and Lipton, 1980; Kong *et al.*, 1994; van Pesch *et al.*, 2001).

### **1.3.1 Recent Discovery of Human Cardioviruses**

As mentioned in the above section, until recently, the *Cardiovirus* genus consisted of two distinct species of rodent viruses. Recent outbreaks of enteric disease which could not be linked to known enteric viruses such as rotavirus, sapovirus or astrovirus have recently been reported worldwide, leading to the conclusion that other pathogens must be causing the outbreaks. In 2007, a virus was isolated from a stool sample collected from an infant in 1981 who presented fever-like symptoms. The virus was amplified in cell culture and the complete genome of the virus sequenced (Jones *et al.*, 2007). The isolate was named Saffold virus (SAFV). Soon after this discovery, several SAFV strains have been isolated and identified worldwide. In Canada, SAFV was isolated from stool samples collected from three children exhibiting respiratory symptoms (Abed and Boivin, 2008). The third strain was isolated in Germany and Brazil, where six stool samples from infants with gastroenteritis tested positive for the virus (Drexler *et al.*, 2008). The next SAFV strain was isolated in California from respiratory secretions collected from a patient exhibiting influenza-like illness and six stool samples from patients suffering from gastroenteritis (Chiu *et al.*, 2008). A more recent recording of the virus was in Asia, where the virus was isolated from stool samples from six children suffering from non-polio acute flaccid paralysis and five children without evident neurological symptoms (Blinkova *et al.*, 2009). In total, the number of SAFV strains isolated and sequenced has now reached eight (Liang *et al.*, 2008). In order to conclusively group these viruses within the *cardiovirus* genus, sequence alignment analysis, phylogenetic analysis and molecular characterisation was conducted on a genotype of the virus, SAFV-3. Although sequences of the new human *cardioviruses* are highly divergent from that of known animal *cardioviruses*, the new viruses are genetically similar mainly to the Theiler's-like virus (TMEV strains), warranting their classification as a *cardiovirus* (Zoll *et al.*, 2009).

The following sections will discuss the genomic organisation, protein processing, replication and assembly of picornaviruses using PV as a model.

### 1.3.2 Picornavirus Genomic Organisation

The picornavirus genome is a single stranded, positive sense RNA molecule of about 7 – 8 kb nucleotides (reviewed by Racaniello, 2001). Illustrated in Figure 1.1 is a schematic representation of the PV genome organisation. As seen in the figure, covalently attached to the 5' untranslated region (UTR) is a small viral protein VPg (virus protein of the genome), which plays a role in the initiation of viral RNA synthesis (Agol, 1991). Within the 5'UTR is a cloverleaf structure known as the internal ribosome entry site (IRES). This site directs the cap-independent internal initiation of translation by recognising and binding to the 40s ribosome unit (Stewart and Semler, 1997; reviewed by Racaniello, 2001; Bedard and Semler, 2004). The polyadenalated (poly-A) tail at the 3' end is thought to play a role in viral infectivity and involved in stabilising viral RNA (Rohll *et al.*, 1995; reviewed by Racaniello, 2001; Bedard and Semler, 2004).

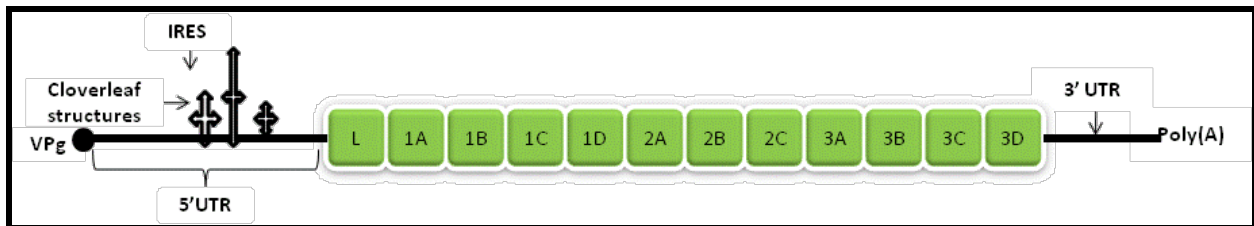


**Figure 1.1: Schematic representation of the PV genome organisation.** Attached at the far end of the 5' UTR is the VPg which acts as a primer for viral RNA synthesis. The 5' UTR comprises of a cloverleaf structure and an IRES region which is followed by the coding region of the viral polyprotein. A poly-A tail is present at the 3' UTR (adapted from Bedard and Semler, 2004).

### 1.3.4 Polyprotein Processing

Once the open reading frame (ORF) has been translated into a single large polyprotein, it undergoes a series of proteolytic cleavages to produce mature viral proteins. The cleavage process is conducted by three virally-encoded proteases,  $2A^{pro}$  and  $3C^{pro}$  and its precursor protein,  $3CD^{pro}$ . The first cleavage event, the separation of the P1 domain from the P2-P3 domains is conducted by the  $2A^{pro}$  (Ryan *et al.*, 1991) and the remaining cleavages are conducted by  $3C^{pro}$  or its precursor protein  $3CD^{pro}$  (Figure 1.2) (reviewed by Racaniello, 2001; Bedard and Semler, 2004).

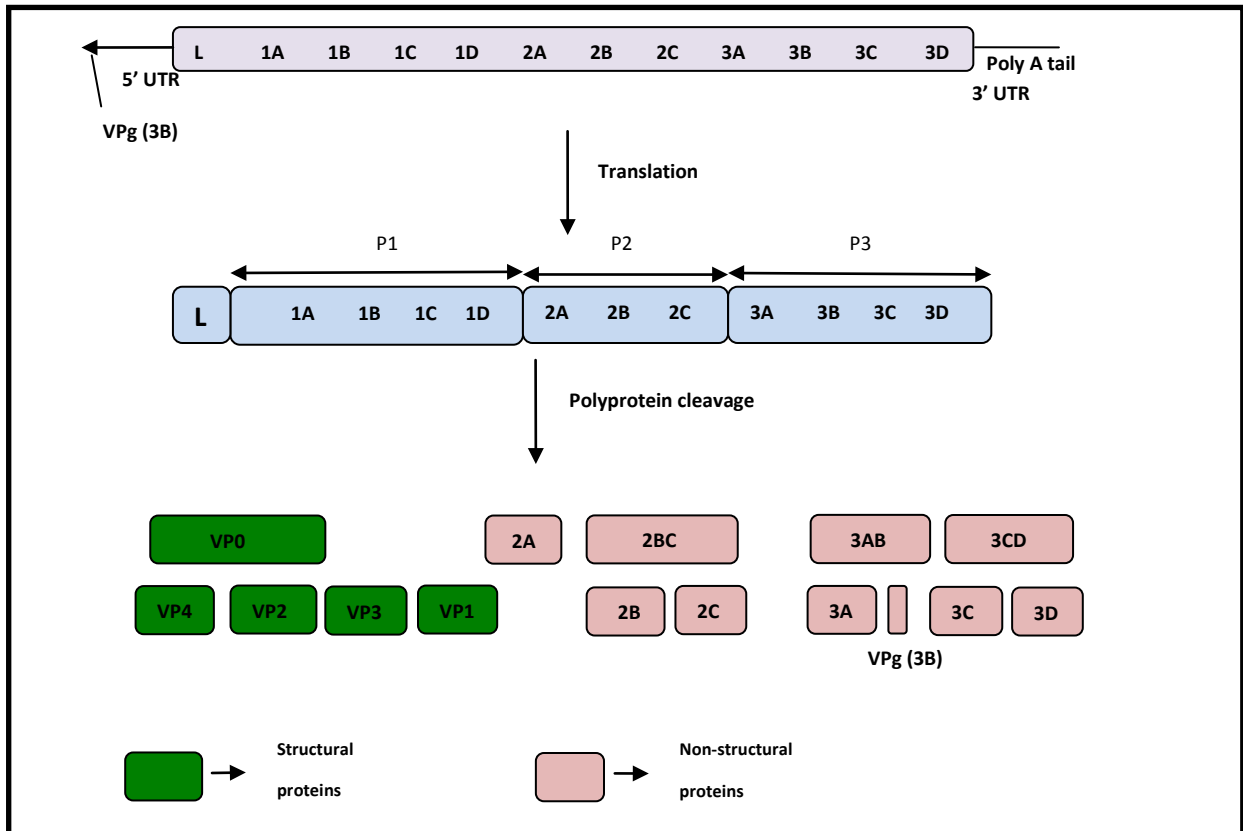


**Figure 1.2: Schematic diagram of picornavirus genomic organisation and polyprotein processing.** The single open reading frame (ORF) is translated into a single polyprotein that is co-translationally cleaved into mature structural proteins (VP1-VP4) from the P1 domain and replicative proteins (2A-3D) from both the P2 and P3 domains (adapted from Bedard and Semler, 2004).

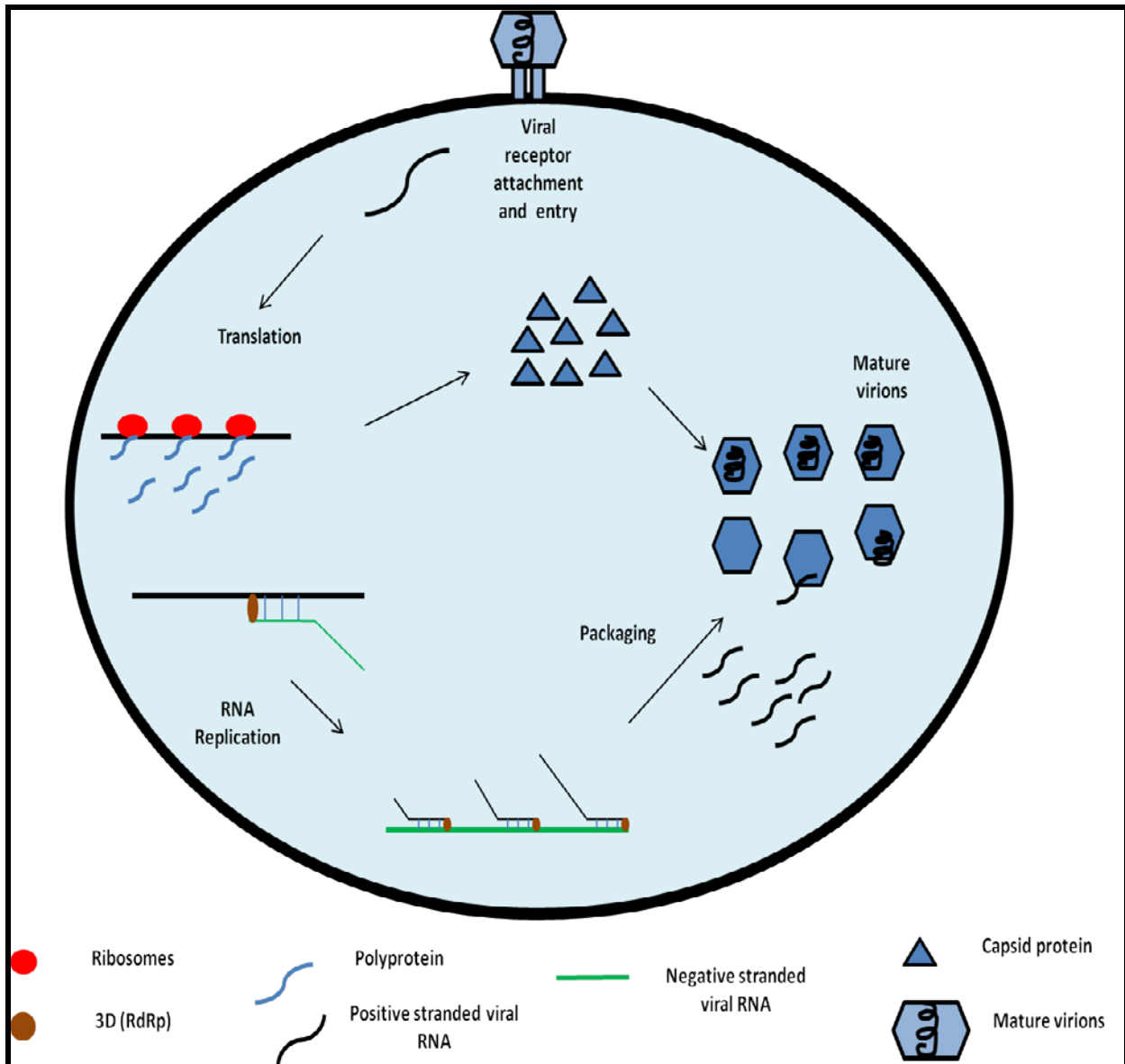
The mature viral proteins are divided into 2 groups, non-structural (NS) and structural (S) proteins. The S proteins, VP1-VP4 are responsible for forming the viral icosahedral capsid and NS proteins (2A-3D) are responsible for viral replication. The proteins and their precursors have different functions (Table 1.2) (reviewed by Buenz and Howe, 2006).

Table 1.2: Picornavirus precursor and mature proteins and the functions they perform (adapted from Buenz and Howe, 2006).

Protein	Function
<b>L</b>	Undefined role in host and tissue tropism
<b>VP1-VP4</b>	Structural proteins, responsible for virion assembly and viral entry into host cells
<b>2A</b>	Viral protease
<b>2B</b>	Alters membrane permeability and involved in RNA synthesis
<b>2C</b>	NTPase, vesicle formation and Guanidine resistance
<b>3AB</b>	Membrane association and stimulation of 3C and 3D
<b>3A</b>	Associates with intracellular membranes
<b>3B</b>	(VPg) primer for RNA synthesis
<b>3CD</b>	3C and 3D precursor, known to have protease activity
<b>3C</b>	Viral protein processing, host protein cleavage and RNA binding and replication
<b>3D</b>	RNA dependent RNA polymerase

### 1.3.3 Replication

The host cytoplasm is the site of replication in picornaviruses. The infection cycle is initiated by receptor-mediated attachment to the cell surface, endocytosis and then uncoating to release viral genome once in the cytoplasm. The responsibility of synthesising new viral genetic material falls on the 3D protein, an RNA-dependent RNA polymerase (RdRp), one of the first viral proteins to be translated. 3D functions in conjunction with another viral protein, 3B (VPg), which serves as a primer for synthesising negative-strand RNA, which is then used as a template for more positive-sense RNA synthesis. Viral replication occurs on membrane vesicles proposed to be formed from the endoplasmic reticulum (ER) by the viral protein 2C (Bienz *et al.*, 1992; Suhy *et al.*, 2000). Some of the newly synthesised viral RNA will be translated into more viral proteins, while the rest is packaged into newly formed viral capsids and the new virions will exit the cell via cell lysis (Figure 1.3) (reviewed by Racaniello, 2001; Bedard and Semler, 2004).



**Figure 1.3: Overview of picornavirus life cycle.** The first step in the replication of the virus is the receptor-mediated attachment to the host cell membrane, followed by penetration and uncoating to release viral RNA into the cytoplasm. Translation of the RNA is accomplished by utilising the host cell machinery to produce the polyprotein, which is cleaved into various viral proteins. The structural proteins form viral capsids, while non-structural proteins are responsible for synthesising negative-strand RNA which will be used as a template to produce more positive-strand RNA. Positive-strand RNA is then packaged into the newly formed viral capsids which exit the cells via cell lysis (adapted from Andino *et al.*, 1999).

### 1.3.4 Assembly

The assembly process of picornaviruses begins with the cleavage of the capsid precursor protein, P1 from the P2/P3 domains. The cleavage is mediated by the viral encoded protease, 2A<sup>pro</sup>. As seen in Figure 1.4, after the first proteolytic cleavage of P1 by 2A<sup>pro</sup>, the precursor polyprotein is cleaved by 3C<sup>pro</sup> and its precursor protein 3CD<sup>pro</sup>. The proteases cleave between VP0–VP3 and VP3–VP1, the cleavage of the subunits from each other is crucial for the formation of the protomer subunit, the cleavage event is required to commence the assembly process. The protomer is the first assembly intermediate, it is formed by the interaction of a single copy of each VP1, VP3 and VP0 subunit. The next step is the association of five protomers, which results in the formation of a pentamer. The association is largely due to hydrophobic interactions that occurs between protomers. It is believed that the formation of the provirion is triggered by the protein-protein interaction between the VPg and the inner surface of the pentamer. The assembly process continues with the addition of eleven pentamers, the condensation and encapsidation of the RNA molecule. The final step to the assembly process is the RNA-dependent cleavage of the VP0 molecules to form VP4 and VP2. This final event results in the formation of a mature virion. The final assembly product is an icosahedral shaped capsid that is made up of 60 copies of each of the four capsid subunits, with VP1-3 on the surface and VP4 embedded within the capsid (as reviewed by Racaniello, 2001).

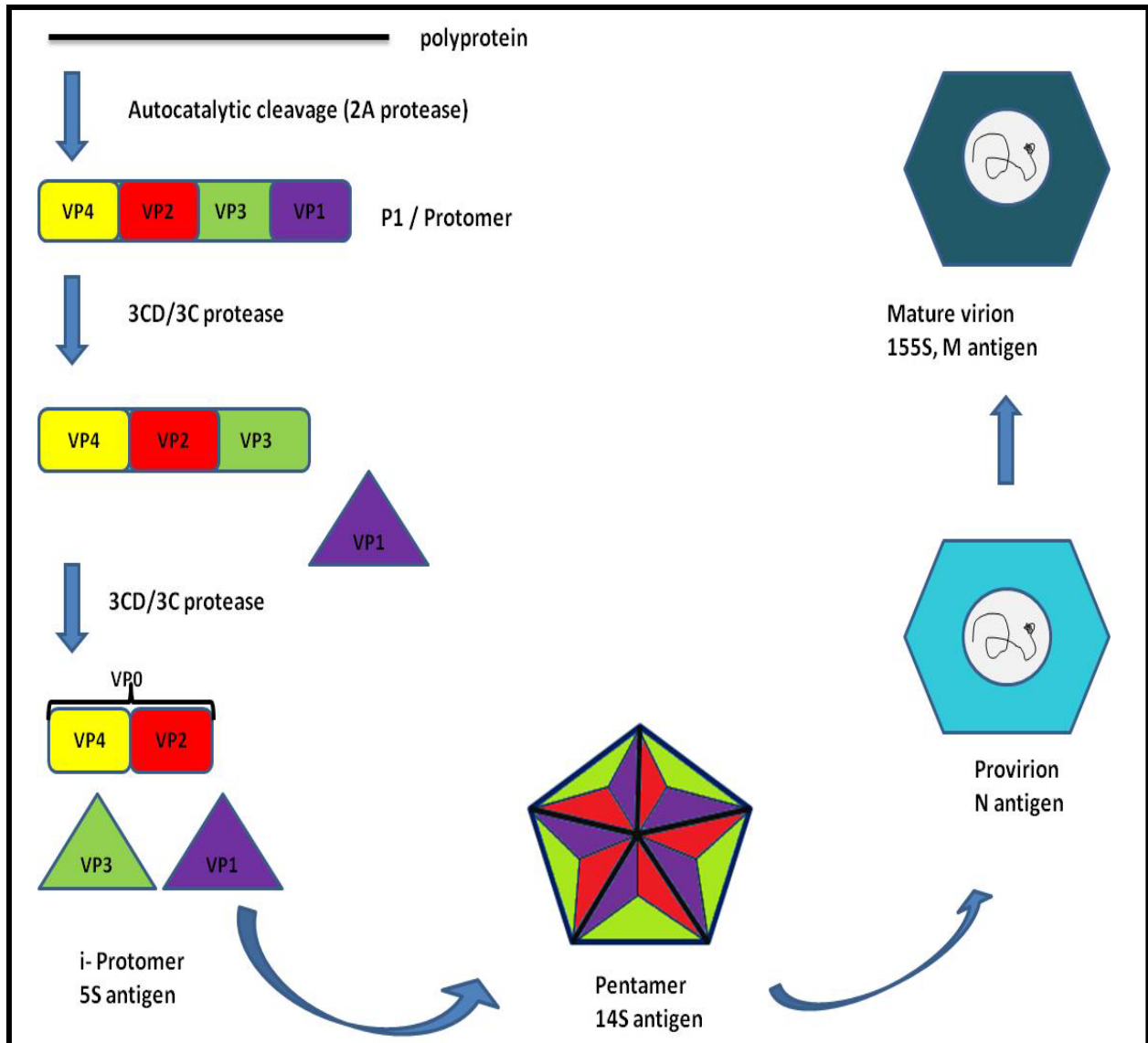


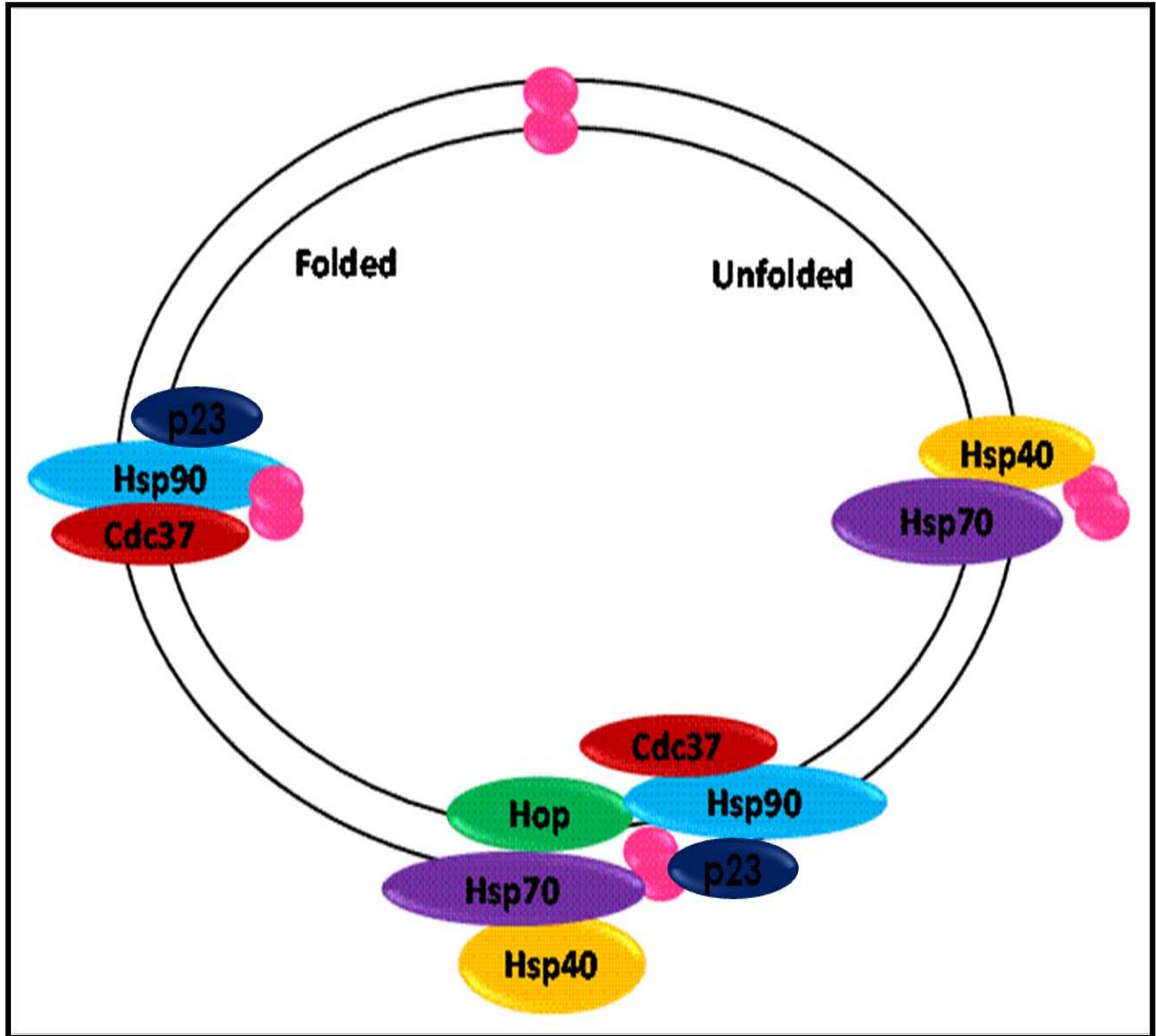
**Figure 1.4: Processing and assembly of the picornavirus capsid.** Once the viral RNA is translated into a single polyprotein, autocatalytic cleavage by  $2A^{pro}$  occurs, separating structural P1 domain from non structural domains, P2 and P3. A series of cleavages by 3C/  $3CD^{pro}$ , yields VP1, VP3 and VP0 (VP2-VP4) proteins which are arranged into a pentamer. A final cleavage of VP0 into VP2 and VP4, results in the maturation of the provirion into mature virion with the capsid being icosahedral in shape and made up of 60 subunits of each protein, VP1, VP2 and VP3 are on the surface while VP4 is buried within the capsid (adapted from Cann, 1997).

Viruses are known to utilise host machinery during different stages of their replication life cycle. Due to the size of their genomic material, the protein coding capacity of viruses is greatly limited. One of the host machinery used by viruses during their life cycle is a group of specialised proteins known as molecular chaperones.

## ***1.4 Molecular Chaperones***

### **1.4.1 Function of molecular chaperones**

The molecular chaperone family, which also consists of several heat shock proteins (Hsps) is a group of proteins that have abundant functions within cells; from protein folding, degradation, translocation, buffering cell mutations, cell survival promotion and regulating the apoptosis process (reviewed by Ellis, 1987; Feldman and Frydman, 2000; Frydman, 2001). The protein folding process is the primary function of chaperones, they are able to bind selectively to nascent peptides and partially folded intermediates, and distinguish between folded and unfolded proteins by recognising the hydrophobic features of unfolded proteins (reviewed by Fink, 1999). The process generally requires the cooperation of different classes of chaperones. Figure 1.5 illustrates the cycle of a protein from its unfolded state to folded state. Listed in Table 1.3 are the different classes of molecular chaperones, their members, localisation and functions.



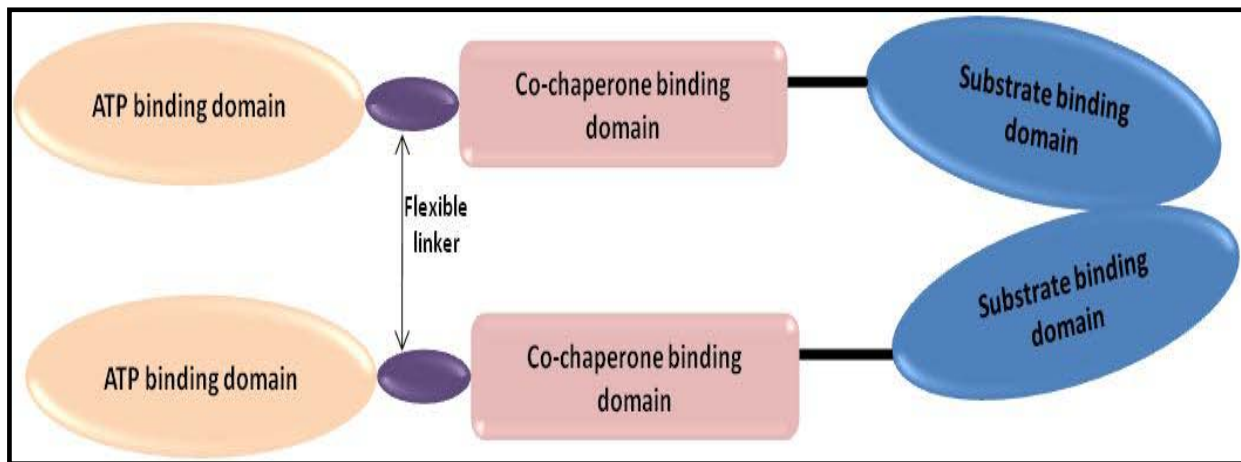
**Figure 1.5: Schematic diagram illustrating how different classes of molecular chaperones function in the cycle to produce a folded and functional protein using the Hsp90 pathway.** The cycle starts with the binding of the nascent protein by Hsp70 and its co-chaperone, Hsp40, to form an early complex, Hsp90 and its co-chaperones Cdc37, p23 and Hop are recruited to form an intermediate complex. The late complex only consists of Hsp90, p23, Cdc37 and the protein of interest, with the end result of the cycle being a functional protein (adapted from Caplan *et al.*, 2007).

Table 1.3: Hsp families, their members, localisation and functions (adapted from Snoeckx *et al.*, 2001; Xu, 2002).

Family	Members	Localisation	Function	Reference
<b>Hsp10</b>	Hsp10, Hsp17	Mitochondria	Works with Hsp60 to promote substrate release	Hartl and Hayer-Hartl, 2002
<b>Small Hsps</b>	Hsp22-23, Hsp27-28	Cytoplasm/ perinuclear  Nucleus (Stress)	F-actin assembly, Chaperone	Arrigo <i>et al.</i> , 1988; Arrigo and Landry, 1994
<b>Hsp40</b>	Hsp32, Hsp40, Hsp47	Cytoplasm/ ER  Nucleus (Stress)	Guides protein folding,  Binds and transports collagen, Hsp70 co-chaperone	Fink, 1999; Rosser and Cyr, 2007; Walsh <i>et al.</i> , 2004
<b>Hsp60</b>	Hsp58, Hsp60, Hsp65	ER, Mitochondrial	Assemble polypeptides, chaperone, translocates proteins across membranes, works with Hsp10	Kirchhoff <i>et al.</i> , 2002; Soltys and Gupta 1996
<b>Hsp70</b>	Hsp68, Hsc70, Hsx70, Hsp72-73, Hsp75, Hsp78, BiP	Cytoplasm, peroxisomes, mitochondria, ER  Nucleus (Stress)	Guide and folds proteins, ATPase activity	Mayer and Bukau, 1998, 2005
<b>Hsp90</b>	Hsp83, Hsp87, Hsp90 $\alpha$ , Hsp90 $\beta$	Cytoplasm, Nuclear membrane, ER  Nucleus (Stress)	Binds cytoplasmic hormone receptors, guides certain kinases to cell membrane, molecular chaperone	Fink, 1999; Picard, 2002; Chiosis <i>et al.</i> , 2004

### 1.4.2 Heat shock protein 90 (Hsp90)

One of the most abundant heat shock proteins is Hsp90 which makes up about 1% of the soluble proteins in eukaryotes (Lai *et al.*, 1984). Like other chaperones Hsp90 is involved in the folding, transportation, maturation and degradation of many proteins (Cowen and Lindquist, 2005). Hsp90 has 3 domains, the highly conserved N-terminal ATP-binding domain, a C-terminal domain which has the client binding domain, and a middle domain where co-chaperones bind (Figure 1.6).



**Figure 1.6: Schematic diagram of the three functional domains of Hsp90.** Hsp90 exists as a dimer within the cell. Located on the N-terminus domain the ATP binding domain. A flexible linker connects the N-terminus and Middle domain, the Middle domain responsible for binding Hsp90 co-chaperones and the substrate binding domain is located on the C-terminus (adapted from Whitesell and Lindquist, 2005).

As mentioned above, the N-terminal domain is the most conserved and most studied domain out of the three. The domain comprises of approximately 220 amino acids and has been shown to bind both ATP and ADP. The presence of the structurally unique ATP-binding site classifies Hsp90 into the GHLK family along with bacterial DNA gyrase, the DNA repair protein MutL and several bacterial histidine kinases (Dutta and Inouye, 2000). Although the listed proteins are part of the same family and require the binding of ATP to function, they do not function in the same way (Dutta and Inouye, 2000). The binding and hydrolysis of ATP causes a conformational change in Hsp90 which is related to its chaperoning activities (Prodromou *et al.*, 1997a; 1997b; 2000). The N-terminal ATP-binding site is also the binding site of Hsp90 inhibitors, geldanamycin (GA) and its analogues, as well as radicicol (Grenert *et al.*, 1997; Stebbins *et al.*,

1997; Roe *et al.*, 1999). Hsp90 is known to interact with numerous co-chaperones as seen in Figure 1.5. In order for the co-chaperones to bind to Hsp90, they have to contain 34 amino acid tetratricopeptide repeats (TPRs), which they utilise to interact with the MEEVD motif that is located at the end of the C-terminus (Prodromou *et al.*, 1999; Ramsey *et al.*, 2000). Some Hsp90 co-chaperones that contain the TRPs are Hsp70-90 organising protein (Hop), the immunophilins FKBP51, FKBP52, and cyclophilin-40, protein phosphatase 5, the Ah receptor-interacting protein AIP, the E3 ubiquitin ligase CHIP and the myosin-binding protein UNC-45 (Chen *et al.*, 1998; Carrello *et al.*, 1999). Also located at the C-terminus is another ATP-binding site. It is believed that the site opens up when the N-terminal ATP-binding site is occupied (Sóti *et al.*, 2002). Hsp90 inhibitors, novobiocin (Nov), cisplatin and taxol are known to bind the C-terminal ATP-binding site (Marcu *et al.*, 2000a; reviewed by Donnelly and Blagg, 2008). Nov and GA will be discussed in detail in Chapter 3, as they were selected for analysis in this study.

The function of Hsp90 in cells under normal conditions is to maintain cell homeostasis. This is achieved by correctly folding and stabilising client proteins. Recently it has been discovered that Hsp90 plays a role in the regulation of several factors involved in apoptosis. Hsp90 is also involved in buffering cell mutation, cell survival promotion and recently been linked to the preservation of transformation states of several cell types. The proteins that are controlled by Hsp90 are involved in different roles in cells such as controlling the cell cycle, cell growth and cell death and the inhibition of Hsp90 leads to the degradation of the various proteins via the ubiquitin cycle resulting in arrested cell growth (reviewed by Chiosis *et al.*, 2004). Two cytosolic isomers of Hsp90 (Hsp90 $\alpha$  and Hsp90 $\beta$ ) have been identified and are expressed differently in the cell, with the  $\beta$  form being induced by growth hormones and the  $\alpha$  form expressed under stress conditions (Buchner, 1999). A third form of Hsp90 called TRAP1 or Hsp75 was discovered and is found in lower levels suggesting that it has a specialised function in the cell (Buchner, 1999).

### **1.4.3 Heat shock protein 70 (Hsp70)**

Another well-studied chaperone is Hsp70. This class of chaperones is crucial in protein folding, membrane translocation, disruption of protein aggregates and also rearranging multiprotein complexes (reviewed by Mayer and Bukau, 1998; 2005; Fink, 1999; Pratt and Toft, 2003). Hsp70s are highly conserved and are present in all organisms. Hsp70 consists of three domains,

an N-terminal ATPase domain of about ~44kDa, substrate binding domain ~15kDa and a ~10kDa C-terminal lid (Figure 1.7) (Flaherty *et al.*, 1990; Zhu *et al.*, 1996; reviewed by Fink, 1999). An EEVD motif is located on the far end of the C-terminus of the Hsp70 protein. This motif is responsible for the interaction of the chaperone with its co-chaperones. Similar to Hsp90, in order for an interaction to occur between the co-chaperones and the EEVD motif of Hsp70, they require the 34 amino acid TPRs as seen in the case of HOP (Scheufler *et al.*, 2000; Odunuga *et al.*, 2003).

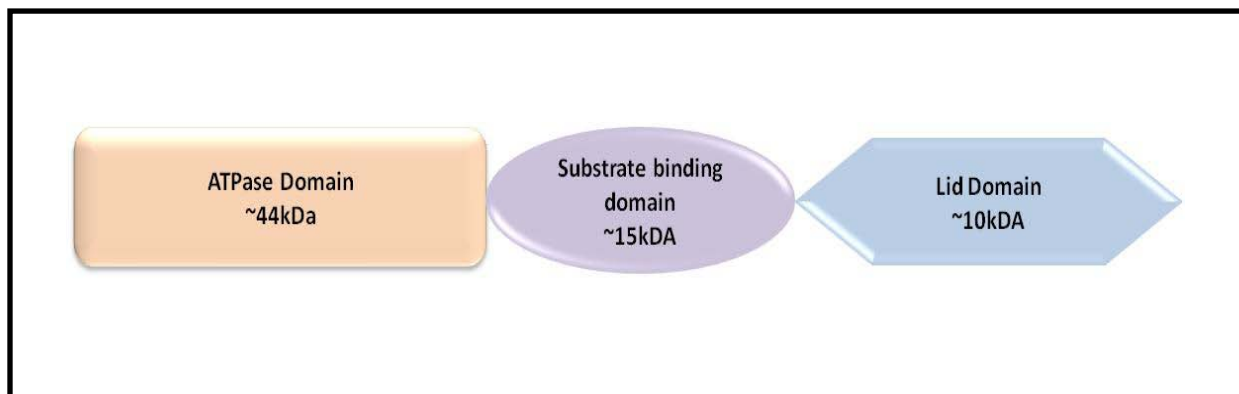


**Figure 1.7: Schematic representation of Hsp70 domains.** A ~44kDa ATPase domain, is located on the N-terminus of the protein and is the site where ATP binds. The substrate binding domain (SBD) of about 15kDa is located in the middle of the protein and is the site where client proteins/substrates of Hsp70 bind. The lid domain (LD) is located on the C-terminus of the protein and is the site where co-chaperones bind and also is responsible for covering the SBD.

The mode of Hsp70 function is the binding of substrates which is facilitated by the energy provided by the hydrolysis of ATP (McCarty *et al.*, 1995; Theyssen *et al.*, 1996). In the ATP bound form, Hsp70 has low affinity for substrate binding, but once ATP hydrolysis occurs with the help of Hsp70 co-chaperone, Hsp40, a conformational change occurs and ADP-bound Hsp70 has substrate binding affinity greatly increased (reviewed by Mayer and Bukau, 1998; 2005). Numerous isomers of Hsp70 are expressed under different conditions and location. Heat-shock cognate 70 (Hsc70) is the cytosolic constitutive form and under stress conditions, Hsp70 expression is inducible. Bip and mHsp70 are the ER and mitochondrial forms, respectively (reviewed by Fink, 1999).

### 1.4.4 Heat shock protein 40 (Hsp40)

The Hsp40s are molecular chaperones also known as the J domain family because this domain defines a protein as a member of the Hsp40 family. To date over a hundred Hsp40s have been identified, forty four of the known Hsp40 are found in mammalian cells and localise to the ER, nucleus, mitochondria, cytosol and ribosomes. Twenty homologues of Hsp40 such as Ydj1 have been found in *Saccharomyces cerevisiae* and six in *Escherichia coli* (*E. coli*) where there mostly known as DnaJ (reviewed by Qiu *et al.*, 2006). Hsp40s are divided into three different groups based on their structural domains, namely, type 1 Hsp40s with a J domain, present in all Hsp40s, a G/F rich domain and a zinc domain. Type 2 have the J and G/F domains but lack the zinc domain and type 3 Hsp40s only have the J domain (Figure 1.8) (reviewed by Cheetham and Caplan, 1998). The different domains within the Hsp40s have different functions.

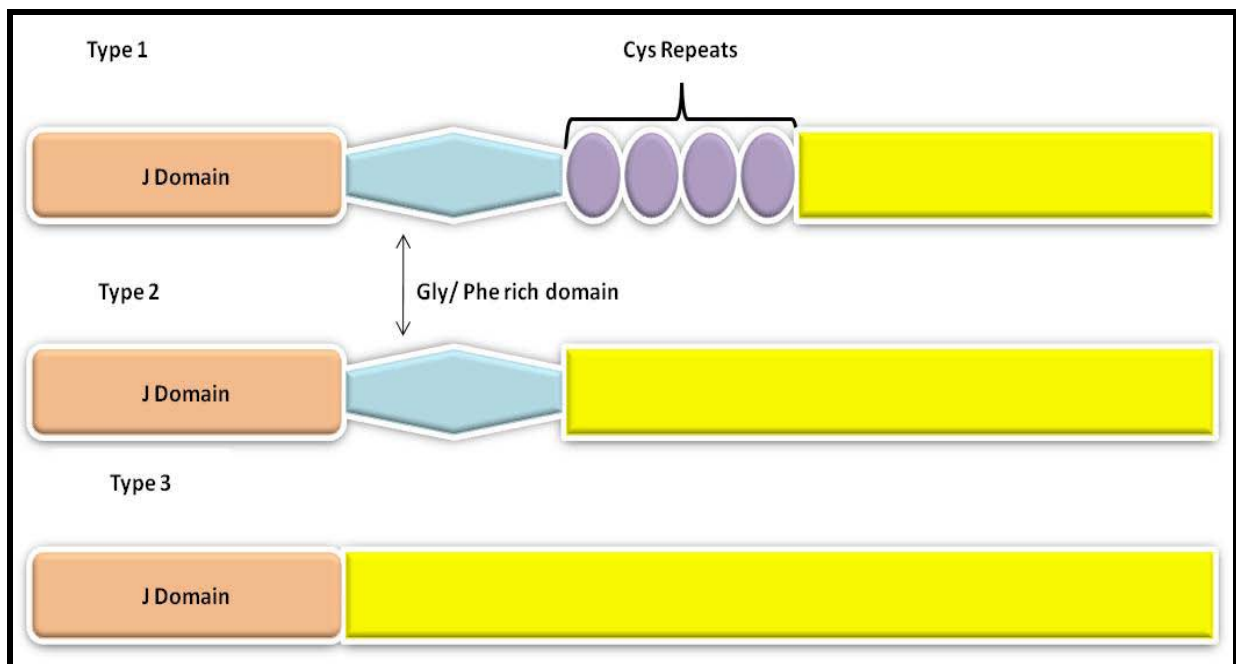


**Figure 1.8: Schematic diagram of the three different types of Hsp40s.** Classification depends on the presence of the different domains. The J domain is present in all Hsp40s and is involved in facilitating the interaction between Hsp40s and Hsp70s. The G/F rich domain is found in type 1 and 2 and is responsible for stimulating the J domain. The zinc domain which consists of four cysXXcys repeats is only present in type 1 (adapted from Qiu *et al.*, 2006; Rosser and Cyr, 2007).

Structurally, the J domain is made up of four alpha-helices and no beta sheets. The most important part of the J domain is the exposed finger structure made up by the compression of two of the helices making up the J domain (second and third helices). The finger tip is a loop between helices 2 and 3 and it contains the functionally significant HPD motif, and this motif is found in all Hsp40-like proteins. The side chain of the motif extends out from the structure and is believed to facilitate the interaction between Hsp40 and Hsp70 (reviewed by Cheetham and Caplan, 1998). Studies have shown that the J domain is involved in the interaction and stimulation of the ATPase activity of Hsp70 and the HPD motif is essential for this interaction as mutation of the HPD motif leads to the loss of the interaction (Feldheim *et al.*, 1992; Wall *et al.*, 1994; Tsai and Douglas, 1996). The function of the G/F domain is to stimulate the J domain when it interacts with Hsp70 and its function appears to be dependent on the peptide binding state of Hsp70 because it has been shown that in the presence of bound peptide, the J domain can stimulate the ATPase activity of Hsp70 in the absence of the G/F domain (Karzai and McMacken, 1996). The zinc domain is only present in type 1 Hsp40s, it contains a cys-rich region that has a cysXXcys motif repeated four times, and similar repeats are found in DNA binding proteins. It has been suggested that the Hsp40 cys-rich domain might be involved in the stabilisation of Hsp70-substrate complexes (Szabo *et al.*, 1994; Banecki *et al.*, 1996).

One of the most important functions of Hsp40s is to act as a co-chaperone to Hsp70s. Hsp40s are classified as Hsp70 co-chaperones because they are able to bind Hsp70, pass substrates to Hsp70 and finally stimulate the ATPase activity of Hsp70. In order for Hsp70 to take part in these functions, its affinity for substrates is regulated by its nucleotide binding state. When bound to ATP, Hsp70 has low affinity for substrate proteins but when hydrolysis of ATP to ADP occurs, the affinity of Hsp70 to substrates increases due to a conformational change that occurs. In order for Hsp70 to act as a chaperone, it needs to undergo repeated cycles of ATP hydrolysis and nucleotide exchange, allowing it to bind and release substrates numerous times (Figure 1.9) (reviewed by Fink, 1999; Mayer and Bukau, 2005; Qiu *et al.*, 2006; Rosser and Cyr, 2007).

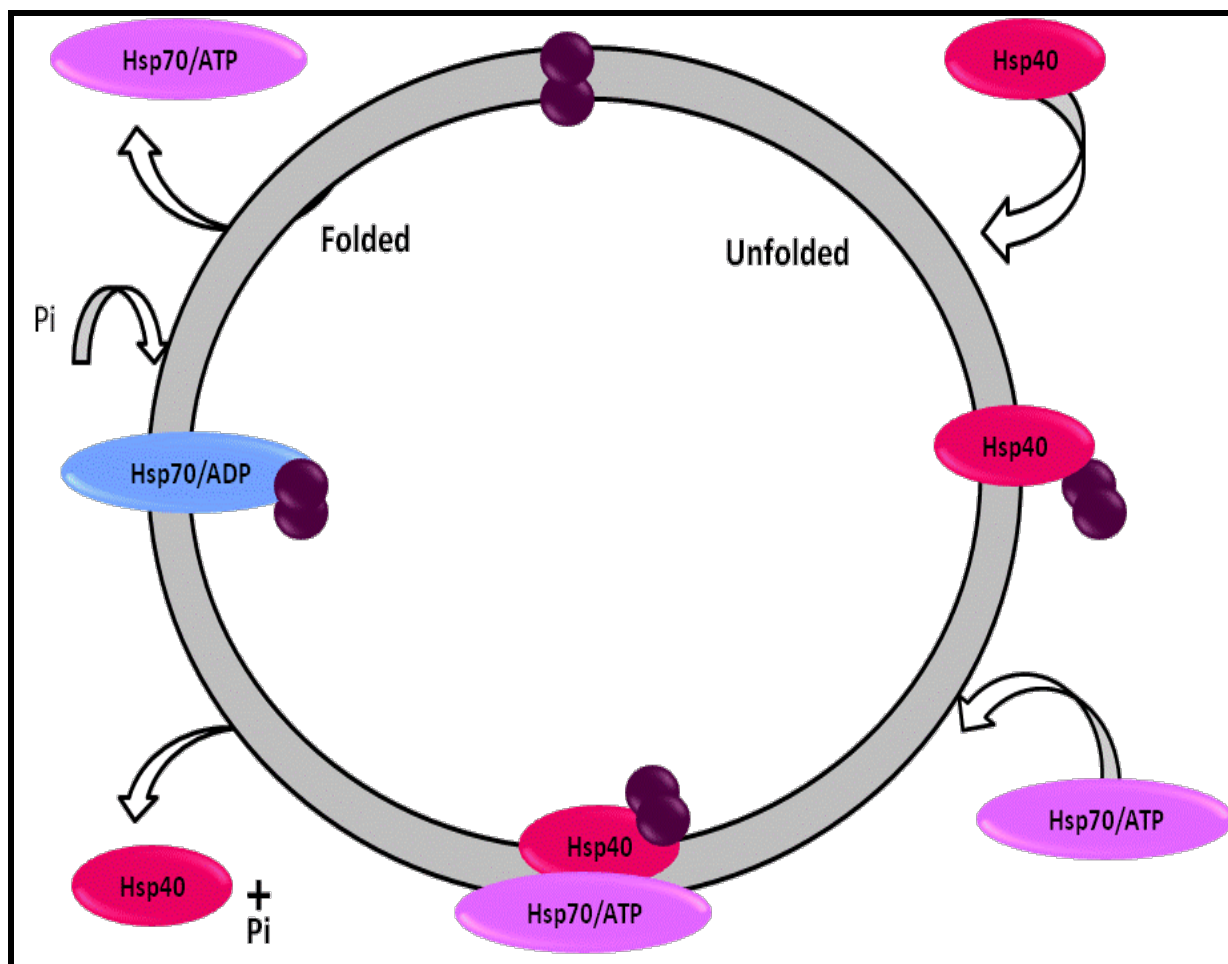


**Figure 1.9:** Systematic diagram illustrating the functions of Hsp40 as a co-chaperone to Hsp70. In its ATP bound form, Hsp70 has low affinity for binding to substrates, Hsp40 is essential in changing the ATP bound to Hsp70 to ADP, this increases the binding affinity of Hsp70 to its substrate (adapted from Fan *et al.*, 2003).

Due to their versatile roles within the cell, Hsp40 and other chaperones have been targets of exploitation by viruses of many families and genera as discussed below.

## ***1.5 Virus-Chaperone Interaction***

### **1.5.1 General viral-chaperone interactions**

Since the discovery of minute particles using light microscopical techniques as disease causing agents, extensive research has been conducted to understand these killers. The particles, termed “viruses” seem to hijack host cell machinery and pathways in order to undergo their infectious cycle. The relationship between chaperones and viruses has been widely documented,

implicating the majority of these proteins as unwilling participants in viral entry, replication and assembly (extensively reviewed by Sullivan and Pipas, 2001; Xiao, 2010).

### **a) Viral entry**

Viruses are known to interact with chaperones during their entry into the host cell. The role of chaperones during viral entry is to act as viral receptors or assist in the viral uncoating process. Rotaviruses require the presence of Hsc70 during their entry into the host cell. The interaction occurs during a post-attachment step, where the chaperone brings about a conformational change to the viral capsid, facilitating the entry of the virus into the cytoplasm (Guerrero *et al.*, 2002; Zarate *et al.*, 2003). Other examples of chaperone-virus interactions that mediate viral entry include Hsp90/ Hsp70 and Dengue virus (Reyes-Del Valle *et al.*, 2005), Hsp70 and Japanese encephalitis virus (Das *et al.*, 2009) and GRP78 (Hsp70) and Coxsackievirus (CV) A9 (Triantafilou *et al.*, 2002).

### **b) Chaperone regulation by viruses**

There is evidence of certain viruses inducing directly or indirectly the expression of cellular chaperones such as Hsc70, Hsp90 and Hsp40 (reviewed by Sullivan and Pipas, 2001). It has been suggested that the expression of these chaperones is an automatic response to the stress the cell undergoes during viral infection and not to facilitate viral replication. This situation has been noted in cells infected by viruses from the *Polyomaviridae*, where infection induces an increase in the expression of Hsc70 but the protein does not have any functions in viral replication (Sainis *et al.*, 1994). However, the increase of Hsc70 expression in avian Adenovirus is a clear indication of how the virus is dependent on the presence of the chaperone. Hsc70 expression is upregulated by the virus and shown to be essential in viral DNA nuclear import and binding to capsid proteins (Saphire *et al.*, 2000). The increase of gp96 (ER Hsp90) levels in Hepatitis B virus (HBV)-infected cells correlates considerably with disease progression (Zhu *et al.*, 2004).

### **c) Replication and gene expression**

The majority of virus-chaperone interactions occur during the replication of viral genomic material. DNA viruses such as Hepadnaviruses replicate via the mechanism of protein-primed reverse transcription using a specialised reverse transcriptase (RT) and it has been shown that the presence of Hsp70 and to some degree, Hsp90, is required for the activation of the RT (Stahl *et*

*al.*, 2007). In duck HBV, Hsp90 activates the RT by forming a bridge between the two separate domains of the protein, enabling the formation of a ribonucleoprotein complex and viral RNA (Hu and Anselmo, 2000). In Influenza A virus, Hsp90 stimulates the activity of the RNA polymerase and this leads to efficient transcription and replication of viral RNA (Momose *et al.*, 2002). In *E.coli*, *in vivo* experiments illustrated how the presence of DnaJ and other chaperones, DnaK (Hsp70) and GrpE are required for the initiation of bacteriophage lambda DNA replication (Alfano and McMacken, 1989; Zylicz *et al.*, 1989; Hoffmann *et al.*, 1992). Earlier studies showed that these chaperones are crucial for DNA replication as mutated forms of the three listed chaperones resulted in no DNA replication initiation when introduced to a crude *in vivo* system containing the lambda DNA replication system (Zylicz and Georgopoulos, 1984; Zylicz *et al.*, 1985; 1987).

In both Influenza A and B viruses, Hsp40 has been shown to interact with the M2 protein (Guan *et al.*, 2010). The M2 protein functions as an ion channel and is important for virus uncoating and essential for virus replication. Hsp40 has been illustrated to be a regulator of the PKR, a crucial component of the host cell in the defence against viral infections. Hsp40 regulates the PKR pathway by interacting with the cellular inhibitor of PKR, p58<sup>IPK</sup> (Melville *et al.*, 1997). It is proposed that the M2 protein forms a stable complex with both Hsp40 and p58<sup>IPK</sup> which enhances the autophosphorylation of PKR which in turn induces cell death (Guan *et al.*, 2010). The resulting apoptosis has been shown to be beneficial for influenza virus replication (Oslen *et al.*, 1996; Wurzer *et al.*, 2003).

The Hepatitis C virus (HCV) RNA-dependent RNA polymerase has been shown to interact with cyclophilin A (a chaperone with isomerase activity) in order to facilitate its maturation by exploiting its chaperone and isomerase activities (Chatterji *et al.*, 2009). Within the same virus, Hsp90 was identified as a crucial factor in the maturation of the protease protein, NS2/3, a vital protein for viral replication (Waxman *et al.*, 2001). In papillomaviruses, Hsp40 and Hsp70 improve the binding of the viral protein E1, a replication initiator helicase to the origin of replication on viral DNA, unwittingly enhancing viral replication (Liu *et al.*, 1998).

Hsp90 has also been found to play a role in the assembly and function of the Flock house virus (FHV) RNA replication complex (Kampmueller and Miller, 2005; Castorena *et al.*, 2007). One of the normal functions of Hsp90 in a cell is to transport mitochondrial proteins to the outer

mitochondrial membrane import receptors. Using the same pathway, Hsp90 is able to facilitate FHV RNA replication complex assembly and function by transporting the RNA replication complex to the mitochondria membranes where it is assembled (Castorena *et al.*, 2007). Weeks and co-workers, illustrated how the yeast homologue Ydj1 facilitates viral replication, while Hsp70 was shown to be a crucial regulator of FHV polymerase synthesis (Weeks *et al.*, 2008; 2010).

Human immunodeficiency virus-1 (HIV-1) has also adapted its replication strategy to utilise chaperones. The Nef protein is one of the most important viral proteins necessary for viral pathogenesis and disease progression. The protein has also been implicated in viral replication and gene expression. Through *in vivo* and *in vitro* experiments, it was found that the Nef protein induced the expression of Hsp40 in HIV-1-infected cells. The interaction is important because it increases Hsp40 translocation into the nucleus of infected cells which, in turn, facilitates viral gene expression by becoming part of the cyclin-dependent kinase 9-associated transcription complex, regulating long terminal repeat-mediated gene expression (Kumar and Mitra, 2005). In HIV-2, Hsp40 interacts with Vpx, a protein required for nuclear translocation of the viral pre-integration complex (PIC) in dormant cells. Over-expression of Hsp40 was found to enhance the nuclear import functions of Vpx (Cheng *et al.*, 2008).

The positive strand RNA virus, Brome mosaic virus, a member of the alphavirus-like superfamily which replicates in yeast and plant cells also depends on Ydj1 for the accumulation of negative strand RNA synthesis. A mutation in Ydj1 resulted in the absence of viral RNA, leading to the conclusion that Ydj1 is involved in forming replication complexes needed for RNA synthesis (Tomita *et al.*, 2003).

Recent research has shown that Hsp40 is required in the Measles virus life cycle for its role as a co-chaperone to Hsp70. Couturier *et al.*, (2009) have illustrated how Hsp40's ATP hydrolysis activity is required in the binding of Hsp70 to the measles virus' nucleoprotein in order to stimulate viral transcription and genome replication. Other examples of Hsp40 functioning in conjunction with other cell components to facilitate viral replication are illustrated by Nanda *et al.*, 2004, where mitochondrial Hsp40 along with Hsp70 and Hsp60 have been shown to bind to

the 3' untranslated region of Murine hepatitis virus (MHV) genome prior to viral RNA import into the mitochondria.

#### **d) Chaperone-mediated viral assembly**

The chaperone-viral protein interaction is not only observed in viral replication but also in virion assembly, although this interaction has not been studied in-depth. An example of a chaperone assisting in virion assembly is seen in the case of Hsc70 and HIV-1, where Hsc70 is found enclosed within the HIV-1 virions suggesting an interaction between the chaperone and virus during the assembly process (Brenner and Wainberg, 1999). The ER chaperone calnexin is involved in the formation of the HCV envelope, the chaperone assists in the assembly of the two glycoproteins, E1 and E2 (Dubuisson and Rice, 1996; Choukhi *et al.*, 1998; Dubuisson, 1998). In Polyomavirus, it has been shown that Hsc70 binds to the VP1 capsid protein, regulating quality and the location of virus assembly (Chromy *et al.*, 2003). Another example of chaperone-mediated viral assembly is the indirect involvement of GRP78/BiP, calnexin and calreticulin in the assembly process of Rotavirus viral particles (Maruri-Avidal *et al.*, 2008). Also, the regulation of GRP78/BiP levels during Human cytomegalovirus infection enhances virion assembly in the cytoplasm (Buchkovich *et al.*, 2008). In picornaviruses, it was found that Hsp70 and Hsp90 play a role in the assembly process (Macejak and Sarnow, 1992; Geller *et al.*, 2007). The association of Hsp70 and Hsp90 in picornavirus assembly will be discussed in-depth in an upcoming section.

#### **e) Chaperone-like viral proteins**

The requirement for chaperones in viral replication is so crucial that some viruses have resorted to mimicking the functional domains of the chaperones. Simian virus 40 (SV40) has been intensively studied and has become a model to decipher the origin of cancer due to its uncanny ability to control different phases of the cell cycle (Hahn *et al.*, 2002). This ability has been attributed to the large tumour antigen TAg, which has been shown to be essential for efficient virus replication. The interesting feature of this protein is found on the N-terminal region, which has functions similar to that of the J domain of Hsp40. The J domain enables TAg to interact with endogenous Hsp70 as its natural co-chaperone and this interaction enables the virus to

complete its viral cycle without utilising host Hsp40 (Campbell *et al.*, 1997; Genevoux *et al.*, 2003).

The virally-encoded capsid-associated protein 80 is known to assist in the proper folding of the major capsid protein p73 of African swine fever virus (Cobbold *et al.*, 2001). The R1 subunit of Herpes simplex virus (HSV) ribonucleotide reductase has been shown to have chaperone-like activities similar to those of Hsp27 that assist in the protection of the cells from apoptosis during infection (Chabaud *et al.*, 2003). Also, the non-structural Rotavirus NSP4 glycoprotein regulates the folding of the structural protein VP4 and facilitates protein transportation through the ER membrane during virion assembly similar to ER chaperones (Suzuki, 1996).

#### ***d) Negative effects of chaperone-virus interactions***

Not all virus-chaperone interactions are beneficial or facilitate viral replication. Some of these interactions are detrimental to the survival of the virus. Unlike the other virus examples listed above, the presence of Hsp40s seem to have a suppressive function on the replication ability of HBV. The chaperones are able to suppress HBV replication by accelerating the degradation of the viral core and HBx proteins. Inhibition of the Hsp40s resulted in an increase of HBV replication, showing that the presence of Hsp40s is responsible for the virus's inability to replicate (Sohn *et al.*, 2006a; 2006b). Some of the viral-chaperone interactions discussed above are summarised in Table 1.4.

Table 1.4: Summary of selected virus-chaperone interactions.

<b>Virus</b>	<b>Chaperone</b>	<b>Function</b>	<b>Reference</b>
<b>Hepatitis B virus</b>	Hsp40	Suppresses viral replication	Prange, <i>et al.</i> , 1999; Beck and Nassal, 2001; 2003; Cho <i>et al.</i> , 2003; Hu <i>et al.</i> , 2004; Sohn <i>et al.</i> , 2006a; 2006b
	Hsp70	Viral morphogenesis and replication	
	Hsp90	Binds viral polymerase	
<b>HIV-1/2</b>	Hsp40	Facilitates viral gene expression, enhances the Vpx nuclear import functions	Brenner and Wainberg, 1999; Kumar and Mitra, 2005; Cheng <i>et al.</i> , 2008
	Hsp70	Associated with viral transcription	
<b>Herpes simplex virus-1</b>	Hsp90	Helps localise viral polymerase to the nucleus	Burch and Weller, 2005
<b>Bacterial phage lambda</b>	Hsp40 (DnaJ) Hsp70 (DnaK) GrpE	Initiates bacteriophage lambda DNA replication	Alfano and McMacken, 1989; Zylicz <i>et al.</i> , 1989; Hoffmann <i>et al.</i> , 1992
<b>Adenovirus</b>	Hsc70	Viral replication, import of viral DNA into nucleus	Saphire <i>et al.</i> , 2000
<b>Influenza A virus</b>	Hsp90	Stimulates RNA polymerase	Momose <i>et al.</i> , 2002
<b>Measles virus</b>	Hsp70/ Hsp40	Stimulates viral transcription and replication	Couturier <i>et al.</i> , 2009
<b>Hepadnavirus</b>	Hsp70/ Hsp90	Activates reverse transcriptase	Stahl <i>et al.</i> , 2007
<b>Flock house virus</b>	Hsp90	Assemble viral replication complexes	Kampmueller and Miller, 2005; Castorena <i>et al.</i> , 2007
<b>Ebola virus</b>	Hsp90	Involved in viral replication	Smith <i>et al.</i> , 2010
<b>Porcine circovirus type 1-2</b>	Hsp40	Interacts with capsid proteins	Finsterbusch <i>et al.</i> , 2009

## **1.6 Picornaviruses and Chaperones**

As described above for other virus families, picornaviruses are also known to utilise molecular chaperones during their life cycle. Recent studies have shown that chaperones are also involved in the assembly process of enteroviruses, PV, HRV and CV (Geller *et al.*, 2007). The two chaperones implicated are Hsp90 and Hsp70. Both of these chaperones have been shown to only interact with picornavirus structural proteins and have no association with any of the non-structural proteins. The studies conducted on Hsp70 and Hsp90 show that interaction occurs with the capsid precursor protein, P1. Immunoprecipitation experiments showed that P1 was the only viral protein to co-precipitate with the two chaperones (Geller *et al.*, 2007; Macejak and Sarnow, 1992). The interaction between Hsp70 and P1 was shown to be highly stable as high salt and high detergent concentrations did not disrupt the association between the two proteins (Macejak and Sarnow, 1992). When inhibition studies on Hsp90 using GA were conducted, it was observed that when Hsp90 ATPase activity was inhibited, P1 could not fold into the proper conformation necessary for the final cleavage step and this resulted in no viral capsid formation and no new viral particles produced. The study also revealed that chaperone-mediated P1 protein folding was governed by strict evolutionary constraints since the virus could not adapt to the inhibition of Hsp90 and form an alternative folding strategy as seen by the absence of mutant viruses that could replicate in the presence of GA (Geller *et al.*, 2007).

## **1.7 Project Motivation**

The involvement of host cell factors such as molecular chaperones in facilitating the replication cycles of numerous viruses has been extensively researched. Molecular chaperones have been shown to be involved in viral entry, replication, protein activation, assembly and exit and picornaviruses are no exception.

In light of the information given above that highlights the importance of chaperones in enteroviruses, this study intends to further investigate the role of chaperones in picornaviruses. In picornaviruses, studies have been conducted to examine the involvement of Hsp70 and 90, but not Hsp40, a chaperone that is known to work in conjunction with Hsp70 and is part of the

Hsp90 pathway. Secondly, no studies have been conducted to investigate the role of chaperones in the replication of TMEV and cardioviruses, in general. With the discovery of new human cardioviruses, using TMEV as a study model will aid in elucidating the host-virus interactions of these viruses. By understanding these specific interactions, antivirals that target them may be developed.

## ***1.8 Hypothesis***

Hsp40, Hsp70 and Hsp90 are host factors involved in the replication and assembly of TMEV.

## ***1.9 Aims and Objectives***

### **Overall Aim**

The main aim of this research was to investigate the role of Hsp40, Hsp70 and Hsp90 in the life cycle of TMEV by determining the effects of Hsp90 inhibitors on replication and examining localisation of Hsp90, Hsp70 and Hsp40 in TMEV-infected and mock-infected Baby BHK-21 cells.

### **Objectives**

- Conduct *in silico* analysis, to identify sequence or structural similarities between picornavirus P1 polyproteins and examine protein domains of Hsp90 cellular and viral client proteins using protein domain architecture.
- Determine the effects of Hsp90 inhibitors, Nov and GA on the development of CPE in TMEV-infected BHK-21 cells and detect viral proteins in drug-treated and untreated cells using anti-TMEV 2C antibodies.
- Examine the localisation of Hsp40, Hsp70 and Hsp90 in TMEV-infected and mock-infected BHK-21 cells by indirect immunofluorescence (IF) and confocal microscopy.

## **Chapter 2: *In Silico* Analysis of Picornavirus Capsid Proteins and Hsp90 Client Proteins**

### **2.1 Introduction**

This chapter involves a bioinformatic analysis of the picornavirus capsid precursor protein P1, focusing on the VP1 capsid subunit to identify sequence and structural conservations present within the capsid protein. Protein domain features of Hsp90 cellular and viral client proteins were also examined. Due to the small size of the viral genetic material, the protein coding capacity of viruses is greatly limited. In order to complete their replication cycles, viruses have evolved the ability to utilise host machinery including Hsps. Recently, Hsps have become the focus of intensive research in virology because numerous viruses have been shown to utilise them during different stages of the viral replication cycle (reviewed by Sullivan and Pipas, 2001; Xiao, 2010) and picornaviruses are no exception. Studies have shown that an interaction between Hsp90 and Hsp70 with the enterovirus capsid precursor polyprotein, P1 is essential during the assembly process, in assisting folding and maturation of capsid proteins (Macejak and Sarnow, 1992; Geller *et al.*, 2007). While numerous studies have been conducted to better understand the virus-chaperone connection in viruses such as HIV (Brenner and Wainberg, 1999; Kumar and Mitra, 2005; Cheng *et al.*, 2008), HBV (Hu and Anselmo, 2000; Sohn *et al.*, 2006a; 2006b) and Influenza viruses (Momose *et al.*, 2002; Guan *et al.*, 2010), only two studies have focused on the interaction between picornavirus proteins and chaperones (Hsp90 and Hsp70) (Macejak and Sarnow, 1992; Geller *et al.*, 2007).

Hsp90, one of the most studied chaperones, was chosen for analysis because studies have indicated that Hsp90 interacts with a diverse group of specialised cellular proteins such as transcriptional factors, kinases and several co-chaperones (reviewed by Young *et al.*, 2004; Picard, 2002; Pratt and Toft, 2003). Along with its chaperoning role, Hsp90 is also involved in different functions and processes such as translocation, buffering cell mutations, cell survival promotion and regulation of apoptosis (reviewed by Ellis, 1987; Frydman, 2001) within the cells. The ability of Hsp90 to interact with a diverse group of proteins has made the chaperone a target of exploitation by viruses to facilitate their life cycles by hijacking numerous pathways and exploiting cellular processes mediated by Hsp90.

The aim of this chapter was to discover identical or similar amino acid residues or protein structures within picornavirus capsid proteins, focusing mainly on the VP1 capsid subunit. In addition, examine protein domains of cellular and viral proteins to highlight the diversity of the Hsp90 client proteins. The specific objectives were:

- To discover identical or similar amino regions within the sequence of several picornavirus VP1 proteins by conducting multiple sequence alignment analysis.
- To construct a three dimensional structure of TMEV GDVII VP1 protein and determine structural similarities between VP1 proteins of various picornaviruses.
- To compare protein domains of cellular and viral clients of Hsp90 through protein domain architecture using SMART.

## **2.2 Methods and Materials**

### **2.2.1 Multiple sequence alignment**

Alignment was performed with the ClustalW algorithm (Thompson *et al.*, 1994) under the BioEdit Sequence Alignment Editor Software, version 7.0.4.1 (Hall, 1999) with BLOSUM62 scoring matrix and default parameters. The accession numbers of the VP1 protein sequences used in the multiple sequence alignments were: cardiocorviruses (TMEV GDVII (AAA62147); SAFV 1 (YP\_001210296; ECMV (NP\_056777)), enterocorviruses (PV 1 (NP\_041277); HRV 14 (NP\_041009), CV B3 (ACY40750)) and aphthocorviruses (FMDV Type O (NP\_658990)).

### **2.2.2 Modelling of the VP1 Subunit of the TMEV GDVII P1 protein**

The TMEV GDVII VP1 sequence (Accession No. AAA62147) was submitted to the Internet-based modelling server HHPred to identify templates, search results were restricted to templates with resolved structures. A model for TMEV GDVII VP1 was generated by the MODELLER (Sali *et al.*, 1995) software using TMEV DA VP1 (PDB ID: 1TME) as a template. Generated TMEV GDVII VP1 model was compared to resolved three dimensional structures of several picornaviruses available in the Protein Data Bank (PDB). Three dimensional structures used: CV (PDB entry 1Z7S), HRV (PDB entry 1AYM), PV (PDB entry 1POV). Model was rendered using the open-source software PyMol v0.98 (2005 DeLano Scientific LLC).

### **2.2.3 Protein domain architecture**

Protein domain architecture was carried out using the Internet based Simple Molecular Architecture Research Tool [SMART] (<http://smart.embl-heidelberg.de>, Schultz *et al.*, 1998; Letunic *et al.*, 2008) under default parameters, SMART mode: normal, search databases: outlier homologues, PFam domains, signal peptides, internal repeats and intrinsic protein disorders. The accession numbers of protein sequences used were: TMEV GDVII P1 (AAA62147); Insulin receptor (AAA59452); Estrogen receptor (NP\_0319821); Glucocorticoid receptor (NP\_00166458); Her2 (AAU019101); Stat3 (BAH47273); p23 (AAA18537); Influenza A virus RNA polymerase (AAP04505).

## **2.3 Results**

### **2.3.1 Identification of conserved amino acid residues in the capsid protein of picornaviruses**

Multiple sequence alignment of VP1 amino acid sequences from three cardioviruses (TMEV, ECMV, SAFV), three enteroviruses (PV, HRV, CV) and one aphthovirus (FMDV) was conducted to identify within the VP1 sequences, regions that were highly conserved in identity or similarity which may suggest that they have similar functional significance within the family. Results are presented in Figure 2.1.

The size of the sequences alignment ranged from 211 amino acids (FMDV) to 302 amino acids (PV). The figure also illustrated several residue deletions, with the major deletions occurring within the VP1 protein sequence of FMDV. The alignment analysis revealed that the number of amino acid residues conserved or similar within query sequences was extremely low, as indicated by the number of amino acids highlighted red and blue, representing identical and similar residues, respectively. Overall, 29 out of 302 (10%) amino acids were found to be identical and 35 out of 302 (12%) amino acids share similar physical properties.

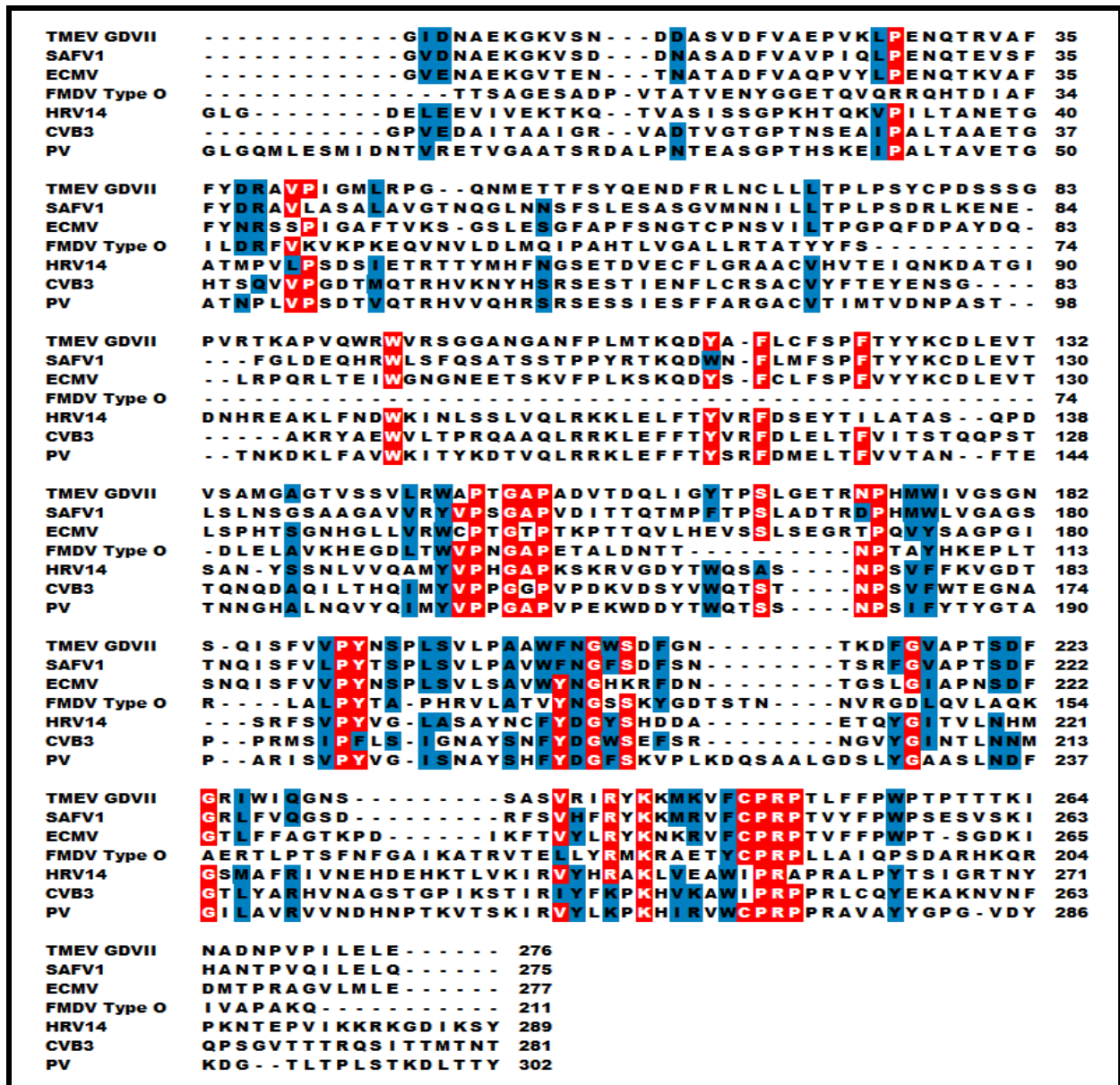


Figure 2.1: Multiple sequence alignment of picornavirus VP1 protein sequences using ClustalW. A multiple sequence alignment was conducted on sequences of the VP1 subunit of the capsid precursor protein, P1 from the following picornaviruses: TMEV GDVII (AAA62147); FMDV Type O (NP\_658990); SAFV 1 (YP\_001210296); PV 1(NP\_041277); ECMV (NP\_056777); HRV 14 (NP\_041009); CV B3 (ACY40750). Identical amino acids are highlighted in red and amino acids with similar chemical properties are highlighted in blue (software used under default parameters and BLOSUM62 scoring matrix).

### **2.3.2 Three dimensional structural modelling and comparison analysis of picornavirus VP1 proteins**

The following analysis involved the use of MODELLER to construct a TMEV GDVII VP1 three dimensional model using TMEV DA (ITME) as a template. To determine structural conservation or similarity between picornavirus capsid proteins, the predicted structural model of TMEV GDVII was compared to resolved VP1 structures of PV, CV and HRV. Results are presented in Figure 2.2.

Structural analysis of the selected picornavirus VP1 protein (compare panels i-iv of Figure 2.2), all had alpha-helices (coloured red), but the positions and number differed for each proteins. The most striking difference between the models is the length and conformation of the loops (coloured green) connecting the secondary structures. Interestingly, an eight-stranded anti-parallel beta-barrel structure (coloured yellow) was present in all analysed VP1 proteins.

It is important to note that the TMEV GDVII VP1 structure was previously resolved by Luo *et al.*, 1996.

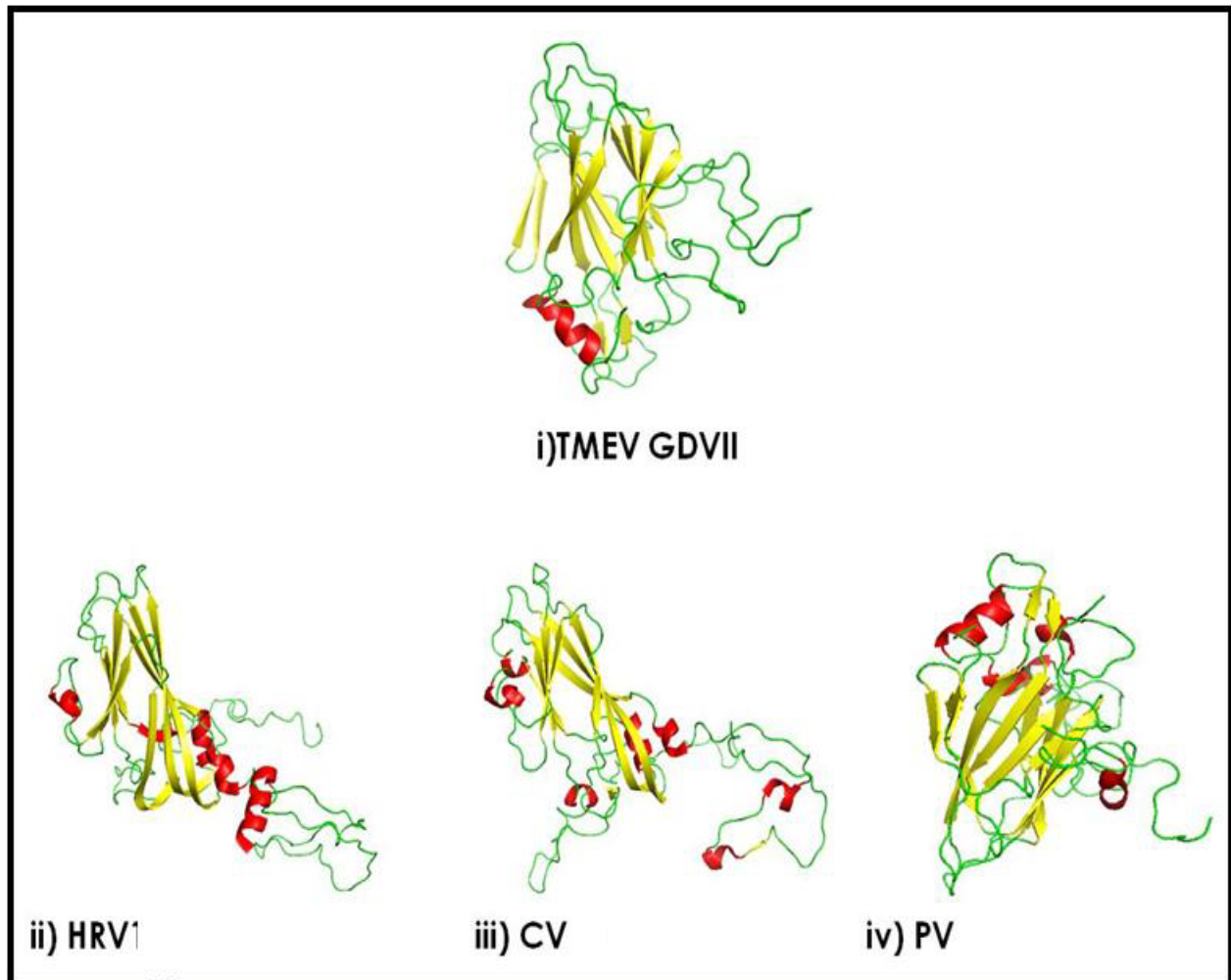


**Figure 2.2: Structural model of TMEV GDVII and resolved structures of various picornavirus VP1 proteins.** Cartoon representation of various picornaviruses VP1 capsid proteins; (i) MODELLER predicted structure of TMEV GDVII; resolved structures of (ii) HRV (1NCQ), (iii) CV (1Z7S), (iv) PV (1POV). Beta-sheets, alpha-helices and loops are coloured yellow, red and green, respectively. Model was rendered using PyMol v0.98 software.

### 2.3.3. Protein domain comparison of cellular and viral Hsp90 client proteins

To illustrate the diversity of Hsp90 client proteins, protein domain architecture was conducted on several well studied Hsp90 cellular and viral client proteins, with the exception of TMEV P1. Results are presented in Figure 2.3.

The SMART program was used as an alternative evaluation tool to multiple sequence alignment which is commonly used in comparison analysis. The Pfam database was used to analyse the domain organisation of the proteins because it is large and widely used as it contains a vast

amount of protein domains and families. The six cellular client proteins chosen for comparison are part of the co-chaperone family (p23), transcription factors (STAT3, glucocorticoid receptors, estrogen receptor) and kinases (HER2 and insulin receptor). Extensive studies have been conducted to characterise the interaction of Hsp90 and the listed proteins, STAT3 (Sato *et al.*, 2003), p23 (Sullivan *et al.*, 2002), estrogen receptor (Bouhouche-Chatelier *et al.*, 2001), glucocorticoid receptor (Bohen, 1995), insulin receptor (Takata *et al.*, 1997) and HER2 (Citri *et al.*, 2004). The Influenza A virus polymerase was chosen for analysis as the viral client protein (Momose *et al.*, 2002). The features of selected client proteins were compared to those of the TMEV P1, since it was the protein of interest.

The black lines and the multiple coloured shapes in Figure 2.3 represent the protein sequence and the different protein domains, respectively. The figure illustrated that the proteins differ in complexity as seen by the variation of protein domains within each protein. The insulin receptor consists of six different domains, four in STAT3 and the estrogen receptor, three domains in the glucocorticoid receptor and only one in the Her2, p23 and the Influenza A virus polymerase sequences. Although, three protein domains were identified in TMEV P, they were all classified as capsid domains. In addition, common and unique protein domains were also identified within the proteins. Some common domains present in more than one protein were; the ligand binding domain, the tyrosine kinase catalytic domain, and the zinc finger domain. Majority of the domains were unique to one protein such as the furin-like repeats, STAT interaction domain, fibronectin type 3 domain, picornavirus capsid domain, DNA binding domain, all alpha helical domain and polymerase domain. The main observation was that, no common protein domain was identified within the proteins.

It is important to note that the protein domains identified amongst the proteins do not represent all the domains that may be present but limited to those found within the PFam database.

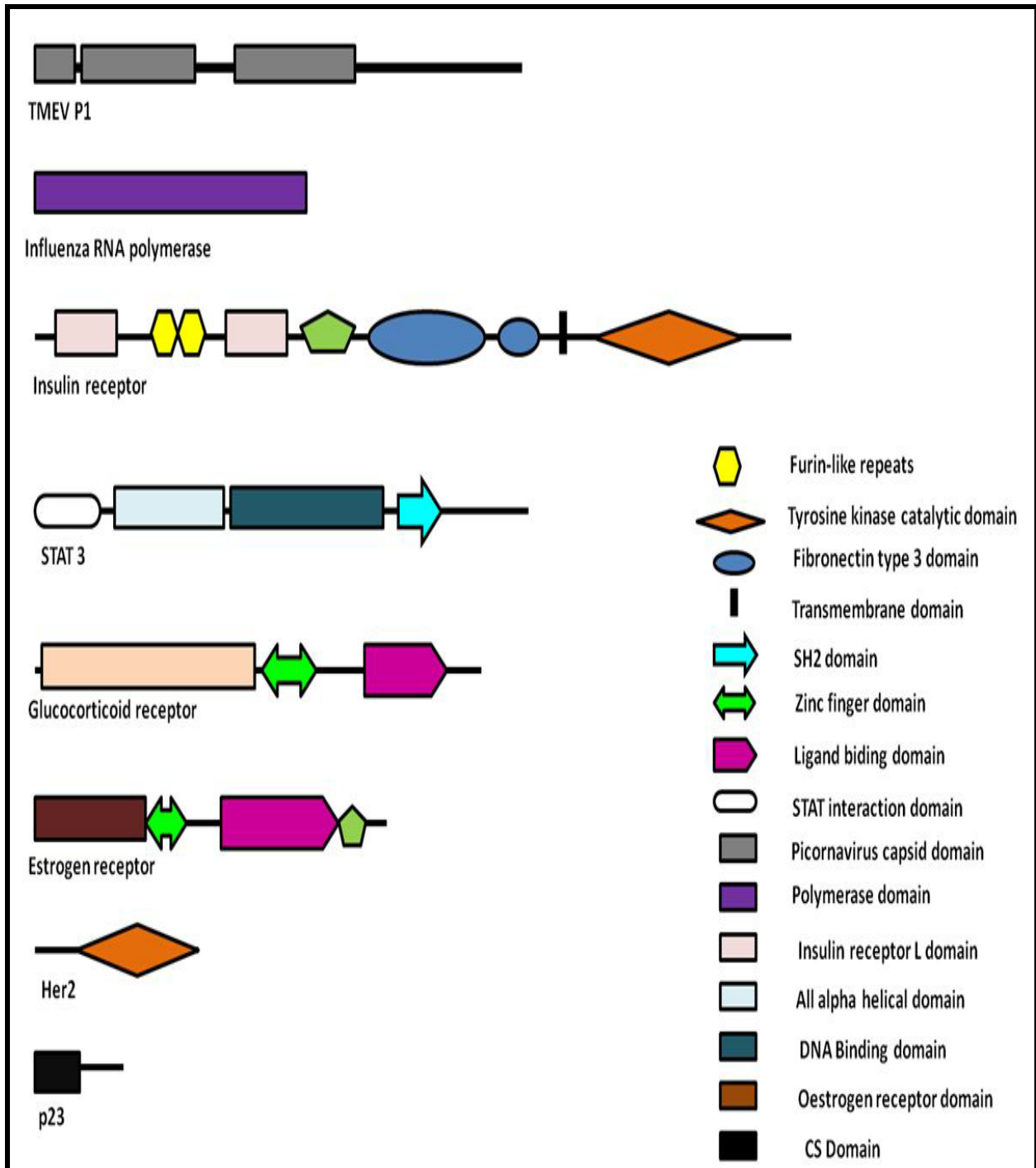


**Figure 2.3: Schematic representation of the protein domains of cellular and viral Hsp90 client proteins.** Protein domain architecture generated by submitting the amino acid sequence of each protein to SMART program. Program used under default parameters.

## **2.4 Discussion**

Multiple sequence alignment analysis of various picornavirus VP1 protein sequences was conducted in an attempt to identify a region or regions within the query sequences that might show a high degree of conservation or similarity. The VP1 protein in picornaviruses forms the virus capsid along with three other proteins, VP2, VP3 and VP4, where 60 copies of each subunit are required for the formation of the icosahedral capsid (Racaniello, 2001). Although studies have shown VP1 to be the most variable capsid protein in terms of length, sequence and charge which makes the alignment of the sequences complicated (Palmenberg, 1989), it was selected for further analysis. The variability makes VP1 the best suited capsid protein for prediction studies under the assumption that any series of amino acid residues or regions found conserved throughout the family may suggest that they have a vital role in the function of the protein. Figure 2.1 showed that the VP1 protein sequences were highly divergent within picornaviruses. VP1 sequences play an important role in the determination of virus tropism and antibody neutralisation (Oberste *et al.*, 1999; reviewed by Racaniello, 2001), which might contribute to the sequence divergence. Insertions and deletions within VP1 protein sequences also contributed to the low sequence identity and similarity. According to the literature, FMDV lacks surface canyons or “pits”, which are known to be receptor binding sites within cardio- and enteroviruses (Luo *et al.*, 1987; Muckelbauer *et al.*, 1995; Kolatkar *et al.*, 1999), suggesting the lack of these surface structures might be linked to the deleted residues. Another possible explanation for the observed sequence divergence could be due to the presence of the CD loops (I and II) only found in cardioviruses, which play a vital role in virus pathogenicity and persistence (Wada *et al.*, 1994; McCright *et al.*, 1999). Interestingly, although the loops are only present within cardioviruses VP1 sequences, the loop regions vary greatly within the genus (Zoll *et al.*, 2009).

Since the multiple sequence alignment analysis illustrated the divergence of the capsid protein sequences, the structural model of TMEV GDVII and resolved structures of several picornavirus VP1 proteins were analysed. Analysis was conducted in an attempt to identify structural similarities between the analysed picornavirus (TMEV, PV, HRV, and CV) capsid proteins. Although a resolved structure for TMEV GDVII VP1 protein exists (Luo *et al.*, 1996), a modelled structure was used in this study. All VP1 proteins had a similar conserved core, a wedge shaped eight-stranded anti-parallel beta-barrel structure (also called a beta-barrel jelly roll

or a Swiss-roll beta-barrel). The wedge shape of the structure is thought to facilitate the packaging of structural subunits to form a dense and ridged protein shell, allowing the virus particles to be acid-stable and to retain infectivity at various pHs (reviewed by Racaniello, 2001). Interestingly, the conserved eight-stranded anti-parallel beta-barrel also makes up the core of both VP2 and VP3 capsid proteins. Due to the size of VP4 (17 to 34 amino acids) compared to VP1 (209-302 amino acids), VP2 (218-267 amino acids) and VP3 (219-246 amino acids) (Palmenberg, 1989), it is the only capsid protein that does not possess the eight-stranded anti-parallel beta-barrel structure. Overall, the structure of VP1 capsid proteins is highly conserved within the family and may be linked to the assembly process being highly conserved within the family. The conservation of the capsid protein structure, which is thought to be linked to the assembly process, suggests that the involvement of Hsp90 in facilitating the proper folding and maturation of the capsid proteins as seen in enteroviruses, (Geller *et al.*, 2007) may also be required in TMEV and other picornaviruses.

Protein domain architecture was conducted on several cellular and viral proteins known to be Hsp90 clients, with the exception of TMEV P1. Through protein domain comparison, several differences were observed that highlighted the diversity of Hsp90 client proteins. The complexity of each protein contributed to the differences observed. The first difference observed was the absence of a pattern in the number of protein domains present within each client; seven domains were identified in the insulin receptor, four in STAT3 and the estrogen receptor and only one in p23, HER2 and the Influenza A virus polymerase. Secondly, the insulin receptor had repeats of identical domains, the furin-like repeats domain and fibronectin type 3 domain. Interestingly, this feature was only observed in one other protein, TMEV P1, a protein not known to interact with Hsp90. Thirdly, the majority protein domains were unique to one protein as seen in the case of the polymerase domain, STAT interacting domain and CS domain which belong to the Influenza A virus polymerase, STAT3 and p23, respectively. The unique domains might be linked to the specific function of each protein within the cell or virus. Some protein domains were present within more than one protein and this might be because the proteins having function equivalence within the cell as seen in the cases of HER2 and the insulin receptor and the glucocorticoid and estrogen receptors which are known to be part of the kinases and transcription factors, respectively. Interestingly, although all analysed proteins are known Hsp90 client proteins with the exception of TMEV P1, no common protein domain that could be functionally connected to

Hsp90 was identified. As mentioned, the protein domains identified during this study were those only present within the PFam database, meaning that if the domain linked to Hsp90 is not part of the PFam database, therefore it could not be identified. Also, even though the client proteins chosen for analyses represented different classes of Hsp90 client proteins, the number of proteins analysed might not have been significant to recognise any possible subtle sequence motifs/patterns that might be common between Hsp90 client proteins. Alternatively, this observation suggests that Hsp90 most likely recognises surface features rather than a sequence motif/pattern. Several studies have suggested that surface features such as exposed hydrophobic residues in partially denatured regions might be responsible for the formation of stable complexes between Hsp90 and its client proteins, such as p53 (Müller *et al.*, 2004), a well characterised Hsp90 client. Identifying a similar or identical hydrophobic feature on the surface of all known Hsp90 client protein and then on the TMEV P1 protein, would suggest that TMEV P1 might also interact with Hsp90.

## **2.5 Conclusion**

By using multiple sequence alignment analysis and structural comparison analysis, the identification of a conserved structure in the VP1 capsid protein of picornaviruses was successful. The following conclusions were reached with regards to the VP1 protein:

- The amino acid sequences of the VP1 proteins are highly divergent within the *Picornaviridae* as highlighted by the presence of few identical and similar amino acid residues. The divergence in the sequences might be linked to the function of VP1 in determining virus tropism and antibody neutralisation.
- All analysed VP1 proteins had a similar conserved core structure, a wedged-shaped eight-stranded anti-parallel beta-barrel structure. This structure is thought to be involved in the packaging of structural subunits to form the picornavirus protein capsid and possibly linked to the conversation of the assembly process between picornaviruses.

Differences in the features of selected Hsp90 client proteins were successfully identified using protein domain architecture analysis. From the analysis it was concluded that:

- The analysed client proteins differed in their complexity as seen by the existence of varying numbers of domains and repeats of identical domains and the presence of unique domains within any particular protein, which might be linked to the different functions of each protein.
- No common protein domains or domain that could be functionally connected to Hsp90 were identified. Suggesting that Hsp90 most likely recognises a surface feature rather than a sequence pattern/motif.

The next chapter describes the effects of Hsp90 inhibitors, GA and Nov on TMEV growth.

## **Chapter 3: Effects of Hsp90 Inhibitors, Geldanamycin and Novobiocin on TMEV Growth in BHK-21 Cells**

### ***3.1: Introduction***

This chapter describes the effects of Hsp90 inhibitors, Nov and GA, on the growth of TMEV in BHK-21 cells. Protein domain architecture analysis of Hsp90 client proteins (previously conducted in chapter 2), illustrated the ability of Hsp90 to interact with a diverse group of proteins including viral proteins. In recent years, evidence from several studies has shown that viruses have evolved to require host factors including Hsp90 during different stages of their life cycles such as viral entry, genome replication, activation and expression and viral assembly (discussed in section 1.5 of chapter 1). The requirement of Hsp90 during the life cycles of numerous viruses despite the type of genetic material (RNA or DNA), genome strandedness (double or single), genome sense (positive, negative or ambisense) and host range (animal, human, plant and bacteria) is widely documented (reviewed by Sullivan and Pipas, 2001; Xiao, 2010).

Further importance of Hsp90-viral interactions has been illustrated by the consequences of inhibiting Hsp90 on various stages of the virus replication. The inhibition of Hsp90 in virus-infected cells seemed to reduce or inhibit viral replication. For example, in FHV, the inhibition of Hsp90 activity using GA suppressed the production of infectious virions and prevented the accumulation of viral RNA (Kampmueller and Miller, 2005). In enteroviruses, the production of new virions or the development of drug-resistant viruses was prevented in infected cells treated with GA (Geller *et al.*, 2007). Inhibition of Hsp90 using numerous inhibitors such as GA, its analogue 17-allylamino-17-demethoxygeldanamycin (17AGG) and radicicol were shown to significantly reduce and/or inhibit replication of the Ebola virus (Smith *et al.*, 2010). In Vesicular stomatitis virus (VSV), the inhibition of Hsp90 using GA and radicicol was able to reduce viral replication irrespective of the virus load used for infection (Connor *et al.*, 2007). The listed examples illustrate the possibility of using non-toxic Hsp90 inhibitors as universal antivirals, since many viruses require the chaperone to facilitate one or more aspect of their replication.

Currently there are several well-known and characterised Hsp90 inhibitors such as GA, 17AGG, Nov and radicicol. For this study, Nov and GA were selected for analysis. Nov is a coumarin antibiotic isolated from several strains of *Streptomyces* (reviewed by Donnelly and Blagg, 2008). As an antibiotic, Nov was found to exhibit potent activity against Gram-positive bacteria. Along with other coumarin antibiotics, Nov binds to type II topoisomerases including DNA gyrase, the binding inhibits ATP hydrolysis that is catalysed by the enzymes, resulting in the inhibition of DNA synthesis (Reece and Maxwell, 1991; Ali *et al.*, 1993; Lewis *et al.*, 1996; Laurin *et al.*, 1999). Recently Nov has been shown to bind weakly to the newly discovered C-terminal nucleotide binding site of Hsp90 (Marcu *et al.*, 2000a). The binding of Nov to the ATP binding site results in the disruption of Hsp90 late multi-chaperone complexes, resulting in the release and degradation of Hsp90 client proteins (Marcu *et al.*, 2000b; Yun *et al.*, 2004).

The other drug of interest, GA, is a naturally occurring antitumor antibiotic (DeBoer *et al.*, 1970). Initially, GA was thought to be a nonspecific kinase inhibitor until it was discovered that it specifically binds to Hsp90 and its ER homologue, GRP94 (Whitesell *et al.*, 1994; Chavany *et al.*, 1996). The antitumor activity of GA is suggested to be a result of the drug's ability to deplete the cell of essential growth-regulatory signalling proteins known to interact with Hsp90 such as the progesterone receptor (Smith *et al.*, 1995), erB-2 (Miller *et al.*, 1994; Chavany *et al.*, 1996) and the glucocorticoid receptor (Whitesell and Cook, 1996). GA inhibits Hsp90 by binding to the nucleotide-binding site located on the N-terminal region of the chaperone. When GA binds to the ATP site, it prevents a conformational change in Hsp90 that is essential for the binding of p23, a co-chaperone that is part of the multi-chaperone complex of the Hsp90 pathway (Sullivan *et al.*, 1997). The inability of Hsp90 to bind to p23 results in the accumulation of intermediate complexes, retardation of ATP-driven substrate maturation and folding and ultimately the degradation of substrates (Grenert *et al.*, 1997; Stebbins *et al.*, 1997).

Although there is substantial evidence of viruses requiring chaperones during their life cycles, at present there are only two studies that have been conducted to examine the interaction of chaperones with picornaviruses (Macejak and Sarnow, 1992; Geller *et al.*, 2007). Only one of these studies observed the effects of inhibiting Hsp90 using GA, and found that the drug had an inhibitory effect on virus assembly (Geller *et al.*, 2007). To the best of our knowledge, no studies

have been conducted to examine any interactions between Hsp90 and the virus of interest, TMEV, or determine the effects of inhibiting Hsp90 on virus growth.

Based on the above information that illustrates the importance of Hsp90 in the replication of various viruses including picornaviruses, the overall aim of this chapter was to determine if the inhibition of Hsp90 in TMEV-infected BHK-21 cells would have the same effects on virus growth as observed for other viruses. The specific objectives of this chapter were:

- To prepare a TME virus stock and determine the virus titre by plaque assay.
- To examine the effects of Nov and GA on the development of CPE in TMEV-infected BHK-21 cells over a 48hr time period.
- To detect virally-expressed non-structural TMEV 2C protein in Nov- and GA-treated BHK-21 cells 48hrs post-treatment.

## **3.2 Methods and Materials**

### **3.2.1 Mammalian cell lines and culture conditions**

BHK-21 cells (Kind donation from Professor Martin Ryan, St Andrews University, UK) were used in this study. Cells were maintained in HEPES-buffered Dulbecco modified Eagle's medium (DMEM, Lonza Group Ltd., Basel, Switzerland) containing 5 % fetal calf serum (FCS) (Sigma-Aldrich, St Louis, USA) and 1 % penicillin, streptomycin and fungizone (PSF) (Lonza Group Ltd., Basel, Switzerland) and incubated at 37°C with 10 % CO<sub>2</sub>.

### **3.2.2 Reagents and antibodies**

Geldanamycin (Biomol International Inc, PA, USA) was resuspended in DMSO and used at a final concentration of 0.125 µM. Novobiocin (Sigma Aldrich, St Louis, USA) was resuspended in sterile water and used at a final concentration of 250 µM. Polyclonal anti-TMEV 2C antibodies generated in rabbits using a peptide region of the non-structural TMEV 2C protein previously described (Jauka *et al.*, 2010) were used in the detection of virally-expressed TMEV 2C by Western analysis.

### **3.2.3 Maintaining a BHK-21 cell line**

#### **3.2.3.1 Subculturing cells**

Cells at 100 % confluency (percentage of cell growth where the growth surface is completely covered by cells), were subcultured into fresh complete medium (DMEM containing 5 % FCS and 1 % PSF). Spent medium was discarded and cells rinsed in phosphate buffered saline (PBS) [137 mM NaCl, 2.7 mM Na<sub>2</sub>HPO<sub>4</sub>, 2 mM KH<sub>2</sub>PO<sub>4</sub> (pH 7.4)]. Cell matrix and cell-cell interactions were interrupted by the addition of trypsin (Sigma-Aldrich, St Louis, USA) and the cells resuspended in 1 ml of complete medium and seeded into 5ml of fresh complete medium.

#### **3.2.3.2 Cryopreservation of BHK-21 cells**

To prepare cell stocks, a 25 cm<sup>2</sup> flask of 100 % confluent BHK-21 cells was resuspended in 1 ml cryopreservation solution (20 % FCS, 10 % glycerol, 1 % PSF, 69 % DMEM). Cells were aliquoted into cryovials and stored at -80°C.

### **3.2.4 Preparation of TMEV stock**

An existing TMEV stock maintained at -80°C (previously prepared in our laboratory) at a titre of  $7 \times 10^8$  plaque forming units/ml (pfu/ml) was used to prepare new TMEV stocks used during this study. A 100 % confluent 25 cm<sup>2</sup> flask was subcultured into a 75 cm<sup>2</sup> flask in 10 ml complete medium. When cells reached 100 % confluency, they were infected with 1 ml TMEV stock and resuspended in serum-free DMEM. Cells were incubated at 37°C for 1 hr with shaking to allow virus adsorption, 9 ml of serum-free DMEM was added and the cells incubated overnight at 37°C with 10 % CO<sub>2</sub>. Cell lysis was accomplished by three cycles of freeze-thawing and cell debris was pelleted by centrifugation for 1 min at 1000 x g. The supernatant was aliquoted into 1 ml fractions in cryovials and placed at -80°C for long-term storage.

### **3.2.5 Plaque assay for TMEV stock titration**

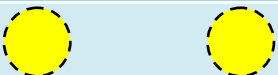
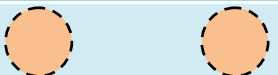
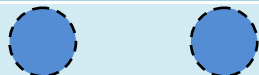
To titre TMEV stocks, a plaque assay was performed to determine the pfu/ml. BHK-21 cells were grown to 100 % confluency in 6-well plates in complete medium. A ten-fold dilution series of the previously prepared TMEV viral stock solution was made in serum-free DMEM in a total volume of 1.5 ml. Spent medium was aspirated from the 6-well plate and cells rinsed with PBS. Virus stock dilutions between  $1 \times 10^{-5}$  and  $1 \times 10^{-10}$  were aliquoted into each well and virus

absorption was conducted at 37°C with gentle shaking for 1 hr. Virus was aspirated, cells rinsed in PBS and overlaid with 3 ml of overlay solution (50 % DMEM, 1.25 % Methocel (Sigma-Aldrich, St Louis, USA), 60 mM NaCl in sterile water). Cells were incubated at 37°C and 10 % CO<sub>2</sub> until zones of clearance (plaques) were visible by light microscopy. Plaques appeared on the cell monolayer after 48 hrs of incubation. The overlay solution was gently washed off using PBS, taking care not to disturb the monolayer. Cells were fixed for 20 mins with shaking at room temperature in 4 % paraformaldehyde and rinsed in PBS. Cells were stained with Coomassie staining solution (45 % methanol, 10 % glacial acetic acid, 0.002 % Coomassie Brilliant Blue) at room temperature for 20 mins, staining solution removed by rinsing with sterile water and plaques visualised as clear zones against the Coomassie-stained cell monolayer. Numbers of plaques were counted for each dilution and virus titre calculated in terms of pfu/ml with dilution factor taken into account.

### **3.2.6 Nov and GA treatments**

BHK-21 cells were sub-cultured into four 6-well plates and grown to 100 % confluency. Treatments are described in Table 3.1. A ten-fold dilution series of TMEV stock (titre:  $5.5 \times 10^{-8}$  pfu/ml) was prepared in serum-free DMEM. Spent medium in the wells was aspirated and cells infected with fresh virus stock at a multiplicity of infection (MOI) of 10 and 0.1 (orange and blue wells respectively). Two wells from each plate were mock-infected with serum-free DMEM (yellow wells). The plates were incubated for 1 hr with shaking at 37°C to allow virus adsorption. Virus dilutions were aspirated and the wells rinsed in PBS before 3 ml of serum-free DMEM containing Nov and GA at final concentrations indicated in section 3.2.2 was added to the wells in duplicate. 3 ml of serum-free DMEM was added to the third plate (untreated sample). The fourth plate was incubated with 3 ml of serum-free DMEM containing 1 µl of DMSO, the solution used to resuspend GA, to ensure that changes observed in GA-treated cells were not due to DMSO. Plates were incubated at 37°C and monitored for the development of cytopathic effect (CPE) over a 48 hr time period. Photographs were captured 24 hrs, 36 hrs and 48 hrs post-treatment using Nikon a CoolPix 990 light microscope under 2x magnification. After the 48 hr time point, cells from each well were collected and analysed by SDS-PAGE and Western analysis.

Table 3.1: Treatment of mock-infected and TMEV-infected BHK-21 cell using Nov and GA. The table illustrates wells of mock-infected cells in yellow, well so cell infected with TMEV at a MOI of 10 in orange and wells of cells infected with TMEV at a MOI of 0.1 in blue.

Plate	Treatment	Mock-infected (Serum-free DMEM)	TMEV MOI ~10	TMEV MOI ~ 0.1
1	- Nov/GA			
2	+ Nov			
3	+ GA			
4	+ DMSO			

### 3.2.7 SDS-PAGE and Western analysis.

All samples analysed by SDS-PAGE were resolved on a 12 % polyacrylamide gel at 100V. For Western analysis, proteins were transferred onto nitrocellulose membrane (Bio-Rad Laboratories, Hercules, USA) for 2 hrs at 250 mA in cold transfer buffer (25 mM Tris-HCl pH 7.4, 192 mM glycine, 10 % methanol). Ponceau stain (0.1 % Ponceau stain in 1 % acetic acid) was used to verify protein transfer. The stain was removed by rinsing the membrane in water and then Tris buffered saline (TBS) [150 mM NaCl, 50 mM Tris-HCl (pH 7.6)]. The membrane was incubated for 1 hr in blocking solution (TBS containing 5 % fat-free powdered milk), followed by an overnight incubation with anti-TMEV 2C rabbit polyclonal antibodies (1:10 000) prepared in blocking solution. The membrane was washed three times for 15 mins in TBS-Tween (TBS containing 2 % Tween-20). For secondary antibody incubation, the membrane was incubated with mouse/ rabbit secondary antibody (1:12 000) provided by the BM Chemiluminescence Western Blotting Kit (Mouse/Rabbit) (Roche, Mannheim, Germany) for an additional 45 mins, followed by three 15 mins washes with TBS-Tween. The reaction was detected by the VersaDoc™ Model 4000 imaging system (Bio-Rad Laboratories, Hercules, USA).

### **3.3 Results**

#### **3.3.1 Titration of TMEV stock by plaque assay**

The concentration of virus particles in the TMEV stock solution was determined as pfu/ml by conducting a plaque assay. The assay was conducted by growing BHK-21 cells to a 100 % confluent monolayer in a 6-well plate and infecting the cells with ten-fold serial dilutions of TMEV between  $10^{-5}$  and  $10^{-10}$ . From the plaque assay, the concentration of virus particles in the prepared virus stock was determined to be  $5.5 \times 10^8$  pfu/ml. The virus titre was used to calculate the MOI used during the different experiments in this study.

#### **3.3.2 Determining the effects of Nov and GA on TMEV growth by monitoring the development of CPE**

To determine the effects of Hsp90 inhibitors, GA and Nov on TMEV growth, BHK-21 cells were mock-infected or infected with the virus and grown in the presence or absence of the two drugs. The development of CPE, defined as change in cell morphology, detachment of cells from growth surface and cell clumping, was used as an indicator of the effects the drugs had on TMEV infection. Cells were monitored over a 48hr period with images being captured at (a) 24 hrs, (b) 36 hrs and (c) 48 hrs post-treatment. Results are presented in Figures 3.1, 3.2 and 3.3.

##### ***a) 24 hrs post-treatment***

Left panels of Figure 3.1 represent images of mock-infected BHK-21 cells subjected to various drug treatments as indicated after 24 hrs. The middle and right columns illustrate images of BHK-21 cells infected with different MOIs, 10 and 0.1 in the absence and presence of both GA and Nov. Compared to mock-infected and untreated cells (left column, upper panel), subtle changes in cell morphology including rounding-up of cells, were observed in cells infected with TMEV in the absence of both GA and Nov, which may indicate the onset of CPE. No indication of CPE was observed in TMEV-infected cells treated with either Nov or GA at this time point (middle and lower panels, respectively).

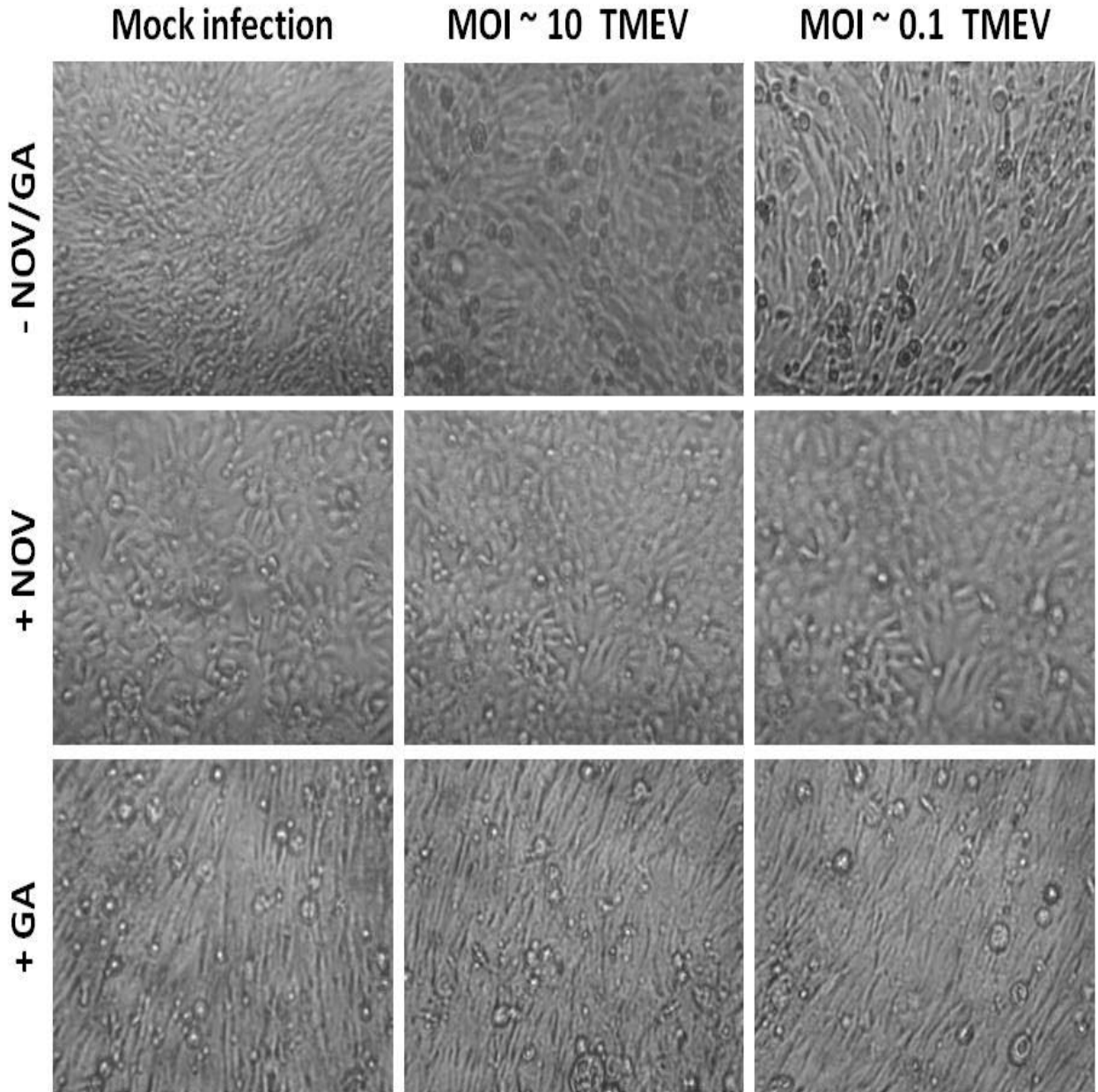


**Figure 3.1: Effects of novobiocin (Nov) and geldanamycin (GA) on the development of CPE in TMEV-infected BHK-21 cells, 24 hrs post-treatment.** BHK-21 cells were infected with TMEV at a MOI of ~10, 0.1 or mock-infected. CPE development was monitored in the absence of both drugs (upper panel), presence of Nov at a final concentration of 250  $\mu$ M (middle panel) or presence of GA at a final concentration of 0.125  $\mu$ M (lower panel). Images were captured using a Nikon CoolPix 900 light microscope under 2x magnification.

***b) 36 hrs post-treatment***

36hrs post-treatment, mock-infected cells not treated with either Nov or GA (left column, upper panel of Figure 3.2) still retained their fibroblast shape. Compared to cells at 24 hrs (Figure 3.1), the cells infected with virus in the absence of both drugs showed advanced stages of CPE (upper panels). Changes in cell morphology, detachment of cells from the growth surface and disruption of the cell monolayer was observed, particularly in the cells infected with a higher MOI of 10 (middle column, upper panel). Infected cells treated with either drug also depicted a change in cell morphology as seen by rounding-up of cells with a “glossy” finish for Nov-treated cells (middle panels) and rounding-up of cells with a “grainy” appearance for GA-treated cells (lower panels). Compared to cells infected in the absence of both drugs (upper panel), the changes in cell morphology were not the typical symptomatic indicators of virus-induced CPE. Mock-infected cells treated with Nov and GA also exhibited the same changes in cell morphology as the infected cells (left columns of middle and lower panels, respectively).

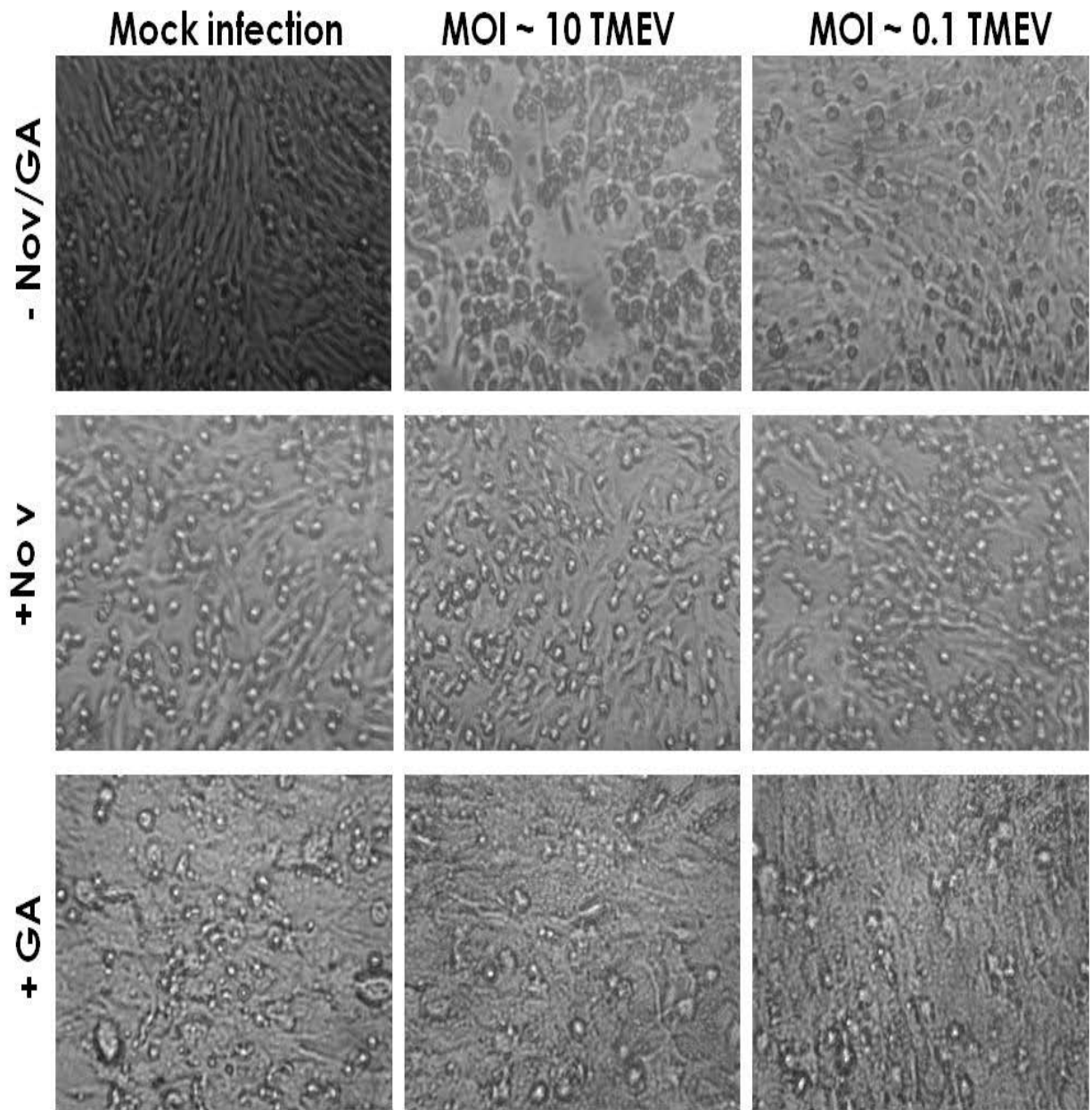


**Figure 3.2: Effects of novobiocin (Nov) and geldanamycin (GA) on the development of CPE in TMEV-infected BHK-21 cells 36 hrs post-treatment.** BHK-21 cells were infected with TMEV at a MOI of ~10, 0.1 or mock-infected. CPE development was monitored in the absence of both drugs (upper panel), presence of Nov at a final concentration of 250  $\mu$ M (middle panel) or presence of GA at a final concentration of 0.125  $\mu$ M (lower panel). Images were captured using a Nikon CoolPix 900 light microscope under 2x magnification.

***c) 48 hrs post treatment***

After 48 hrs, CPE was clearly observed in cells infected with TMEV in the absence of the drugs (upper panels), as detachment of cells from the growth surface and cell clumping was extensive. Mock-infected cells untreated with either Nov or GA still exhibited the typical fibroblast cell morphology after 48 hrs (left column, upper panel). After 48 hrs, typical virus-induced CPE was still not observed in Nov and GA-treated cells (middle and lower panels). The change in cell morphology and detachment of cells from the growth surface was more apparent in Nov- compared to GA-treated cells (compare middle and lower panels of Figure 3.3).

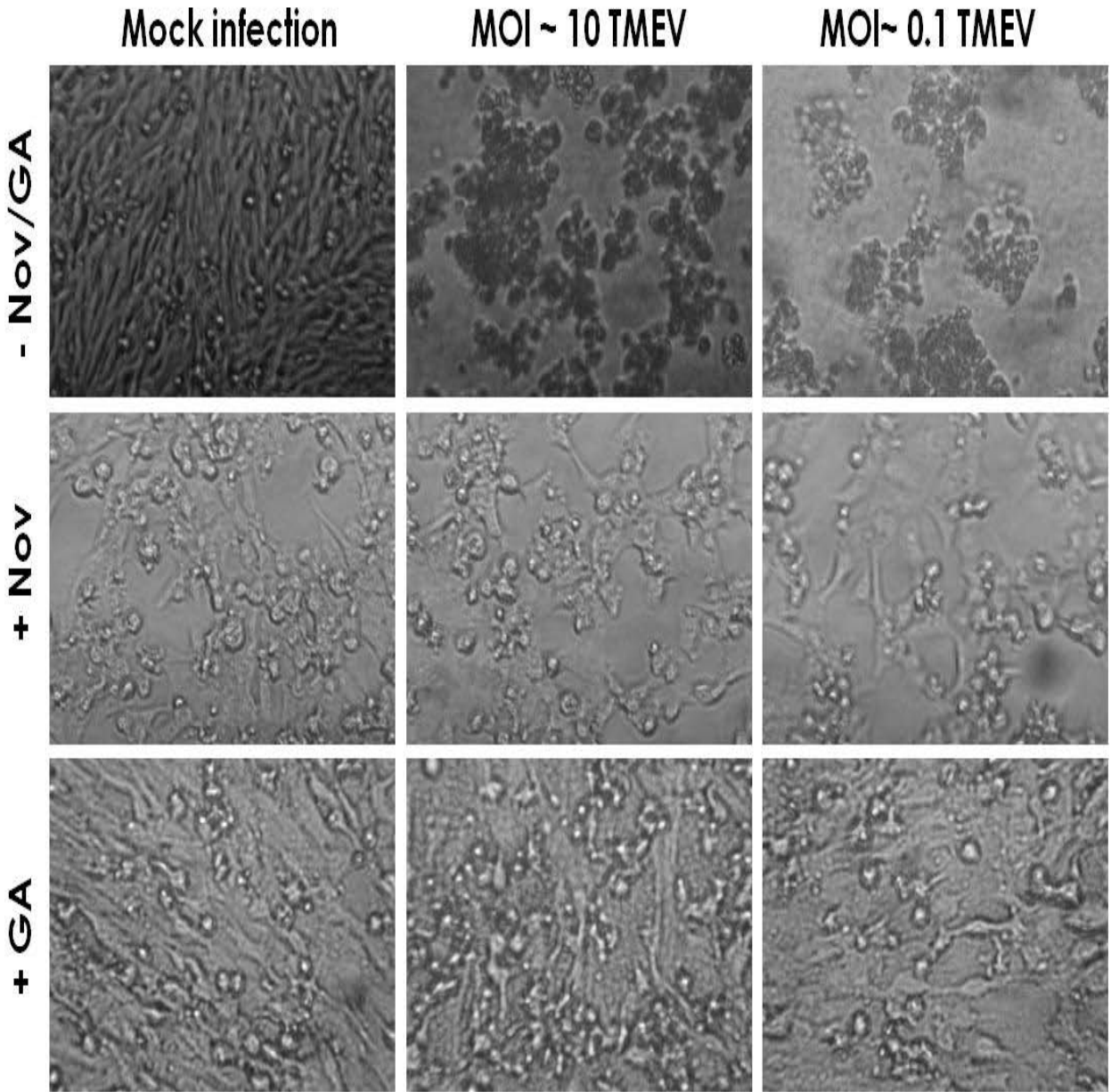


**Figure 3.3: Effects of novobiocin (Nov) and geldanamycin (GA) on the development of CPE in TMEV-infected BHK-21 cells 48 hrs post-treatment.** BHK-21 cells were infected with TMEV at a MOI of ~10, 0.1 or mock-infected. CPE development was monitored in the absence of both drugs (upper panel), presence of Nov at a final concentration of 250  $\mu$ M (middle panel) or presence of GA at a final concentration of 0.125  $\mu$ M (lower panel). Images were captured using a Nikon CoolPix 900 light microscope under 2x magnification.

### 3.3.3 Detection of virally-expressed non-structural TMEV 2C protein in treated cells, 48 hrs post-treatment

In order to determine that TMEV-infection had occurred in Nov- and GA-treated BHK-21 cells, untreated and treated cells were collected from each well after the 48 hr time point. The cells

were lysed, subjected to SDS-PAGE and Western analysis for the detection of the TMEV non-structural 2C protein using anti-TMEV 2C antibodies. Results are presented in Figure 3.4.

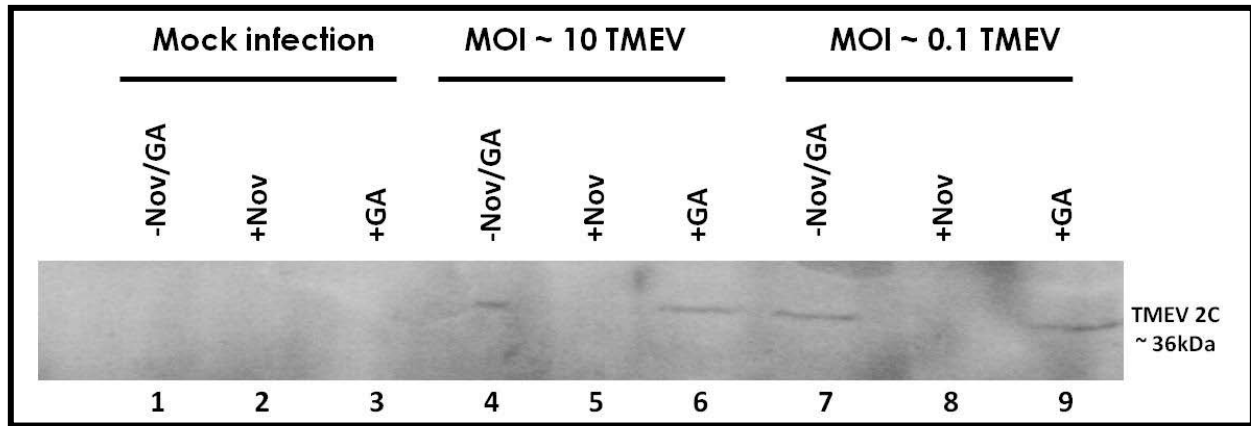


**Figure 3.4: Western analysis of BHK-21 cells infected with TMEV in the presence and absence of Nov and GA using anti-TMEV 2C antibodies.** After the 48 hr time point, treated cells were collected and analysed by SDS-PAGE and Western analysis. Virus presence was verified by detection of the non-structural TMEV 2C protein using anti-TMEV 2C antibodies (1:10 000).

As expected, no 2C signal was detected in mock-infected lysates of cells treated or untreated with Nov or GA (Lanes 1-3). A signal corresponding to TMEV 2C was detected in the lysate infected with TMEV at a MOI of 10 and 0.1 in the absence of both Nov and GA as expected (Lanes 4 and 7). Interestingly, a 2C signal was detected in lysates of cells treated with GA (Lanes 6 and 9) but absent in Nov-treated cells lysates (Lanes 5 and 8).

### **3.4 Discussion**

This chapter describes the effects of Hsp90 inhibitors GA and Nov on virus growth by monitoring the development of CPE in TMEV-infected BHK-21 cells. Detection of TMEV 2C protein in TMEV-infected cells treated with Nov and GA was also conducted by Western analysis.

During the 48 hr time period, it was observed that both Nov and GA prevented the onset of virus-induced CPE in TMEV-infected BHK-21 cells which was apparent in untreated cells. To ensure that the observed changes in cells were due to virus-infection or drug treatments and not due to

cell senescence, mock-infected cells grown in the absence of both drugs were also analysed over the same time period as the infected and treated cells. BHK-21 cells were able to survive and retain their fibroblast cell shape during the 48 hrs of the experiment incubated in serum-free DMEM at 37°C. Another precaution taken during this study was the observation of cells grown in the presence of DMSO, the solvent used to resuspend GA. This was done to ensure that the changes observed in GA-treated cells were due to the drug's effects and not to DMSO. No visible changes were observed in DMSO-treated cells (data not shown), indicating that the solvent did not affect the cells at the concentration applied.

The development of CPE was used as an indicator of the drug's effects on TMEV growth. This was done by observing cells infected with TMEV in the absence of both GA and Nov, and cells infected in the presence of either Nov or GA. Cells infected in the absence of both drugs were used as an indicator of TMEV-induced CPE. 24 hrs post-treatment, slight changes in cell morphology (rounding-up) were observed in cells infected in the absence of both drugs and not in the cells infected in the presence of Nov or GA. This observation indicated that the drugs inhibited or delayed the development of CPE at that time point. After 36 hrs, the progression of TMEV infection was observed in cells infected in the absence of the both drugs as seen by the advanced stages of CPE. Cells had rounded-up and began detaching from the growth surface in cells infected at a MOI of 10. Although changes in cell morphology were observed in infected cells treated with GA or Nov, they were not indicative of TMEV-induced CPE as seen in untreated cells. The changes which included cells rounding-up with a "glossy" finish for Nov-treated cells and cells rounding-up with a "grainy" appearance for GA were a result of the drug and not due to virus since mock-infected cells treated with either drug also exhibited the same changes. After 48hrs, CPE indicative of TMEV infection was still not observed in drug-treated cells even though untreated cells infected with the virus showed advanced stages of CPE as illustrated by the detachment of cells from the growth surface and the formation cell aggregates. These observations suggested that both Nov and GA were able to inhibit TMEV growth in BHK-21 cells.

The ability of GA to inhibit TMEV growth agrees with results described in the literature where the drug's ability to inhibit Hsp90 was able to reduce or inhibit replication of numerous RNA viruses such as FHV (Kampmueller and Miller, 2005), PV (Geller *et al.*, 2007), VSV (Connor *et*

*al.*, 2007), Influenza virus (Chase *et al.*, 2008) and Ebola virus (Smith *et al.*, 2010). The inhibitory effects of Nov on TMEV growth as indicated by the absence of CPE development is also supported by literature where the anti-viral activity of the drug was reported in DNA viruses such as HSV-1 (Franke and Margolin, 1981), Human cytomegalovirus (Landini and Baldassarri, 1982) and murine and avian Retroviruses (Sumiyoshi *et al.*, 1983). An interesting observation made here was that, although Nov is considered to be less cytotoxic than GA, changes in cell morphology and detachment of cells from the growth surface was more advanced in cells treated with Nov than in GA-treated ones. This suggests that the BHK-21 cell line was more susceptible to the drug at the dosage used compared to other cell lines such as human embryo fibroblast cells (Landini and Baldassarri, 1982). This was unexpected since the dosage used (250  $\mu\text{M}$ ) was selected based on numerous studies conducted on fibroblast cells (Landini and Baldassarri, 1982; Sumiyoshi *et al.*, 1983) and it was observed that Nov concentrations below 1000 $\mu\text{M}$  are non-toxic to cells (Hussy *et al.*, 1986). The susceptibility of BHK-21 cells to Nov may be affecting the cells ability to support viral processes, which prevents TMEV replication, hence virus-induced CPE is absence in Nov-treated cells.

To determine the effects of Hsp90 inhibition using GA and Nov on TMEV growth, the detection of the TMEV 2C protein by Western analysis was conducted. Based on the observations of Geller and co-workers (2007), that the inhibition of Hsp90 using GA did not interfere with the processing of non-structural viral proteins, the detection of a replicative, non-structural protein was used as an indicator of virus presence in Nov- and GA-treated cell lysates. The TMEV non-structural protein, 2C was selected for this study because studies are currently being conducted within our laboratory to better understand the functions of the protein. One of these studies resulted in the production of highly specific and sensitive polyclonal anti-TMEV 2C antibodies raised against a peptide region of the protein which have been shown to detect virally-expressed TMEV 2C protein by Western analysis and IF (Jauka *et al.*, 2010). The 2C protein is a non-structural protein of about 36kDa and is highly conserved within the picornavirus family. 2C is a replicative, multifunctional protein that plays a vital role in the picornavirus replication cycle (reviewed by Racaniello, 2001), therefore it was chosen as a marker to indicate the presence of viral proteins.

As expected, no signal for TMEV 2C was detected in the mock-infected lysates of cells grown in the presence or absence of both Nov and GA. These results also illustrated that the antibody used does not cross-react with cellular proteins, indicating the specificity of the antibodies as previously illustrated by Jauka *et al.*, 2010. Also expected was the signal corresponding to the TMEV 2C protein detected in the lysates of TMEV-infected BHK-21 cells at both MOIs of 10 and 0.1 in the absence of both Nov and GA.

A prominent signal for TMEV 2C was detected in GA-treated cell lysates. This suggested that although the drug had a negative effect on TMEV growth as illustrated by the lack of CPE development, the drug did not affect the translation or the processing of the TMEV non-structural protein, 2C. This result supports the findings made by Geller and co-workers (2007) during their study on enteroviruses. The study concluded that the inhibition of Hsp90 using GA in enterovirus-infected cells had no effect on the early, post-infection stages of the viruses or processing of the P2 and P3 polyproteins but affected the processing of the structural polyprotein, P1. As discussed before, GA binds to the ATP-binding site located on the N-terminal of Hsp90 preventing a conformational change that is required for the binding of p23, causing the accumulation of intermediate multi-chaperone complexes. This then blocks substrates from progressing through the Hsp90-mediated protein folding and maturation pathway and proteasome-mediated substrate degradation (Grenert *et al.*, 1997; Stebbins *et al.*, 1997). In picornaviruses, the reduction of new virions was suggested to be a result of P1 degradation due to the inhibition of Hsp90 activity using GA (Geller *et al.*, 2007). Replication processes of picornaviruses is highly conserved within the family, the non-structural proteins of TMEV similar to PV, HRV and CV may not be affected by the inhibition of Hsp90 using GA, hence the TMEV 2C protein could be detected in treated samples.

Interestingly, in three independent experiments, no signal for TMEV 2C was detected in Nov-treated cells. One explanation is that Nov prevented either the production or the processing of TMEV 2C. This observation suggested that, unlike GA, Nov through an unknown mechanism was able to indirectly or directly influence the translation or processing of TMEV 2C. Another possibility is that Nov was able to alter the function of TMEV 3C<sup>Pro</sup>, the viral protease responsible for processing the polyprotein. Another explanation could be that, as observed and discussed in the previous section, the dosage of Nov used during the research might have been

unexpectedly toxic to the cells to the point that they were unable to support TMEV replication or translation and processing of the non-structural viral proteins, hence no TMEV 2C protein was produced. Another explanation as to why TMEV 2C could be detected in GA-treated and not Nov-treated cell lysates may be linked to the different mechanisms involved in the inhibition of Hsp90. Unlike GA, Nov binds to the C-terminal ATP-binding site of Hsp90 and the binding results in the disassociation of the late Hsp90 multi-chaperone complex which leads to the release and degradation of substrates (Marcu *et al.*, 2000a; 2000b; Yun *et al.*, 2004), in this case, TMEV 2C. However, there is no evidence in the literature that supports the theory that an interaction occurs between Hsp90 and any picornavirus 2C protein.

### **3.4 Conclusion**

The effects of the Hsp90 inhibitors, Nov and GA, on virus growth in TMEV-infected BHK-21 cells were successfully examined. Additionally, the presence of TMEV 2C protein in infected cell lysates treated with Nov and GA was investigated by Western analysis using anti-TMEV-2C antibodies. The following conclusions were reached regarding the effects of each drug on TMEV growth:

- At the concentrations used, both Nov and GA were able to inhibit the development of TMEV-induced CPE, 48 hours post-treatment, which suggests that Hsp90 is involved in TMEV replication.
- TMEV 2C was detected in GA- and not Nov-treated, TMEV-infected cell lysates. This suggested that Nov may affect the translation or the processing of the TMEV non-structural protein, 2C.

The next chapter describes the effects of TMEV-infection on the distribution of Hsp90, Hsp70 and Hsp40 in BHK-21 cells by IF.

## Chapter 4: Distribution of Hsp40, Hsp70 and Hsp90 in TMEV-Infected BHK-21 Cells

### 4.1 Introduction

Having established in the previous chapter that the inhibition of Hsp90 using GA and Nov hindered the development of TMEV growth in BHK-21 cells, this chapter examines the distribution of Hsp90, Hsp70 and Hsp40 in TMEV-infected and mock-infected cells. Hsp90, Hsp70 and Hsp40 were selected for analysis based on the available evidence that Hsp90 and Hsp70 are host factors that play a role in picornavirus replication (Macejak and Sarnow, 1992; Geller *et al.*, 2007) and that Hsp40 works in conjunction with Hsp70 in numerous virus activities (Alfano and McMacken, 1989; Zylitz *et al.*, 1989; Hoffmann *et al.*, 1992; Liu *et al.*, 1998; Couturier *et al.*, 2009; Weeks *et al.*, 2008). Examples of specific interactions are described in chapter 1, section 1.5.

In recent years, confocal, fluorescence and electron microscopy have become major techniques in understanding interactions between viral proteins and host factors. IF and confocal microscopy has been instrumental in deciphering various aspects of the picornavirus life cycle, such as entry and genome replication. As mentioned and illustrated in chapter 1 section 1.3.3, the first step in picornavirus replication is the receptor-mediated attachment of the virus to the host membrane. Through the use of confocal microscopy Triantafilou *et al.*, (1999; 2002) identified and verified that, along with the receptor integrin  $\alpha_v\beta_1$ , CVA9 requires the chaperone GRP78 as a co-receptor to successfully enter the host cell. Similarly, Echovirus requires a specific surface receptor, in this case, the  $\alpha_2\beta_1$  integrin to successfully attach to the host cell and initiate entry (Roivainen *et al.*, 1994; Xing *et al.*, 2004). Confocal analysis was also crucial in deciphering a new caveolar pathway utilised by Echovirus to gain entry into host cells (Marjomäki *et al.*, 2002; Upla *et al.*, 2004; Pietiäinen *et al.*, 2004). Caveolae have been described as invaginations in the plasma membrane of about ~ 50- 80 nm in size and are involved in the potocytosis of small molecules and the trafficking of cholesterol (reviewed by Kurzchalia and Parton, 1999; Pelkmans and Helenius, 2002; Parton 2003). Caveolae have been shown to be the alternative route for clathrin-dependent endocytosis for viruses such as SV40 (Mukherjee *et al.*, 1997; Norkin, 1999; Parton and Lindsay, 1999). Through the use of confocal microscopy,

colocalisation of Echovirus capsid proteins and SV40 capsid proteins was observed, verifying that Echovirus utilises the caveolae during endocytosis (Marjomäki *et al.*, 2002; Pietiäinen *et al.*, 2004).

IF and confocal analysis have also been used to understand picornavirus-host cell interactions during viral genome replication. Confocal analysis has been used to identify cellular compartments where various picornavirus and host proteins localise during replication. By expressing FMDV non-structural proteins in BHK cells, FMDV 3C<sup>pro</sup> was identified as the viral protein responsible for altering cell morphology by changing the distribution of microtubule and intermediate filament components (Armer *et al.*, 2008). With the aid of fluorescence microscopy, it was shown that FMDV structural and non-structural proteins co-localised next to the nucleus, close to the Golgi complex in punctuate structures that represented the sites of replication for the virus (Knox *et al.*, 2005). Using confocal microscopy, FMDV non-structural proteins 2B, 2C, 2BC and 3A were shown to localise to cellular compartments such as the Golgi apparatus and ER. Using confocal microscopy to track the movement of a GYFP-tagged TsO45 mutant of the VSV G protein (VSVO45 temperature-sensitive glycoprotein) from the ER to the cell surface, 2BC protein was able to obstruct the movement of the tagged G protein through the secretory pathway, suggesting that the protein was able to block ER-to-Golgi transport (Moffat *et al.*, 2005).

Using microscopical techniques, it was shown that, in HAV- and PV-infected cells, 2C and 2BC induced intercellular rearrangement of the ER membrane and also localise to the perinuclear region in punctuate structures when expressed alone (Cho *et al.*, 1994; Aldabe and Carrasco, 1995; Teterina *et al.*, 1997). In CV, the viral protein responsible for host cell membrane permeability in infected cells, 2B, was found to localise to the ER and Golgi membranes using confocal microscopy. This study also provided evidence that the 2B protein forms homomultimers (van Kuppeveld *et al.*, 2002). Confocal microscopy was used to localise TMEV 2C to the Golgi apparatus during infection and in transfected cells (Murray *et al.*, 2009; Jauka *et al.*, 2010).

Although, numerous studies have observed the interaction between viral proteins and chaperones (discussed in chapter 1, section 1.5), information on the distribution of Hsp90, Hsp70 and Hsp40

in infected cells is lacking. To our knowledge, no such studies have been conducted on TMEV or any other picornavirus. Based on the previous chapter, it is clear that TMEV is utilising Hsps including Hsp90 in some aspect of its life cycle. Due to the fact that Hsp90 works in conjunction with Hsp70 and Hsp40 in various cellular pathways and processes, it is possible that Hsp70 and Hsp40 may also be required to facilitate virus replication. The above evidence illustrates that confocal microscopy is a vital tool in examining and understanding the dynamics of viral-host interactions. Therefore, the overall aim of this chapter was to examine the distributions of Hsp90, Hsp70 and Hsp40 in BHK-21 cells mock-infected or infected with TMEV using this technique. Specific objectives were:

- To examine the distribution of Hsp90, Hsp70 and Hsp40 in mock-infected and TMEV-infected BHK-21 cells by IF and confocal microscopy.
- To examine the expression levels of Hsp90, Hsp70 and Hsp40 in TMEV-infected cell lysates by Western analysis.

## ***4.2 Methods and Materials***

### **4.2.1 Preparation of BHK-21 cells for immunofluorescence**

Cells were grown to 80 %-90 % confluence on ethanol-sterilised 13mm glass coverslips in 6-well plates in complete medium. Spent medium was discarded and cells rinsed in serum-free DMEM. Cells were infected with TMEV in serum-free DMEM at a MOI of 50. Cells were mock-infected using 1 ml of serum-free DMEM. The plates were incubated at 37°C for 1 hr with shaking to allow virus absorption. Virus was removed and 4 ml of serum-free DMEM aliquoted into each well and plates incubated at 37°C. 6.5 hours post-infection (h.p.i), the medium was discarded and the cells rinsed in PBS before fixing with 4% paraformaldehyde for 20 mins with shaking at room temperature. Coverslips were rinsed in PBS and transferred to 24-well plates for IF staining. In a separate experiment, to monitor the distribution of Hsp90 over time, cells were fixed 4, 6 and 8 h.p.i as described above.

### **4.2.2 Indirect immunofluorescence staining of BHK-21 cells**

Cells were permeabilised in permeabilising buffer (PBS containing 10 % sucrose, 1 % Triton X-100) for 20 mins with shaking at room temperature (all steps following were conducted at room

temperature with shaking unless stated otherwise). Cells were rinsed twice for 10 mins in wash buffer (PBS containing 0.1 % Tween-20) and blocked in blocking solution (PBS containing 1 % BSA) for 30 mins. Cells were incubated in primary antibodies (described in Table 4.1) prepared in blocking solution for 1hr with shaking at 37°C. To monitor Hsp40 distribution, cells were dual-stained with anti-Hsp40 and anti-TMEV P1 antibodies, for Hsp70 distribution, cells were dual-stained with anti-Hsp70/Hsc70 and anti-TMEV 2C antibodies. To monitor the distribution of Hsp90 at 6.5 h.p.i and at 4, 6 and 8 h.p.i, cells were dual-stained with anti-Hsp90 and anti-TMEV 2C antibodies. Cells were washed twice for 10 mins in wash buffer and then incubated in species-specific Alexa-Fluor 488 and 546-conjugated secondary antibodies (Molecular probes through Invitrogen, Paisley, UK) for 30 mins. Three 10 mins washes were conducted with the second wash containing 0.8 µg/ml of 4', 6- Diamino-2, phenylindole dihydrochloride (DAPI, Sigma, St Louis, USA) in order to stain the cell nucleus. Cover slips were mounted onto glass slides using Dako fluorescence Mounting Medium (Dako North America, Inc, CA, USA) and stored at 4°C.

Table 4.1: Detailed information of primary antibodies utilised in Western analysis and IF.

Antibody Cat #	Dilution (WB)	Dilution (IF)	Type Animal	Source/ Donation
Anti-Actin A2066	1:2000	-	Polyclonal Rabbit	Sigma-Aldrich, St Louis, SA
Anti-TMEV 2C	1:10 000	1:1000	Polyclonal Rabbit	Tembisa Jauka (Rhodes U)
Anti-TMEV P1	1:1000	1:1000	Monoclonal Mouse	Prof Lipton (U of Chicago)
Anti-Hsp40 SMC-100	1:2000	1:500	Polyclonal Rabbit	StressMarq, BC, Canada
Anti-Hsp90 SC-13119	1:1000	1:100	Monoclonal Mouse	Santa Cruz Biotech, Santa Cruz, USA
Anti-Hsp70/Hsc70 SMC-104	1:1000	1:100	Monoclonal Mouse	StressMarq, BC, Canada

Anti-actin antibodies were raised against the C-terminal actin fragment and recognise three isoforms of actin ( $\alpha$ ,  $\beta$  and  $\gamma$ ). Anti-TMEV 2C antibodies were raised against a peptide of TMEV 2C (31-210) and recognise the full length virally-expressed TMEV 2C protein (Jauka *et al.*, 2010). Anti-TMEV P1 antibodies were raised against the VP1 peptide and recognise the TMEV

VP1 subunit of the capsid precursor protein, P1 (Fujinami *et al.*, 1988). Anti-Hsp40 antibodies were raised against recombinant human Hsp40 and recognise all J domain proteins. Anti-Hsp90 antibodies were raised against a peptide of Hsp90 $\beta$  (610-723) and recognise both  $\alpha$  and  $\beta$  isoforms of Hsp90. Anti-Hsp70/Hsc70 antibodies were raised against recombinant Hsp70/Hsc70 and recognise inducible Hsp70 and constitutive Hsc70. Both inducible Hsp70 and constitutive Hsc70 will be referred to as Hsp70.

### **4.2.3 Confocal microscopy and image acquisition**

Cells were visualised using an inverted LSM 510-Meta confocal laser scanning microscope (Carl Zeiss, Germany) using the 40x and 63x oil immersion objective lens. The helium/neon and argon lasers at wavelengths 405, 488 and 543 nm were used to excite DAPI, Alexa-fluor 488 and Alexa-fluor 546 respectively. Images were analysed using the Axiovision LE/ SE freeware software (Carl Zeiss, Germany) and processed using Microsoft Office PowerPoint 2007.

### **4.2.4 Preparation of cell lysates and Western analysis**

Cells were grown in T-75 cm<sup>2</sup> flasks to 90 %-100 % confluency, and infected with TMEV at a MOI of 50 and harvested 0, 2, 4, 6 and 8 h.p.i. Cells were collected by trypsinisation and rinsed with PBS to remove excess trypsin. Cells were resuspended into 100  $\mu$ l of lysis buffer [50 mM Tris-HCl, (pH 7.5), 150 mM NaCl, 2 % Triton X- 100, 1 mM PMSF, 1 mM DTT, 1 x EDTA-free protease inhibitor cocktail (Roche, Mannheim, Germany)] kept on ice for 30 mins with vigorous vortexing every 5 mins. Cells were centrifuged at 1000 x g for 1 min, the supernatant collected and analysed by SDS-PAGE and Western analysis as described in section 3.2.7. Details of antibodies used for Western analysis are summarised in Table 4.1 and described on page 60.

## **4.3 Results**

### **4.3.1 Distribution of Hsp40, Hsp70 and Hsp90 in TMEV-infected and mock-infected BHK-21 cells**

To determine the effects of virus infection on Hsp40, Hsp70 and Hsp90 distribution, BHK-21 cells were mock-infected or infected with TMEV, fixed at 6.5 h.p.i with paraformaldehyde and dual-stained with antibodies against TMEV P1, TMEV 2C, Hsp70, Hsp40 and Hsp90 and examined by confocal microscopy. The results are presented in Figures 4.1, 4.2 and 4.3. It is

important to note that the antibody combinations used in the study were chosen based on the availability of the antibodies. In our possession were anti-TMEV 2C antibodies (rabbit), anti-TMEV-P1 antibodies (mouse), anti-Hsp40 (rabbit), anti-Hsp90 (mouse) and anti-Hsp70/Hsc70 (mouse). Therefore, the following dual-staining combinations were performed:

- Anti-Hsp40 in combination with anti-TMEV P1.
- Anti-TMEV 2C in combination with anti-Hsp90.
- Anti-TMEV 2C in combination with anti-Hsp70/Hsc70.

#### ***a) Distribution of Hsp40***

To monitor the distribution of Hsp40, BHK-21 cells were either mock-infected or infected with TMEV for 6.5 hrs, fixed with paraformaldehyde, dual-stained with anti-TMEV P1 and anti-Hsp40 antibodies and examined by confocal microscopy. Results are presented in Figure 4.1. In mock-infected cells (panel A), no signal for TMEV P1 was observed as expected. Hsp40 was found distributed uniformly in the cytoplasm, concentrated in the perinuclear region and within the nucleus. Panels B and C represent two separate fields of TMEV-infected BHK-21 cells 6.5 h.p.i. The presence of the TMEV P1 signal verified that infection was successful. The signal for P1 was both punctative and diffuse in the cytoplasm, while at the same time same was concentrated around the perinuclear region. In the majority of cells in both panels B and C, Hsp40 was found concentrated mainly in the nucleus but there was still residual cytoplasmic staining. The merged images in panels B and C show that there was some overlap between the signal for TMEV P1 and Hsp40 in the perinuclear region as illustrated by the yellow colour. As can be seen in panel B indicated by the white arrow, there is a cell that did not stain positive for TMEV P1, indicating that the cell was uninfected. Interestingly, the majority of the Hsp40 signal was in the nucleus of the cell, as seen in the case of infected cells. The magnified images of an infected cell (panel D), clearly shows concentration of Hsp40 in the nucleus and TMEV P1 around the perinuclear region and distributed in the cytoplasm in a distinct punctative and diffuse pattern. The overlap of TMEV P1 and Hsp40 signals in the perinuclear region was evident in the merged image.

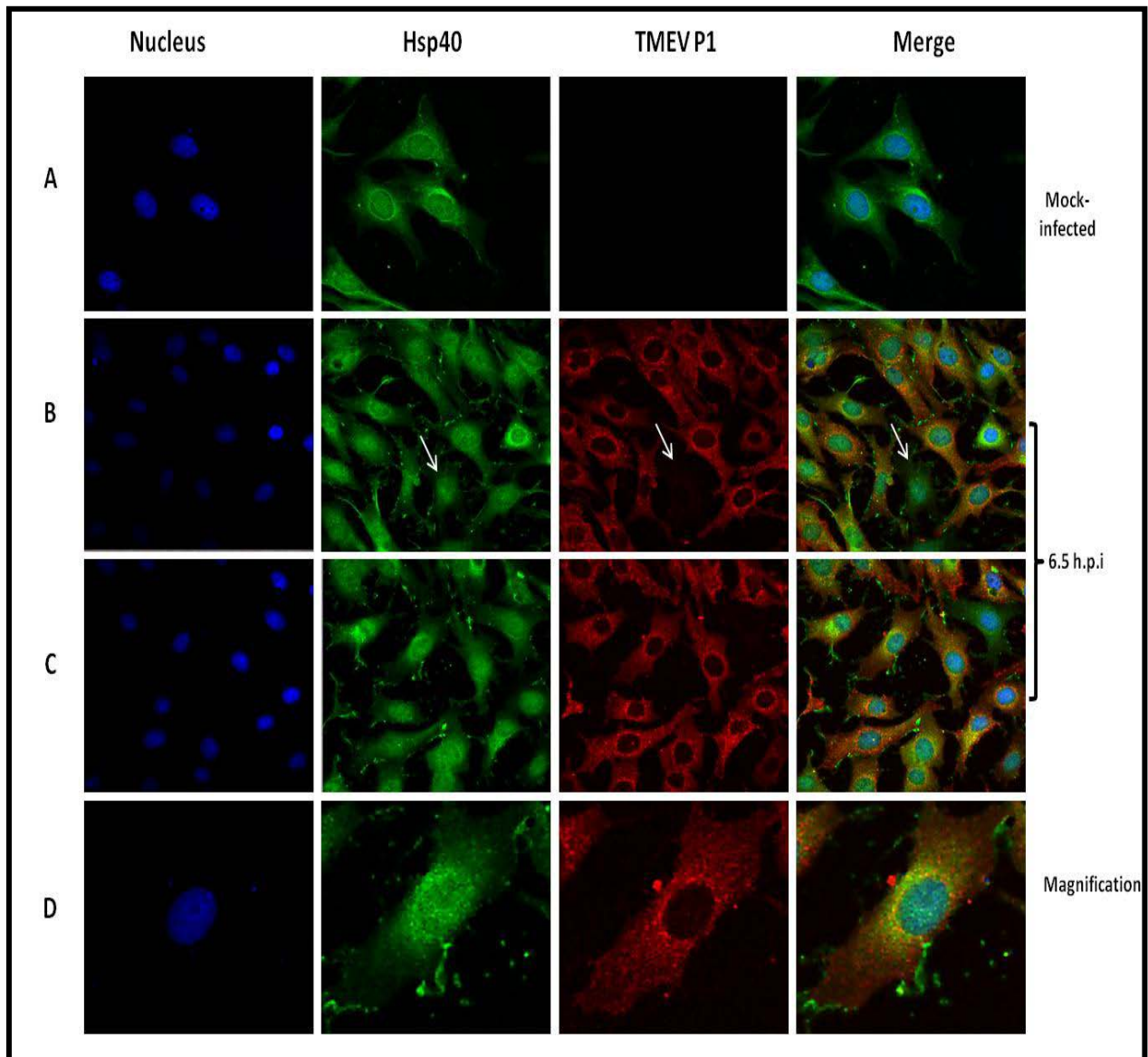


**Figure 4.1: Distribution of Hsp40 in mock-infected and TMEV-infected BHK-21 cells.** Cells were grown on coverslips and mock-infected or infected with TMEV, fixed with 4 % paraformaldehyde at 6.5 h.p.i, permeabilised and dual-stained with anti-Hsp40 and anti-TMEV P1 antibodies. Primary antibodies were detected with species-specific Alexa Fluor 488-conjugated secondary antibodies for Hsp40 or Alexa Fluor 546-conjugated secondary antibodies for TMEV P1. Panel A : Mock-infected cells. Panel B, C and D : TMEV-infected cells. The white arrow indicates an uninfected cell.

### ***b) Distribution of Hsp70***

To monitor the distribution of Hsp70, BHK-21 cells were either mock-infected or infected with TMEV for 6.5 hrs, fixed with paraformaldehyde, dual-stained with anti-TMEV 2C and anti-Hsp70/Hsc70 antibodies and examined by confocal microscopy. Results are presented in Figure 4.2. In mock-infected cells (panel A), no signal for TMEV 2C was observed as expected. The Hsp70 signal was found in punctative structures throughout the cytoplasm and faint staining was also present in the nucleus. Panels B and C represent two separate fields of TMEV-infected BHK-21 cells fixed at 6.5 h.p.i. The presence of the TMEV 2C signal verified that infection was successful. At this time point, two distinct staining patterns of TMEV 2C were observed. The arrow in panel C indicates a cell in an earlier stage of infection (yellow) as indicated by the diffuse staining pattern and the slight concentration of the TMEV 2C signal around the nucleus. The other arrow (white) indicates a cell in a later stage of infection, where the staining pattern for TMEV 2C was concentrated within a large structure adjacent to the nucleus. In the majority of cells in both panels B and C, where the TMEV 2C staining was concentrated next to the nucleus, the signal for Hsp70 was still punctative but found converging around the TMEV 2C-containing structure. In cells where TMEV 2C staining was diffuse in the cytoplasm and slightly concentrated around the perinuclear region, most of the Hsp70 was still distributed in the cytoplasm with the same distinct punctative staining pattern observed in mock-infected cells. In the merged images (panels B and C), it was clear that the signals for Hsp70 and TMEV 2C did not overlap as seen by the separate green and red signals, this is evident in the infected cell depicted in panel D. The magnified image in panel D clearly shows the convergence of Hsp70 around the TMEV 2C-containing replication complex.

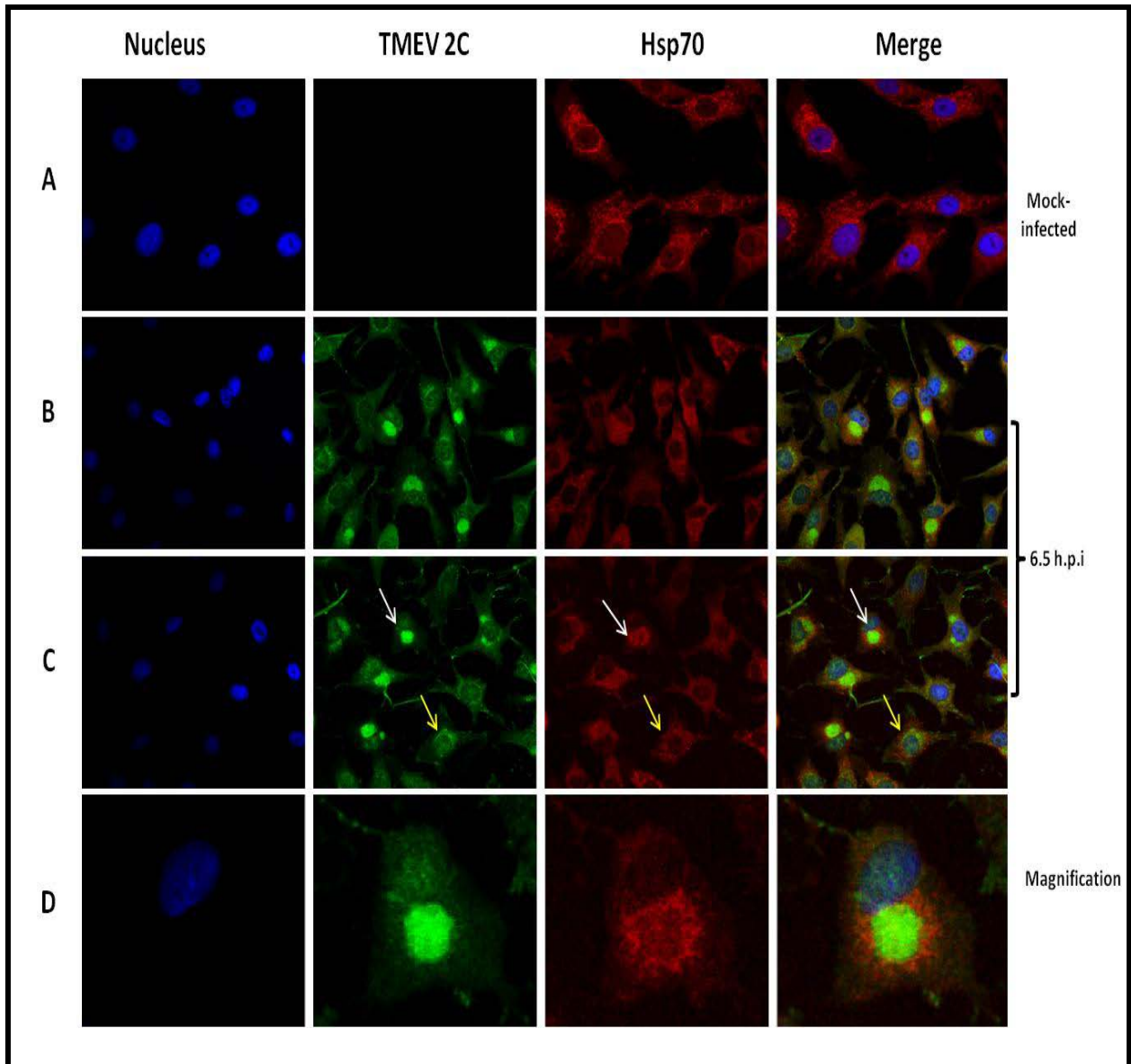


**Figure 4.2: Distribution of Hsp70 in mock-infected and TMEV-infected BHK-21 cells.** Cells were grown on coverslips and mock-infected or infected with TMEV, fixed with 4 % paraformaldehyde at 6.5 h.p.i, permeabilised and dual-stained with anti-Hsp70/Hsc70 and anti-TMEV 2C antibodies. Primary antibodies were detected with species-specific Alexa Fluor 488-conjugated secondary antibodies for Hsp70 or Alexa Fluor 546-conjugated secondary antibodies for TMEV 2C. Panel A: Mock-infected cells. Panel B, C and D: TMEV-infected cells. The yellow and white arrows indicate cells in early and late stages of infections, respectively.

### ***c) Distribution of Hsp90***

To monitor the distribution of Hsp90, BHK-21 cells were either mock-infected or infected with TMEV for 6.5 hrs, fixed with paraformaldehyde, dual stained with anti-TMEV 2C and anti-Hsp90 antibodies and examined by confocal microscopy. Results are presented in Figure 4.3. In mock-infected cells (panel A), no signal for TMEV 2C was observed as expected. The Hsp90 signal was found uniformly distributed throughout the cytoplasm and faint nuclear staining was also present. Panels B and C represent two separate fields of TMEV-infected BHK-21 cells at 6.5 h.p.i. captured during two separate experiments. The presence of the TMEV 2C signal verified that infection was successful. In both panels B and C, two different staining patterns of TMEV 2C were observed as indicated by the two arrows, A and B in panel B. Arrow A indicates an infected cell where the staining of TMEV 2C was mostly diffuse in the cytoplasm, representing an earlier stage of infection. Arrow B points to a cell where the TMEV 2C signal was mostly concentrated around the perinuclear region, representing a later stage of infection. In infected cells (panels B and C), a shift in Hsp90 distribution was observed when compared to mock-infected cells (panel A). The Hsp90 signal was mostly found concentrated around the perinuclear region in cells where the TMEV 2C signal was also concentrated within the same region, but cytoplasmic and nuclear staining was still apparent. The merged images of panels B and C indicate that the TMEV 2C and Hsp90 signals overlapped in the perinuclear region of some cells as seen by the presence of a yellow signal. The yellow colour suggests that the two proteins may colocalise within this region. The magnified images of an infected cell in panel D, verify the observations made in panels B and C. The images clearly indicate that the signal for Hsp90, as well as that of TMEV 2C were concentrated around, and overlapped in the perinuclear region. At the same time, cytoplasmic and nuclear staining of Hsp90 was also visible.

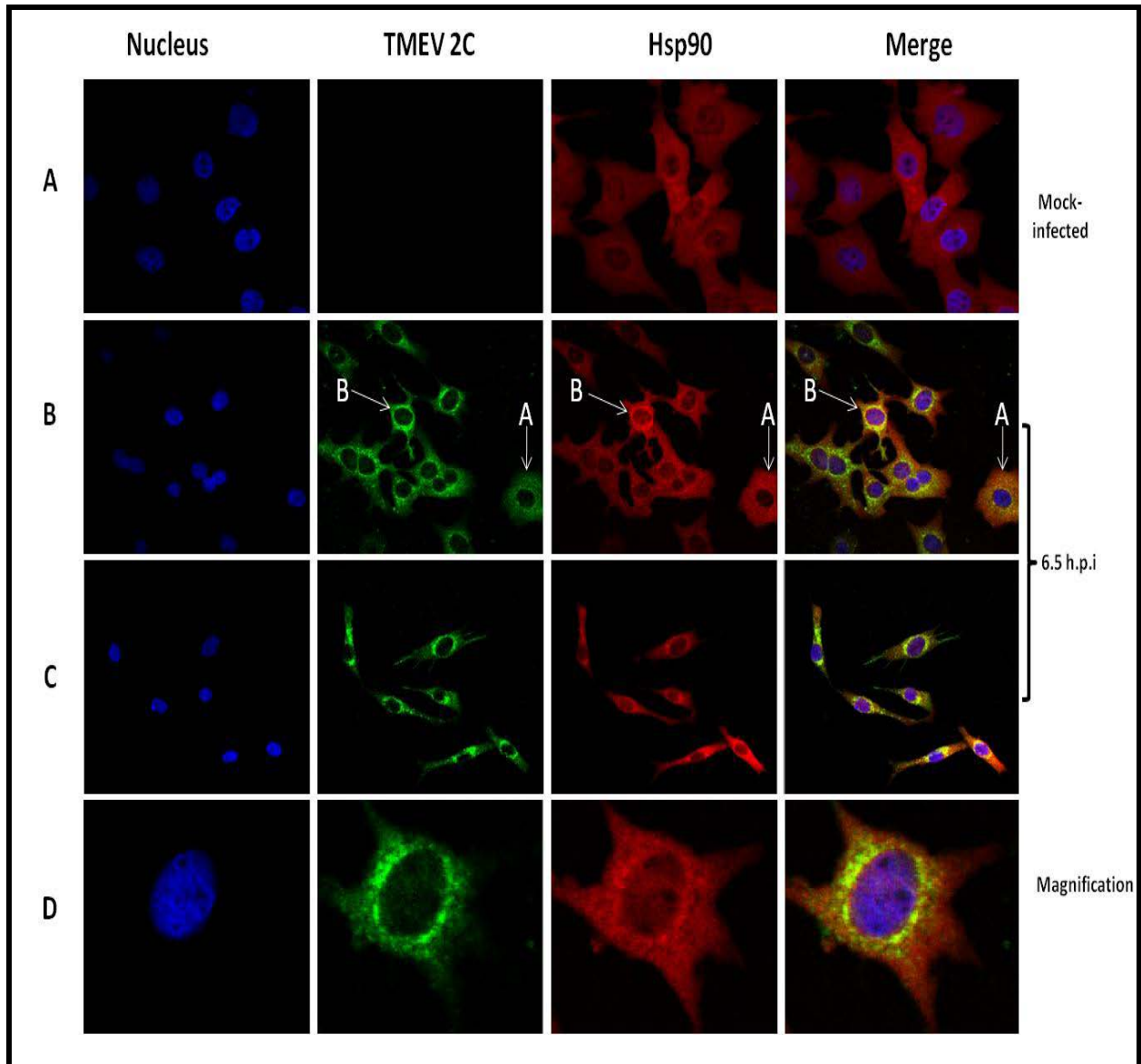


**Figure 4.3: Distribution of Hsp90 in mock-infected and TMEV-infected BHK-21 cells.** Cells were grown on coverslips and mock-infect or infected with TMEV, fixed with 4 % paraformaldehyde at 6.5 h.p.i, permeabilised and dual-stained with anti-Hsp90 and anti-TMEV 2C antibodies. Primary antibodies were detected with species-specific Alexa Fluor 546-conjugated secondary antibodies for Hsp90 or Alexa Fluor 488-conjugated secondary antibodies for TMEV 2C. Panel A: Mock-infected cells. Panel B, C and D. A and B arrows indicate cells in early and late infection stages, respectively.

#### ***d) Distribution of Hsp90 over time***

Based on the observations made during the examination of Hsp90 distribution at 6.5 h.p.i, where Hsp90 staining was observed in different regions during infection, the following experiment monitored the distribution of Hsp90 over time. BHK-21 cells were infected with TMEV, fixed with paraformaldehyde at 4, 6 and 8 h.p.i, dual stained with anti-TMEV 2C and anti-Hsp90 antibodies and examined by confocal microscopy. Results are presented in Figure 4.4. At 4 h.p.i (panel A), which represents an earlier stage of infection, the TMEV 2C signal was found throughout the cytoplasm, while the Hsp90 signal was distributed uniformly in the cytoplasm, with faint nuclear staining. The merged image of panel A shows that the two signals did not overlap at this time point as indicated by the presence of separate red and green signals. At 6 h.p.i (panel B), during the middle stages of infection, the majority of the TMEV 2C signal had concentrated around the nucleus. A concentration of Hsp90 was also observed around the perinuclear region, although cytoplasmic staining was still present. Interestingly, the intensity of the Hsp90 signal had increased in the nucleus (compare panel A and B). The merged image of panel B indicated that, at 6 h.p.i, the Hsp90 and TMEV 2C signals overlapped mainly around the nucleus as indicated by the presence of the yellow signal (white arrow), suggesting that the two proteins colocalised. The images of two cells in panel C were captured at 8 h.p.i during late infection. TMEV 2C was found concentrated in a large structure adjacent to the nucleus in both cells. On the other hand, Hsp90 staining was found in three different locations. Hsp90 was found concentrated next to the nucleus where the majority of the TMEV 2C signal was located. It was also observed in the cytoplasm and within the nucleus.

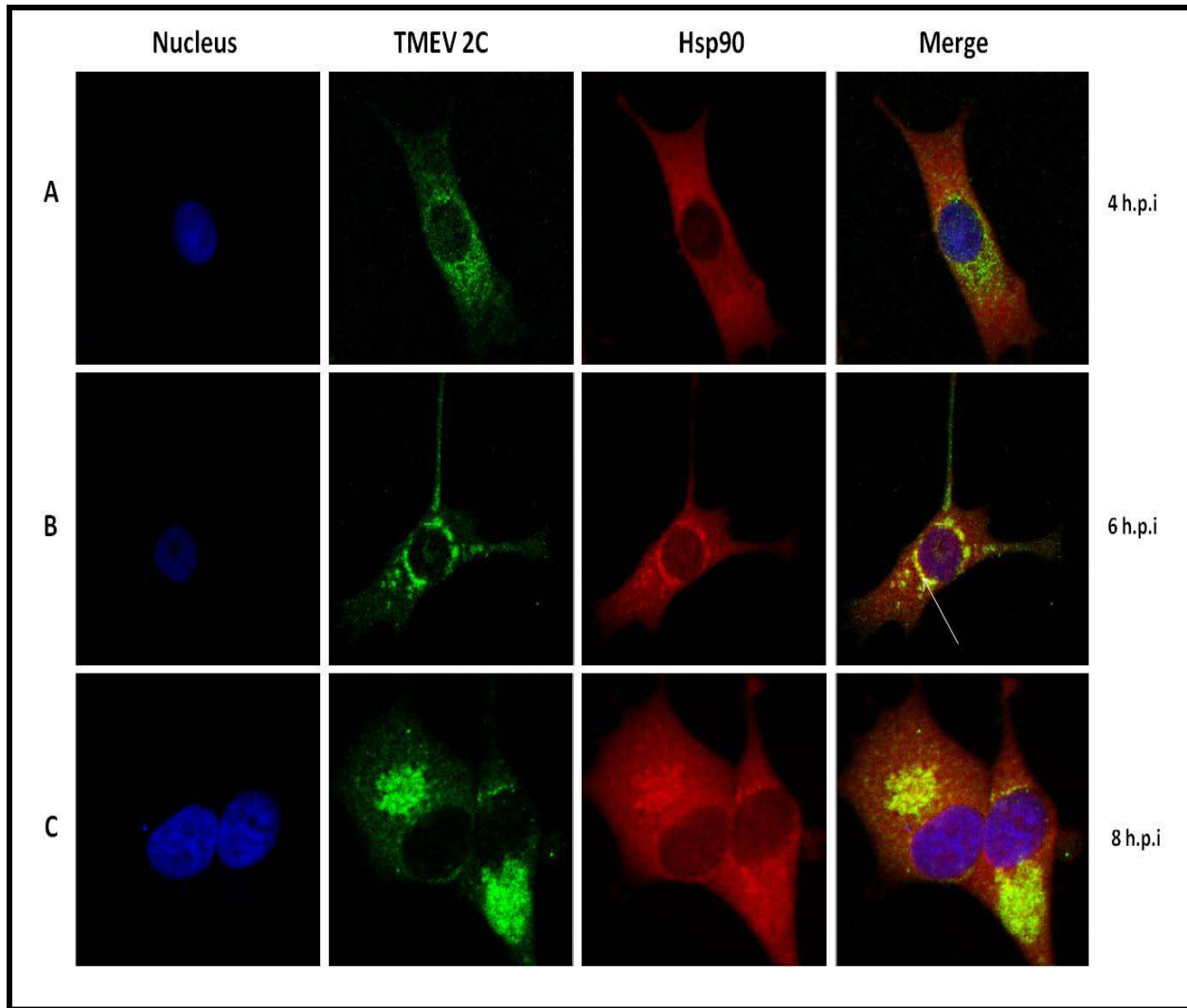


**Figure 4.4: Distribution of Hsp90 in TMEV-infected BHK-21 cells during different stages of infection.** Cells were grown on coverslips and infected with TMEV, fixed with 4% paraformaldehyde at 4 h.p.i (panel A), 6 h.p.i (panel B) and 8 h.p.i (panel C), permeabilised and dual-stained with anti-Hsp90 and anti-TMEV 2C antibodies. Primary antibodies were detected with species-specific Alexa Fluor 546-conjugated secondary antibodies for Hsp90 or Alexa Fluor 488-conjugated secondary antibodies for TMEV 2C. White arrow indicates where Hsp90 and 2C signals overlap.

### 4.3.2 Time course of Hsp expression

Confocal analysis indicated that Hsp90, Hsp70 and Hsp40 are involved in one or other aspect of TMEV infection. Based on this observation, the following experiment sought to examine the expression levels of Hsp90, Hsp70 and Hsp40 during TMEV-infection. In order to conduct such a study, it was necessary to ensure that the antibodies used in the IF experiments could detect the Hsps and viral proteins in infected cell lysates by Western analysis. BHK-21 cells were infected

with TMEV, harvested at 0, 2, 4, 6 and 8 h.p.i, lysed and analysed by SDS-PAGE and Western analysis using antibodies raised against TMEV P1, TMEV 2C, Hsp90, Hsp70 and Hsp40. Actin was also analysed as an internal control. Results are presented in Figure 4.5. As the figure illustrates, all six antibodies tested detected their respective proteins in cell lysates by Western analysis. As expected, no signals for TMEV 2C and TMEV P1 were detected in cell lysates collected at 0 h.p.i. Both viral proteins were only detected at 6 h.p.i (images i and ii), confirming that cells were infected with TMEV at this time point. Host proteins, Hsp40, Hsp70, Hsp90 and actin were detected in all cell lysates collected 0, 2, 4, 6 and 8 h.p.i, as indicated by the presence of the strong signals (images iii, iv, v and vi).

Due to time constraints, the expression levels of Hsp90, Hsp70 and Hsp40 in TMEV-infected cell lysates were not examined. The ability of these antibodies to detect their protein antigens in TMEV-infected cell lysates will allow future experiments involving expression of Hsp90, Hsp70 and Hsp40 in TMEV-infected cells to be conducted. These experiments will be described in Chapter 5.

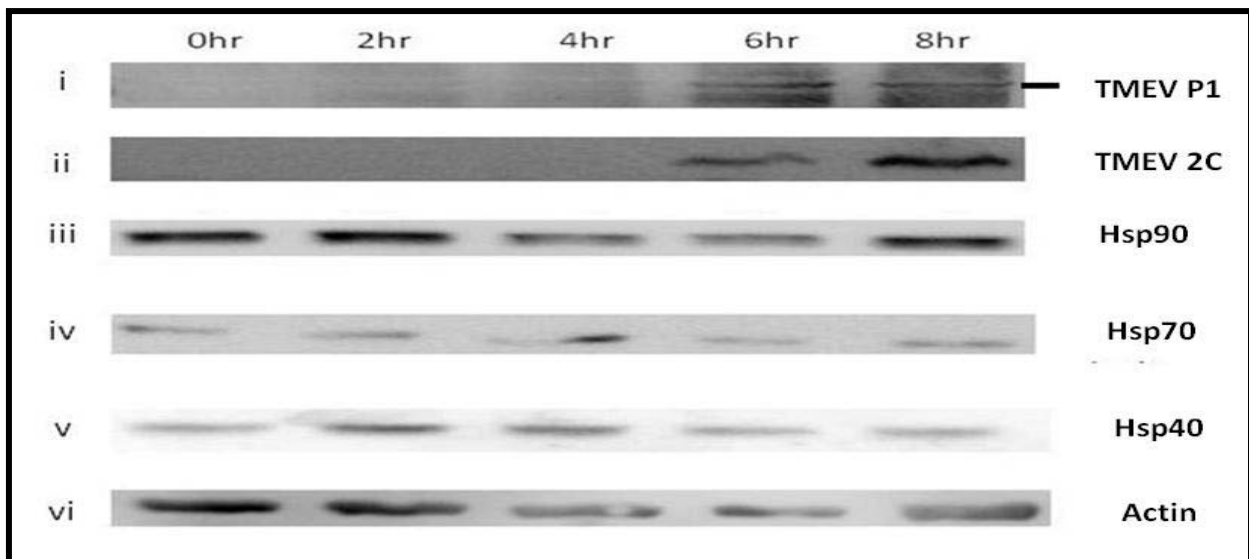


**Figure 4.5: Western analysis of TMEV-infected cell lysates.** Cells were infected with TMEV and collected at 0, 2, 4, 6 and 8 h.p.i and analysed by SDS-PAGE and Western analysis. The following proteins were detected (i) TMEV P1 using anti-TMEV P1 antibodies, (ii) TMEV 2C using anti-TMEV 2C antibodies, (iii) Hsp90 using anti-Hsp90 antibodies, (iv) Hsp70 using anti-Hsp70/Hsc70 antibodies, (v) Hsp40 using anti-Hsp40 antibodies and (vi) Actin using anti-Actin antibodies.

## **4.4 Discussion**

This chapter describes the use of confocal microscopy to examine the distribution of Hsp90, Hsp70 and Hsp40 in mock-infected and TMEV-infected BHK-21 cells. In addition, the distribution of Hsp90 during the course of infection was also examined.

All three Hsps showed a change in distribution in TMEV-infected cells at 6.5 h.p.i. In mock-infected cells, the Hsp40 signal was mostly concentrated in the perinuclear region, with some nuclear staining. In the majority of cells examined, Hsp40 redistributed to the nucleus, suggesting that Hsp40 had a specialised role in the nucleus during infection. Interestingly, it was also observed that, in uninfected cells surrounded by TMEV-infected cells, Hsp40 had also relocated into the nucleus. Although the significance of these observations is not understood, it is tempting to speculate that the re-localisation mimics that of stress situations such as heat and hypoxia, where it has been shown that, in cells under heat stress, Hsp40 is upregulated and relocates to the nucleus (Hattori *et al.*, 1992; 1993; Yamane *et al.*, 1995). However, it must be acknowledged that the anti-Hsp40 antibodies used during this study recognise all J domain proteins because they were raised against the conserved J domain region. The signal detected in the nucleus could represent multiple Hsp40 type proteins. As described in chapter 1 (section 1.4.4), there are numerous Hsp40s in eukaryotic cells, belonging to different classes, namely type 1, type 2 and type 3. Hsp40s are localised in the cytosol, the nucleus, endosomes, mitochondria, the ER, and ribosomes and depending on the type, have different cellular functions (reviewed by Qiu, *et al.*, 2006). For example, type 1 Hsp40s are known to function as chaperones to suppress protein aggregation, and are independent of Hsp70. Type 2 Hsp40s, on the other hand, assist in transferring substrates to Hsp70 and act as co-chaperones (reviewed by Fan *et al.*, 2003; Qiu *et al.*, 2006; Rosser and Cyr, 2007). Type 3 Hsp40s have a more specialised function such as the recruitment of a specific isoform of Hsp70 to a particular site as seen in the case of Sec63 which is anchored in the ER by transmembrane domains. The J domain is exposed in the lumen of ER where it recruits Hsp70 to polypeptides that are in transit to the ER (Corsi and Schekman, 1997). Many viruses have been shown to utilise different types Hsp40s during replication. For example, HIV-1 requires DnaJB6, a type 2 Hsp40 to facilitate nuclear import of viral proteins (Cheng *et al.*, 2008). In both Influenza A and B viruses, Hdj1, another type 2 Hsp40, binds to M2 protein, a protein that is essential for virus uncoating and replication (Guan *et al.*, 2010). Hdj1, along with

Hdj2, a type 1 Hsp40, have been shown to enhance the binding affinity of the human papillomavirus-11 protein E1, a replication initiator helicase, to the origin of replication on viral DNA (Liu *et al.*, 1998). The presence of the Hsp40 signals in the cytoplasm and nucleus in TMEV-infected cells, suggests that different types of Hsp40s play different roles in viral activities. For example, type 2 Hsp40s may be remaining in the cytoplasm to assist Hsp70 in capsid assembly. On the other hand, other types of Hsp40s localise to the nucleus, where they have specialised functions during stress situations, as seen in cells under heat stress (Hattori *et al.*, 1992; 1993; Yamane *et al.*, 1995). In order to identify which Hsp40s are remaining in the cytoplasm or moving in to the nucleus during TMEV infection, antibodies specific to different Hsp40 types will be required to define their respective localisation.

The punctuate Hsp70 staining pattern observed in mock-infected BHK-21 cells using anti-Hsp70/Hsc70 antibodies was unexpected because several studies have illustrated that staining of Hsp70 in cells under homeostatic conditions is uniformly distributed throughout the cytoplasm (Bivik *et al.*, 2006; Leger *et al.*, 2000). The staining pattern observed in this study, however correlates with that reported in clonal striatal cells (Kegel *et al.*, 2000) and hippocampal neurons (Moon *et al.*, 2001) using anti-Hsp70/Hsc70 antibodies. Unlike in the typical stress response induced by heat shock (Ohtsuka and Laszlo, 1992, Hatayama *et al.*, 1993; Hattori *et al.*, 1993; Yamane *et al.*, 1995), Hsp70 in TMEV-infected BHK-21 cells did not localise to the nucleus. Instead, during late infection, Hsp70 converged around the large TMEV 2C-containing structure that was adjacent to the nucleus. This large structure has been identified as the viral replication complex which is the site of viral genome synthesis and is formed in the region of the Golgi apparatus (Jauka *et al.*, 2010). At present, the significance of this observation is currently unknown. However, it may be linked to the observation made by Macejak and Sarnow (1992) who illustrated that Hsp70 interacted and formed a highly stable association with the enterovirus precursor capsid protein suggesting that it plays a role in the virus assembly process. It is possible that, during TMEV infection, Hsp70 converges around the replication complex as opposed to moving into the nucleus because Hsp70 is sequestered by nascent P1 in the cytoplasm to facilitate in the folding of the precursor protein into a conformation that allows the proper cleavage of the protein into mature capsid proteins. Alternatively, Hsp70 may be performing one of its natural roles in the cell which is to transport newly synthesised proteins to various membranes (reviewed by Bukau and Horwich 1998), in this case, those of the replication

complex. Although Hsp70 converged around the replication complex, there was no overlap between the two signals, indicating that TMEV 2C and Hsp70 do not colocalise.

Confocal analysis illustrated that, at 6.5 h.p.i, Hsp90 in mock-infected cells was distributed uniformly in the cytoplasm but, in TMEV-infected cells, had redistributed to the perinuclear region where it overlapped with TMEV 2C during the later stages of infection. It was also observed that Hsp90 moved into the nucleus during late infection.

Based on the localisation pattern observed at 6.5 h.p.i, the distribution of Hsp90 was examined over time at 4, 6 and 8 h.p.i. Analysis of infected cells at the different time points demonstrated that the redistribution of Hsp90 into the perinuclear region and nucleus of TMEV-infected cells was clearly dependent on the stage of infection. Although the significance of this observation is not clearly understood, this stage-dependent redistribution was observed in numerous cells. During early stages of infection (4 h.p.i) 91% of 172 imaged cells showed that Hsp90 was mainly localised in the cytoplasm. Later during infection, (6 h.p.i), a significant amount of Hsp90 was concentrated in the perinuclear region as seen in 89% of 106 imaged cells, where the Hsp90 signal overlapped with TMEV 2C, suggesting the two proteins colocalised at that region. During the late stages of infection (8 h.p.i), the Hsp90 signal was found in the nucleus as well as concentrated within the replication complex, as observed in 84% of 93 imaged cells, suggesting that colocalisation between Hsp90 and TMEV 2C is also occurring during late infection. Currently there is no evidence in the literature that supports the possibility of an interaction between TMEV 2C and Hsp90, although it has been shown that Hsp90 interacts with the capsid precursor protein in enteroviruses where it facilitates in the proper folding and maturation of the protein (Geller *et al.*, 2007).

One explanation for the observation that Hsp90 is concentrated in the perinuclear region of infected cells as well as in the cytoplasm and nucleus could be because it is an abundant protein that makes up ~1% of all soluble proteins (Lai *et al.*, 1994), suggesting that only a small pool of the total protein is required by the virus. Also, based on the model of Geller *et al.*, 2007, the interaction between Hsp90 and P1 could be dynamic, suggesting that once the precursor capsid protein is cleaved into the various mature capsid proteins, Hsp90 is released back into the

cytoplasm and is free to move into the nucleus as seen in heat stressed cells (van Bergen en Henegouwen *et al.*, 1987; Berbers *et al.*, 1988).

Based on the observations made during confocal analysis, where Hsp90, Hsp70 and Hsp40 were illustrated to be involved in TMEV-infection, the following experiment sought to examine the expression levels of Hsp90, Hsp70 and Hsp40 in infected cell lysates. Before the expression levels of Hsps in TMEV-infected cell lysates could be examined, it was crucial to determine that the antibodies used during IF could detect their protein antigens including Hsp90, Hsp70 and Hsp40, as well as TMEV 2C and TMEV P1 by Western analysis in infected cell lysates. Antibodies raised against TMEV 2C and TMEV P1 were able to detect the viral proteins in infected cell lysates at 6 and 8 h.p.i, which confirmed that TMEV-infection was successful. Western analysis also illustrated the specificity of both viral antibodies as indicated by the absence of protein signals in the cell lysate prepared at 0 h.p.i. The antibodies raised against Hsp90, Hsp70 and Hsp40 detected their respective antigens in all cell lysate samples collected 0, 2, 4, 6 and 8 h.p.i. Actin was chosen as an internal control in this experiment because it is a highly conserved protein that is major component of the cytoskeleton in all cells and is known to be the most abundant protein within the cell, accounting for about 15% of proteins within some cells. Due to the abundance of actin compared to other cellular proteins and the fact that the expression levels of actin are constant within cells, actin is commonly used as a loading control during Western analysis. Anti-Actin antibodies were able to detect actin in TMEV-infected lysates. Due to time constraints, examination of Hsp90, Hsp70 and Hsp40 expression levels in TMEV-infected cell lysates could not be conducted.

#### **4.5 Conclusion**

The distribution of Hsp90, Hsp70 and Hsp40 was successfully examined in TMEV-infected BHK-21 cells. In addition, infected cell lysates were probed with antibodies against Hsp90, Hsp70, Hsp40, actin, TMEV 2C and TMEV P1 in order to test their specificity using Western analysis. The following conclusions were reached relating to the localisation and detection of Hsp90, Hsp70 and Hsp40 in TMEV-infected cells:

- Hsp40 localised to the nucleus in infected cells, while some of the protein remained in the cytoplasm. Hsp40 and TMEV P1 signals overlapped in the perinuclear region, suggesting that the two proteins colocalise.
- Hsp70 converged around the large TMEV 2C-containing, juxta-nuclear structure representing replication complex in the late stages of infection. Hsp70 and TMEV 2C signals did not overlap.
- Hsp90 localised to the perinuclear region and the replication complex, where TMEV 2C was also located, during the middle and later stages of TMEV-infection, respectively. Overlap between Hsp90 and TMEV 2C was observed.
- Hsp90, Hsp70, Hsp40 and actin were detected at 0, 2, 4, 6 and 8 h.p.i and TMEV 2C and TMEV P1 were detected 6 and 8 h.p.i in TMEV-infected cell lysates by Western analysis.

## Chapter 5: General Conclusions and Future Work

This study sought to increase the present understanding of picornavirus-Hsp interactions, specifically those between TMEV and Hsp90, Hsp70 and Hsp40. Using confocal microscopy and Western analysis, several important observations were made. Firstly, the inhibition of Hsp90 function in TMEV-infected cells using GA and Nov had a negative effect on TMEV growth as seen by the absence of CPE. In addition, TMEV 2C was detected in the lysates of TMEV-infected cells treated with GA, but not in those treated with Nov. Secondly, confocal microscopy showed that the distribution of Hsp40, Hsp70 and Hsp90 changed in TMEV-infected cells compared to mock-infected cells. Thirdly, the distribution of Hsp90 appeared to be dependent on the stage of infection. In the case of Hsp40, the protein appeared to concentrate in the nucleus during infection. However, some of the protein remained in the cytoplasm and an overlap between the Hsp40 and TMEV P1 signals was observed in the perinuclear region. Hsp70 converged around the TMEV 2C-containing replication complex, but overlap of the two signals was not observed. Hsp90 concentrated in perinuclear region where TMEV 2C was also located and an overlap between the two signals was observed.

The role of Hsp90 in viral activities has been widely documented. Studies have shown that inhibition of Hsp90 in virus-infected cells affects virus growth by either reducing or inhibiting viral replication in viruses such as FHV (Kampmueller and Miller, 2005), enteroviruses (Geller *et al.*, 2007), Influenza virus (Chase *et al.*, 2008) and Ebola virus (Smith *et al.*, 2010). In this study, the Hsp90 inhibitors, GA and Nov, were used to determine if the inhibition of Hsp90 in TMEV-infected BHK-21 cells would inhibit virus growth as observed for other viruses. Absence of TMEV-induced CPE in Nov- and GA-treated cells suggests that Hsp90 is required during some aspect of the TMEV replication process as was seen for enteroviruses where Hsp90 is required to mediate the proper folding and maturation of virus capsid proteins (Geller *et al.*, 2007).

Although, the inhibitory effects of Nov on viruses such as HSV-1 (Franke and Margolin, 1981), Human cytomegalovirus (Landini and Baldassarri, 1982) and murine and avian Retroviruses (Sumiyoshi *et al.*, 1983) have been examined, to our knowledge, no studies have been conducted

to examine the effects of Nov in picornavirus-infected cells. This study provides the first evidence demonstrating that this drug affects the life cycle of the picornavirus, TMEV. Although both drugs affected TMEV growth, they appeared to act differently. A prominent signal for TMEV 2C was detected by Western analysis in infected cell lysates treated with GA, indicating that the drug had no effect on the synthesis and processing of the non-structural protein. These results coincided with those in literature, where it was found that the inhibition of Hsp90 with GA did not affect the translation or processing of viral non-structural proteins (Geller *et al.*, 2007). In contrast, TMEV 2C was not detected in TMEV-infected cells treated with Nov suggesting that, unlike GA, Nov is able to affect the translation or processing of TMEV 2C. This is possibly due to the different mechanisms by which these drugs inhibit Hsp90 function. The absence of the TMEV 2C signal in Nov-treated cells may also be indicative of an additional yet unknown role for Hsp90 during TMEV infection that is somehow linked to the production of TMEV 2C. However, it is clear from the results presented in this study that Hsp90 is involved in TMEV replication. Future studies to examine the mechanism involved will investigate TMEV virus yield in Nov- and GA-treated BHK-21 cells by plaque assays. These experiments will determine if the absence of CPE observed in TMEV-infected cells treated with either Nov or GA is due to a reduction in the production of viable virus particles.

The absence of a TMEV 2C signal in Nov-treated cell lysates and its presence in GA-treated cells is not clearly understood and will need to be further examined. This observation suggests that Nov may affect the translation and processing of TMEV 2C, while GA does not. An important future study will be to investigate the effects of Nov and GA on TMEV protein production by IF and confocal microscopy. For example, BHK-21 cells infected in the presence of Nov and GA can be stained using anti-TMEV 2C or anti-TMEV P1 antibodies at various times post-infection to monitor the presence or absence of these viral proteins. In addition, Western analysis can also be conducted to analyse infected cell lysates treated with Nov and GA for the presence or absence of TMEV P1 and non-structural proteins other than TMEV 2C.

The observation that Hsp90 inhibitors prevented TMEV growth prompted an experiment which sought to examine whether the distribution of Hsp90, as well as Hsp70 and Hsp40, was affected by TMEV infection in cells using IF and confocal microscopy. TMEV 2C and TMEV P1 were used as markers for infection.

It was observed that Hsp40 redistributed to the nucleus during infection although a significant proportion of the signal remained in the cytoplasm and in the perinuclear region. In mock-infected cells, the signal was mostly concentrated in the perinuclear region, although, nuclear staining was also present. In infected cells, partial overlap between Hsp40 and TMEV P1 was observed in the perinuclear region suggesting colocalisation between the two proteins. Future experiments will be conducted to investigate this possibility by performing Z-stack analysis using the Axiovision LE/ SE software (Carl Zeiss, Germany). Co-immunoprecipitation experiments will also confirm possible interactions between TMEV P1 and Hsp40.

Since the antibodies used in this study are raised against all J domain proteins, it is not known which Hsp40s are involved in TMEV infection. Future experiments involving antibodies specific for the different types of Hsp40s will be conducted to investigate their distribution in infected cells.

It is known that Hsps including Hsp40, Hsp70 and Hsp90 may be upregulated in stress situations. In addition, certain viruses are known to up or down regulate Hsps. Preliminary experiments described in this study revealed that Hsp40, Hsp70 and Hsp90 could be detected in cell lysates of infected cells. Future experiments will involve investigating expression levels of Hsp40, Hsp70 and Hsp90 in infected cells by Western analysis. It was also noted that anti-Actin antibodies detect the protein in infected cells. This protein can be used as an internal control to monitor expression of Hsp90, Hsp70 and Hsp40 during infection as has been performed in other studies. Densitometry analysis using the ImageJ Java-based image processing program will be conducted to quantitatively measure Hsp90, Hsp70 and Hsp40 expression levels.

The Hsp70 staining pattern in mock-infected cells was predominantly diffuse and punctative in the cytoplasm. During late infection, it had converged around the large TMEV 2C-containing replication complexes adjacent to the nucleus, and no overlap between the two signals was observed. This observation may possibly be as a result of nascent TMEV P1 sequestering Hsp70 to assist in the folding of the precursor capsid protein into a conformation required for cleavage, as suggested by Macejak and Sarnow, 1992. Additional studies will need to be conducted to further investigate the significance of these observations. These experiments could involve conducting co-immunoprecipitation analysis to examine interactions between Hsp70 and TMEV P1.

The redistribution of Hsp90 was found to be dependent on the stage of infection. During earlier stages of infection, the Hsp90 signal was uniformly dispersed in the cytoplasm, similar to that observed in mock-infected cells. During the middle and late stages of infection, the Hsp90 signal was found concentrated in the perinuclear region and within the replication complex, where TMEV 2C was also located. An overlap between the signals of Hsp90 and TMEV 2C was observed at both regions, suggesting colocalisation. To investigate the possibility of colocalisation between the two proteins, Z-stack analysis can be performed using the Axiovision LE/ SE software (Carl Zeiss, Germany). Co-immunoprecipitation experiments can also be conducted both in the presence or absence of GA and Nov.

In conclusion, this study was able to identify Hsp90, Hsp70 and Hsp40 as possible host cell factors involved in either the replication or assembly process of TMEV. The results reported in this study have set a platform for future studies to examine Hsp-TMEV interactions that will provide better understanding of these conserved and vital proteins in the life cycle of picornaviruses. There are currently no anti-viral agents for the treatment of picornavirus infections which have a devastating effect on human and animal health. It is therefore of vital importance to gain a better understanding of virus-host interactions that can be targeted by novel antiviral therapies.

## Chapter 6: References

**Abed Y & Boivin G** (2008) New Saffold coronaviruses in 3 children, Canada. *Emerging infectious diseases* **14**, 834-836.

**Agol VI** (1991) The 5'-untranslated region of picornaviral genomes. *Advances in virus research* **40**, 103-180.

**Aldabe R & Carrasco L** (1995) Induction of membrane proliferation by poliovirus proteins 2C and 2BC. *Biochemical and biophysical research communications* **206**, 64-76

**Alfano C & McMacken R** (1989) Heat shock protein-mediated disassembly of nucleoprotein structures is required for the initiation of bacteriophage lambda DNA replication. *Journal of biological chemistry* **264**, 10709-10718.

**Ali JA, Jackson AP, Howells AJ & Maxwell A** (1993). The 43-kDa N-terminal fragment of the gyrase B protein hydrolyses ATP and binds to coumarin drugs. *Journal of biochemistry* **32**, 2717–2724.

**Andino R, Bøddeker N, Silvera D & Gamarnik AV** (1999) Intracellular determinants of picornavirus replication. *Trends in microbiology* **7**, 76-82.

**Armer H, Moffat K, Wileman T, Belsham GJ, Jackson T, Duprex WP, Ryan M & Monaghan P** (2008) Foot-and-Mouth Disease Virus, but Not Bovine Enterovirus, Targets the Host Cell Cytoskeleton via the Nonstructural Protein 3C pro. *Society* **82**, 10556-10566.

**Arrigo AP & Landry J** (1994) *Expression and function of the low molecular-weight heat shock proteins*. In: *The Biology of Heat Shock Proteins and Molecular Chaperones*, edited by Morimoto RI, Tissieres A & Georgopoulos C. Cold Spring Harbor, NY: Cold Spring Harbor Laboratory.

**Arrigo AP, Suhan JP & Welch WJ** (1988) Dynamic changes in the structure and intracellular locale of the mammalian low-molecular weight heat shock protein. *Molecular and cell biology* **8**, 5059–5071.

**Banecki B, Liberek K & Wall D** (1996) Structural-function analysis of the zinc finger region of the DnaJ molecular chaperone. *Journal of biological chemistry* **271**, 14840-14848.

**Beck R & Nassal M** (2001) Reconstitution of a Functional Duck Hepatitis B Virus Replication Initiation Complex from Separate Reverse Transcriptase Domains Expressed in *Escherichia coli*. *Society* **75**, 7410-7419.

**Beck J & Nassal M** (2003) Efficient Hsp90-independent in vitro activation by Hsc70 and Hsp40 of duck hepatitis B virus reverse transcriptase, an assumed Hsp90 client protein. *Journal of biological chemistry* **278**, 36128-36138.

**Bedard KM & Semler BL** (2004) Regulation of picornavirus gene expression. *Microbes and infection / Institut Pasteur* **6**, 702-713.

**Berbers GA, Kunnen R, van Bergen en Henegouwen PM & van Wijk R** (1988). Localization and quantitation of hsp84 in mammalian cells. *Experimental cell research* **177**, 257-271.

**Bienz K, Egger D, Pfister T & Troxler M** (1992) Structural and functional characterization of the poliovirus replication complex. *Journal of virology* **66**, 2740–2747.

**Bivik C, Rosdahl I & Ollinger K** (2007) Hsp70 protects against UVB induced apoptosis by preventing release of cathepsins and cytochrome *c* in human melanocytes. *Carcinogenesis* **28**, 537–544.

**Blinkova O, Kapoor A, Victoria J, Jones M, Wolfe N, Naeem A, Shaukat S, Sharif S, Alam MM, Angez M, Zaidi S & Delwart EL** (2009) Cardioviruses are genetically diverse and cause common enteric infections in South Asian children. *Journal of virology* **83**, 4631-4641.

**Bohen SP** (1995) Hsp90 mutants disrupt glucocorticoid receptor ligand binding and destabilize aporeceptor complexes. *Journal of biological chemistry* **270**, 29433-29438.

**Bouhouche-Chatelier I, Chadli A & Catelli M** (2001). The N-terminal adenosine triphosphate binding domain of Hsp90 is necessary and sufficient for interaction with estrogen receptor. *Cell stress and chaperones* **6**, 297-305.

**Brenner BG & Wainberg MA** (1999) Heat shock protein-based therapeutic strategies against human immunodeficiency virus type 1 infection. *Infectious diseases in obstetrics and gynaecology*, **7**, 80-90.

**Buchkovich NJ, Maguire TG, Yu Y, Paton AW, Paton JC, Alwine JC** (2008) Human cytomegalovirus specifically controls the levels of the endoplasmic reticulum chaperone BiP/GRP78, which is required for virion assembly. *Journal of virology* **82**, 31–39.

**Buchner J** (1999) Hsp90 & Co. - a holding for folding. *Trends in biochemical sciences* **24**, 136-141.

**Buenz EJ & Howe CL** (2006) Picornaviruses and cell death. *Trends in microbiology* **14**, 28-36.

**Bukau B & Horwich AL** (1998) The Hsp70 and Hsp60 chaperone machines. *Cell* **92**, 351-366.

**Burch AD & Weller SK** (2005) Herpes Simplex Virus Type 1 DNA Polymerase Requires the Mammalian Chaperone Hsp90 for Proper Localization to the Nucleus. *Society* **79**, 10740-10749.

**Cann AJ** (1997) Principles of Molecular Virology, 2<sup>nd</sup> edition. London, UK: Academic Press.

**Campbell KS, Mullane KP, Aksoy IA, Stubdal H, Zalvide J, Pipas JM, Silver PA, Roberts TM, Schaffhausen BS & DeCaprio JA** (1997) DnaJ/hsp40 chaperone domain of SV40 large T antigen promotes efficient viral DNA replication. *Genes and development* **11**, 1098-1110.

**Caplan AJ, Mandal AK & Theodoraki MA** (2007) Molecular chaperones and protein kinase quality control. *Trends in cell biology* **17**, 87-92.

**Carrello A, Ingle E, Minchin RF, Tsai S & Ratajczak T** (1999) The common tetratricopeptide repeat acceptor site for steroid receptor- associated immunophilins and Hop is located in the dimerization domain of Hsp90. *Journal of biological chemistry* **274**, 2682–2689.

**Castorena KM, Weeks SA, Stapleford KA, Cadwallader AM & Miller DJ** (2007) A functional heat shock protein 90 chaperone is essential for efficient flock house virus RNA polymerase synthesis in *Drosophila* cells. *Journal of virology* **81**, 8412-8420.

**Chabaud S, Lambert H, Sasseville AM, Lavoie H, Guilbault C, Massie B, Landry J, Langelier Y** (2003) The R1 subunit of herpes simplex virus ribonucleotide reductase has chaperone-like activity similar to Hsp27. *FEBS letters* **545**, 213–218.

**Chase G, Deng T, Fodor E, Wah Leung B, Mayer D, Schwemmle M & Brownlee G** (2008) Hsp90 inhibitors reduce influenza virus replication in cell culture. *Virology* **377**, 431-439.

**Chatterji U, Bobardt M, Selvarajah S, Yang F, Tang H, Sakamoto N, Vuagniaux G, Parkinson T, Gallay P** (2009) The isomerase active site of cyclophilin A is critical for hepatitis C virus replication. *Journal of biological chemistry* **284**, 16998–17005.

**Chavany C, Mimnaugh E, Miller P, Bitton R, Nguyen P, Trepel J, Whitesell L, Schnur R, Moyer J & Neckers L** (1996) p185erbB2 binds to GRP94 in vivo. Dissociation of the p185erbB2/GRP94 heterocomplex by benzoquinone ansamycins precedes depletion of p185erbB2. *Journal of biological chemistry* **271**, 4974-4977.

**Cheetham ME & Caplan AJ** (1998) Structure, function and evolution of DnaJ: conservation and adaptation of chaperone function. *Cell stress and chaperones* **3**, 28-36.

**Chen S, Sullivan WP, Toft DO & Smith DF** (1998) Differential interactions of p23 and the TPR-containing proteins Hop, Cyp40, FKBP52 and FKBP51 with Hsp90 mutants. *Cell stress and chaperones* **3**, 118–129.

**Cheng X, Belshan M & Ratner L** (2008) Hsp40 Facilitates Nuclear Import of the Human Immunodeficiency Virus Type 2 Vpx-Mediated Preintegration Complex. *Journal of virology* **82**, 1229-1237.

**Chiosis G, Vilenchik M, Kim J & Solit D** (2004) Hsp90: the vulnerable chaperone. *Drug discovery today* **9**, 881-888.

**Chiu CY, Greninger AL, Kanada K, Kwok T, Fischer K, Runckel C, Louie J, Glaser C, Vagi S, Schnurr D, Haggerty TD, Parsonnet J, Ganem D & Van Der Vusse GJ** (2008) Identification of cardioviruses related to Theiler's murine encephalomyelitis virus in human infections. *Proceedings of the national academy of sciences of the United States of America* **105**, 14124-14129.

**Cho MW, Teterina N, Egger D, Bienz K & Ehrenfeld E** (1994) Membrane rearrangement and vesicle induction by recombinant poliovirus 2C and 2BC in human cells. *Virology* **202**, 129-45.

**Cho DY, Yang GH, Ryu CJ & Hong HJ** (2003) Molecular chaperone GRP78/BiP interacts with the large surface protein of hepatitis B virus in vitro and in vivo. *Journal of virology* **77**, 2784–2788.

**Choukhi A, Ung S, Wychowski C & Dubuisson J** (1998) Involvement of endoplasmic reticulum chaperones in the folding of hepatitis C virus glycoproteins. *Journal of virology* **72**, 3851–3858.

**Chromy LR, Pipas JM & Garcea RL** (2003) Chaperone-mediated in vitro assembly of Polyomavirus capsids. *Proceedings of the national academy of sciences of the United States of America* **100**:10477–10482.

**Citri A, Gan J, Mosesson Y, Vereb, G, Szollosi J & Yarden Y** (2004). Hsp90 restrains ErbB-2/HER2 signalling by limiting heterodimer formation. *EMBO reports* **5**, 1165-1170.

**Cobbold C, Windsor M & Wileman T** (2001) A virally encoded chaperone specialized for folding of the major capsid protein of African swine fever virus. *Journal of virology* **75**, 7221–7229.

**Connor JH, McKenzie MO, Parks GD & Lyles DS** (2007) Antiviral activity and RNA polymerase degradation following Hsp90 inhibition in a range of negative strand viruses. *Virology* **362**, 109 - 119.

**Corsi AK & Schekman R** (1997) The luminal domain of Sec63p stimulates the ATPase activity of BiP and mediates BiP recruitment to the translocon in *Saccharomyces cerevisiae*. *Journal of cell biology* **137**, 1483-1493.

**Couturier M, Buccellato M, Costanzo S, Bourhis J, Shu Y, Nicaise M, Desmadril M, Flaudrops C, Longhi S & Oglesbee** (2009) High affinity binding between Hsp70 and the C-terminal domain of the measles virus nucleoprotein requires an Hsp40 co-chaperone. *Journal of molecular recognition*.

**Cowen LE & Lindquist S** (2005) Hsp90 potentiates the rapid evolution of new traits: Drug resistance in Diverse Fungi. *Science* **309**, 2185-2189.

**Das S, Laxminarayana SV, Chandra N, Ravi V & Desai A** (2009) Heat shock protein 70 on Neuro2a cells is a putative receptor for Japanese encephalitis virus. *Virology* **385**, 47–57.

**DeBoer C, Meulman PA, Wnuk RJ & Peterson DH** (1970) Geldanamycin, a new antibiotic. *Journal of antibiotics* **23**, 442–447.

**Donnelly A & Blagg BSJ** (2008) Novobiocin and additional inhibitors of the Hsp90 C-terminal nucleotide-binding pocket. *Current medical chemistry* **15**, 2702–2717.

**Drexler J, de Souza L, Stocker A, Silva Almeida P, Medrado Ribeiro T, Pertersen N, Herzog P, Pedroso C, Huppertz H, de Costa Ribeiro H, Baumgarte S & Drosten C** (2008) Circulation of 3 lineages of a novel saffold cardiovirus in humans. *Emerging infectious diseases* **14**, 1398-1405.

**Dubuisson J & Rice CM** (1996) Hepatitis C virus glycoprotein folding: disulfide bond formation and association with calnexin. *Journal of virology* **70**, 778–786.

**Dubuisson J** (1998) The role of chaperone proteins in the assembly of envelope proteins of hepatitis C virus. *Bulletin et memoires de l'Academie royale de medecine de Belgique* **153**, 343–349.

**Dutta R & Inouye M** (2000) GHKL, an emergent ATPase/kinase superfamily. *Trends in biochemical science* **25**, 24–28.

**Ellis J** (1987) Proteins as molecular chaperones. *Nature* **328**, 378-379.

**Fan C, Lee S & Cyr DM** (2003) Mechanisms for regulation of Hsp70 function by Hsp40. *Cell stress and chaperones* **8**, 309-316.

**Feldheim D, Rothblatt J & Schekman R** (1992) Topology and functional domain of Sec63p, an endoplasmic reticulum membrane protein required for secretory protein translocation. *Molecular and cell biology* **12**, 3288-3296.

**Feldman DE & Frydman J** (2000) Protein folding in vivo: the importance of molecular chaperones. *Current opinion in structural biology* **10**, 26-33.

**Fendrick A, Monto A, Nightengale B & Sarnes M** (2003) The economic burden of non influenza-related viral respiratory tract infections in the United States. *Archives of internal medicine* **163**, 487-494.

**Fink AL** (1999) Chaperone-mediated protein folding. *Physiological reviews* **79**, 425-449.

**Finsterbusch T, Steinfeldt T, Doberstein K, Rödner C & Mankertz A** (2009) Interaction of the replication proteins and the capsid protein of porcine circovirus type 1 and 2 with host proteins. *Virology* **386**, 122-131.

**Flaherty KM, DeLuca-Flaherty C & McKay DB** (1990) Three-dimensional structure of the ATPase fragment of a 70K heat-shock cognate protein. *Nature* **346**, 623-628.

**Franke B & Margolin J** (1981) Effect of novobiocin and other gyrase inhibitors on virus replication and DNA synthesis in Herpes Simplex virus type 1-infected BHK-21 cells. *Journal of general virology* **52**, 401-404.

**Friedmann A & Lipton HL** (1980) Replication of Theiler's murine encephalomyelitis virus in BHK-21 cells: an electron microscopic study. *Virology* **101**, 389-398.

**Frydman J** (2001) Folding of newly translated protein in vivo: The role of molecular chaperones. *Annual review of biochemistry* **70**, 603-647.

**Fujinami RS, Zurbriggen A & Powell HC** (1988) Monoclonal antibody defines determinant between Theiler's virus and lipid like structures. *Journal of neuroimmunology* **20**, 25-32.

**Geller R, Vignuzzi M, Andino R & Frydman J** (2007) Evolutionary constraints on chaperone-mediated folding provide an antiviral approach refractory to development of drug resistance. *Genes & development* **21**, 195-205.

**Genevaux P, Lang F, Vartikar JV, Rundell K, Pipas JM, Georgopoulos C & Kelley WL** (2003) Simian Virus 40 T Antigens and J Domains : Analysis of Hsp40 Cochaperone Functions in Escherichia coli. *Society* **77**, 10706-10713.

**Grenert JP, Sullivan WP, Fadden P, Haystead TAJ, Clark J & Mimnaugh E** (1997) The amino-terminal domain of heat shock protein 90 (hsp90) that binds geldanamycin is an ATP/ADP switch domain that regulates hsp90 conformation. *Journal of biological chemistry* **272**, 23843–23850.

**Grubman MJ & Baxt B** (2004) Foot-and-Mouth Disease. *Clinical microbiology reviews* **17**, 465-493.

**Guan Z, Liu D, Mi S, Zhang J, Ye Q, Wang M, Gao GF & Yan J** (2010) Interaction of Hsp40 with influenza virus M2 protein: implications for PKR signalling pathway. *Protein cell* **1**(10), 944-955.

**Guerrero CA, Bouyssounade D, Zarate S, Isa P, Lopez T, Espinosa R, Romero P, Mendez E, Lopez S & Arias CF** (2002) Heat shock cognate protein 70 is involved in rotavirus cell entry. *Journal of virology* **76**, 4096–4102.

**Hahn WC, Dessain SK, Brooks M, King JF, Elenbaas B, Sabatini DM, DeCaprio JM & Weinberg RA** (2002) Enumeration of the simian virus 40 early region elements necessary for human cell transformation. *Molecular and cell biology* **22**, 2111-2123.

**Hall TA** (1999) BioEdit: a user-friendly biological sequence alignment editor and analysis program for Windows 95/98/NT. *Nucleic acids research* **41**, 95-98.

**Hartl FU & Hayer-Hartl M** (2002) Molecular chaperones in the cytosol: From nascent chain to folded protein. *Science* **295**, 1852-1858.

**Hatayama T, Asai Y, Wakatsuki T, Kitamura T & Imahara H** (1993) Regulation of Hsp70 induction in thermotolerant HeLa cells. *Biochimica et biophysica acta* **1179**, 109–116.

**Hattori H, Kaneda T, Lokeshwar B, Laszio A & Ohtsuka K** (1993) A stress-inducible 40 kDa protein (hsp40): purification by modified two-dimensional gel electrophoresis and co-localization with hsc70(p73) in heat-shocked HeLa cells. *Journal of cell science* **104**, 629-638.

**Hattori H, Liu YC, Tohnai I, Ueda M, Kaneda T, Kobayashi T, Tanabe K & Ohtsuka K** (1992) Intracellular localization and partial amino acid sequence of a stress-inducible 40-kDa protein in HeLa cells. *Cell structure and function* **17**, 77- 86.

**Hoffmann HJ, Lyman SK, Lu C, Petit Ma & Echols H** (1992) Activity of the Hsp70 chaperone complex--DnaK, DnaJ, and GrpE--in initiating phage lambda DNA replication by sequestering and releasing lambda P protein. *Proceedings of the national academy of sciences of the United States of America* **89**, 12108-12111.

**Hu J & Anselmo D** (2000) In vitro reconstitution of a functional duck hepatitis B virus reverse transcriptase: posttranslational activation by Hsp90. *Journal of virology* **74**, 11447-11455.

**Hu J, Flores D, Toft D, Wang X & Nguyen D** (2004) Requirement of Heat Shock Protein 90 for Human Hepatitis B Virus Reverse Transcriptase Function. *Journal of virology* **78**, 13122-13131.

**Hussy P, Maass G, Tummler B, Grosse F & Schomburg U** (1986) Effect of 4-quinolones and novobiocin on calf thymus DNA polymerase a primase complex, topoisomerase I and II, and growth of mammalian lymphoblasts. *Antimicrobial agents and chemotherapy* **29**, 1073-1078.

**Jauka T, Mutsvunguma L, Boshoff A, Edkins AL & Knox C** (2010) Localisation of Theiler's murine encephalomyelitis virus protein 2C to the Golgi apparatus using antibodies generated against a peptide region. *Journal of virological methods* **168**, 162-169.

**Jones M, Lukashov V, Ganac R & Schnurr D** (2007) Discovery of a novel human picornavirus from a pediatric patient presenting with fever of unknown origin. *Journal of clinical microbiology* **45**, 2144-2150.

**Kampmueller KM & Miller DJ** (2005) The Cellular Chaperone Heat Shock Protein 90 Facilitates Flock House Virus RNA Replication in Drosophila Cells. *Journal of virology* **79**, 6827-6837.

**Karzai AW & McMacken R** (1996) A bipartite signalling mechanism involved in DnaJ-mediated activation of the Escherichia coli DnaK protein. *Journal of biological chemistry* **271**, 11236-11246.

**Kegel KB, Kim M, Sapp E, McIntyre C, Castano JG, Aronin N & DiFiglia M** (2000) Huntingtin expression stimulates endosomal-lysosomal activity, endosome tubulation, and autophagy. *Journal of neurological science* **20**, 7268-7278.

**Kirchhoff S, Gupta S, Knowlton AA** (2002) Cytosolic HSP60, apoptosis, and myocardial injury. *Circulation*. **105**, 2899–2904.

**Knox C, Moffat K, Ali S, Ryan M & Wileman T** (2005) Foot-and-mouth disease virus replication sites form next to the nucleus and close to the Golgi apparatus, but exclude marker proteins associated with host membrane compartments Printed in Great Britain. *Journal of general virology* **86**, 687-696.

**Kolatkhar PR, Bella J, Olson NH, Bator CM, Baker TS & Rossmann MG** (1999) Structural studies of two rhinovirus serotypes complexed with fragments of their cellular receptor. *EMBO Journal* **18**, 6249–6259.

**Kong W, Ghadge G & Roos R** (1994) Involvement of cardiovirus leader in host cell restricted virus expression. *Proceedings of the national academy of sciences of the United States of America* **91**, 1796-1800.

**Kumar M & Mitra D** (2005) Heat shock protein 40 is necessary for human immunodeficiency virus-1 Nef-mediated enhancement of viral gene expression and replication. *Journal of biological chemistry* **280**, 40041-40050.

**Kurzchalia TV & Parton RG** (1999) Membrane microdomains and caveolae. *Current opinions in cell biology* **11**, 424–431.

**Lai BT, Chin NW, Stanek AE, Keh W & Lanks KW** (1984). Quantitation and intracellular localization of the 85K heat shock protein by using monoclonal and polyclonal antibodies. *Molecular and cell biology* **4**, 2802-2810.

- Landini MP & Baldassarri B** (1982) Early inhibition of cytomegalovirus replication by novobiocin. *Journal of antimicrobial chemotherapy* **10**, 533-537.
- Laurin P, Klich M, Dupis-Hamelin C, Mauvais P, Lassaingne P, Bonnefoy A & Musicki B** (1999) Synthesis and *in vitro* evaluation of novel highly potent coumarin inhibitors of gyrase B. *Bioorganic and medicinal chemistry letters* **9**, 2079–2084.
- Leger JP, Smith FM & Currie RW** (2000) Confocal microscopic localization of constitutive and heat shock-induced proteins HSP70 and HSP27 in the rat heart. *Circulation* **102**, 1703–1709.
- Lehrich J, Arnason B & Hochberg F** (1976) Demyelinating myelopathy in mice induced by the DA virus. *Journal of neurological science* **29**, 149-160.
- Letunic I, Doerks T & Bork P** (2008) SMART 6: recent updates and new developments. *Nucleic acid research* **37**, 229-232.
- Levine AJ** (1996) *The origins of virology*. In: *Fundamental Virology*, 3<sup>rd</sup> edition, edited by Fields BN, Knipe DM & Howley. PM. Philadelphia, USA: Lippincott-Raven Publishers, pp 1-14.
- Levy JA, Fraenkel-Conrat H & Owens RA** (1994) *Virology*, 3<sup>rd</sup> edition. New Jersey, USA: Prentice Hall.
- Lewis RJ, Tsai FTF & Wigley DB** (1996) Molecular mechanisms of drug inhibition of DNA gyrase. *BioEssays* **18**, 661–671.
- Liang Z, Manoj Kumar AS, Jones MS, Knowles NJ & Lipton HL** (2008) Phylogenetic analysis of the species Theilovirus: Emerging murine and human pathogens. *Journal of virology* **82**, 11545–11554.
- Lipton HL & Dal Canto MC** (1976) Chronic neurological disease in Theiler's virus infection in SJL/J mice. *Journal of neurological science* **30**, 201-107.
- Lipton HL & Dal Canto MC** (1979) The TO strain of Theiler's virus causes a "slow virus-like" infection in mice. *Annual neurology* **6**, 25-28.

**Lipton HL** (1975) Theiler's virus infection in mice: an unusual biphasic disease process leading to demyelination. *Infection immunology* **11**, 1147-1155.

**Lipton HL** (1980) Persistent Theiler's murine encephalomyelitis virus infection in mice depends on plaque size. *Journal of general virology* **46**, 169-177.

**Liu JS, Kuo SR, Makhov AM, Cyr DM, Griffith JD, Broker TR & Chow LT** (1998) Human Hsp70 and Hsp40 chaperone proteins facilitate human papillomavirus-11 E1 protein binding to the origin and stimulate cell-free DNA replication. *Journal of biological chemistry* **273**, 30704–30712.

**Luo M, Vriend G, Kamer G, Minor I, Arnold E, Rossmann MG, Boege U, Scraba DG, Duke GM & Palmenberg AC** (1987) The atomic structure of Mengo virus at 3.0 Å resolution. *Science* **235**, 182–191.

**Luo M, Toth KS, Zhou L, Pritchard A & Lipton HL** (1996) The structure of a highly virulent Theiler's murine encephalomyelitis virus (GDVII) and implications for determinants of viral persistence. *Virology* **220**, 246-250.

**Macejak DG & Sarnow P** (1992) Association of heat shock protein 70 with enterovirus capsid precursor P1 in infected human cells. *Journal of virology* **66**, 1520-1527.

**Marcu MG, Chadli A, Bouhouche I, Catelli M & Neckers LM** (2000a) The heat shock protein 90 antagonist novobiocin interacts with a previously unrecognised ATP-binding domain in the carboxyl terminus of the chaperone. *Journal of biological chemistry* **275**, 37181-37186.

**Marcu MG, Schulte TW & Neckers L** (2000b) Novobiocin and related coumarins and depletion of heat shock protein 90-dependent signalling proteins. *Journal of the national cancer institute* **92**, 242-248.

**Marjomäki V, Pietiäinen V, Matilainen H, Upla P, Ivaska J, Nissinen L, Reunanen H, Huttunen P, Hyypiä T & Heino J** (2002) Internalization of Echovirus 1 in Caveolae. *Society* **76**, 1856-1865.

- Maruri-Avidal L, Lopez S & Arias CF** (2008) Endoplasmic reticulum chaperones are involved in the morphogenesis of rotavirus infectious particles. *Journal of virology* **82**, 5368–5380.
- Mayer MP & Bukau B** (1998) Hsp70 Chaperone systems: diversity of cellular functions and mechanisms of action. *Biological chemistry* **379**, 261-268.
- Mayer MP & Bukau B** (2005) Hsp70 chaperones: cellular functions and molecular mechanism. *Cellular and molecular life sciences* **62**, 670-684.
- McCarty JS, Buchberger A, Reinstein J & Bukau B** (1995) The role of ATP in the functional cycle of the DnaK chaperone system. *Journal of molecular biology* **249**, 126–137.
- McCright IJ, Tsunoda I, Whitby FG & Fujinami RS.** (1999) Theiler's viruses with mutations in loop I of VP1 lead to altered tropism and pathogenesis. *Journal of virology* **73**, 2814–2824.
- Melville MW, Hansen WJ, Freeman BC, Welch WJ & Katze MG** (1997) The molecular chaperone hsp40 regulates the activity of P58IPK, the cellular inhibitor of PKR. *Proceedings of the national academy of sciences of the United States of America* **94**, 97-102.
- Miller P, DiOrio C, Moyer M, Schnur RC, Bruskin A, Cullen W & Moyer JD** (1994) Depletion of the erbB-2 gene product p185 by benzoquinoid ansamycins. *Cancer research* **54**, 2724–2730.
- Moffat K, Howell G, Knox C, Belsham GJ, Manahan P, Ryan MD & Wileman T** (2005) Effects of foot-and-mouth disease virus nonstructural proteins on structure and function of the early secretory pathway: 2BC but not 3A blocks endoplasmic reticulum-to-Golgi transport. *Journal of virology* **79**, 4382-4395.
- Momose F, Naito T, Yano K, Sugimoto S, Morikawa Y & Nagata K** (2002) Identification of Hsp90 as a stimulatory host factor involved in influenza virus RNA synthesis. *Journal of biological chemistry* **277**, 45306-45314.
- Moon IS, Park IS, Schenker LT, Kennedy MB, Moon J & Jin I** (2001) Presence of both Constitutive and Inducible Heat Shock Protein 70 in the Cerebral Cortex and Hippocampal Synapses. *Cerebral Cortex* **11**, 238-248.

**Muckelbauer JK, Kremer M, Minor I, Diana G, Dutko FJ, Groarke J, Pevear DC & Rossmann MG** (1995) The structure of coxsackievirus B3 at 3.5 Å resolution. *Structure* **3**, 653–667.

**Mukherjee S, Ghosh RN & Maxfield FR** 1997 Endocytosis. *Physiological reviews* **77**,759-803.

**Müller L, Schaupp A, Walerych D, Wegele H & Buchner J** (2004) Hsp90 Regulates the Activity of Wild Type p53 under Physiological and Elevated Temperatures. *Journal of biological chemistry* **279**, 48846–48854.

**Murray L, Luke G, Ryan, MD, Wileman T & Knox C** (2009) Amino acid substitutions within the 2C coding sequence of Theiler's Murine Encephalomyelitis virus alter virus growth and affect protein distribution. *Virus research* **144**, 74–82.

**Nanda SK, Johnson RF, Liu Q & Leibowitz JL** (2004) Mitochondrial HSP70, HSP40, and HSP60 bind to the 3' untranslated region of the Murine hepatitis virus genome. *Archives of virology* **149**, 93-111.

**Norkin LC** (1999) Simian virus 40 infection via MHC class I molecules and caveolae. *Immunological reviews* **168**, 13–22.

**Oberste MS, K. Maher K, Kilpatrick DR & Pallansch MA** (1999) Molecular evolution of the human enteroviruses: correlation of serotype with VP1 sequence and application to picornavirus classification. *Journal of virology* **73**, 1941–1948.

**Odunuga OO, Hornby JA, Bies C, Zimmermann R, Pugh DJ & Blatch GL** (2003) Tetratricopeptide repeat motif-mediated Hsc70-mSTI1 interaction. Molecular characterization of the critical contacts for successful binding and specificity. *The Journal of biological chemistry* **278**, 6896-6904.

**Ohtsuka K & Laszlo A** (1992) The relationship between HSP70 localization and heat resistance; *Experimental cell research* **202**, 507–518.

**Olsen CW, Kehren JC, Dybdahl-Sissok NR & Hinshaw VS** (1996). bcl-2 alters influenza virus yield, spread, and hemagglutinin glycosylation. *Journal of virology* **70**, 663–666.

**Palmenberg AC** (1989) Sequence alignment of picornaviral capsid proteins. In: *Molecular Aspects of picornavirus Infection and Detection*, edited by Semler BL & Ehrenfeld E. Washington D.C, USA: American Society of Microbiology, pp211-241.

**Parton RG** (2003) Caveolae—from ultrastructure to molecular mechanisms. *National review of molecular cell biology* **4**, 162–167.

**Parton RG & Lindsay M** (1999) Exploitation of major histocompatibility complex class I molecules and caveolae by simian virus 40. *Immunology reviews* **168**, 23–31.

**Pelkmans L & Helenius A** (2002) Endocytosis via caveolae. *Traffic* **3**, 311–320.

**Picard D** (2002) Heat-shock protein 90, a chaperone for folding and regulation. *Cellular and molecular life sciences* **59**, 1640-1648.

**Pietiäinen V, Marjomäki V, Upla P, Pelkmans L, Helenius A & Hyypiä T** (2004) Echovirus 1 Endocytosis into Caveosomes Requires Lipid Rafts, Dynamin II, and Signaling Events. *Molecular biology of the cell* **15**, 4911- 4925.

**Prange R, Werr M & Loffler-Mary H** (1999) Chaperones involved in hepatitis B virus morphogenesis. *Biological chemistry* **380**, 305–314.

**Pratt WB & Toft DO** (2003) Regulation of signaling protein function and trafficking by the hsp90/hsp70-based chaperone machinery. *Experimental biology and medicine* **228**, 111-133.

**Prodromou C, Panaretou B, Chohan S, Siligardi G, O'Brien R, Ladbury JE, Roe SM, Piper PW & Pearl LH** (2000) The ATPase cycle of Hsp90 drives a molecular 'clamp' via transient dimerization of the N-terminal domains. *EMBO Journal* **19**, 4383-4392.

**Prodromou C, Roe SM, O'Brien R, Ladbury JE, Piper PW & Pearl LH** (1997a) Identification and structural characterization of the ATP/ADP-binding site in the Hsp90 molecular chaperone. *Cell* **90**, 65-75.

**Prodromou C, Roe SM, Piper PW & Pearl LH** (1997b) A molecular clamp in the crystal structure of the N-terminal domain of the yeast Hsp90 chaperone. *Nature structural biology* **4**, 477–482

**Prodromou C, Siligardi G, O'Brien R, Woolfson DN, Regan L, Panaretou B, Ladbury JE, Piper PW & Pearl LH** (1999) Regulation of Hsp90 ATPase activity by tetratricopeptide repeat (TPR)- domain cochaperones. *EMBO Journal* **18**, 754-762.

**Qiu X, Shao Y, Miao S & Wang L** (2006) Review The diversity of the DnaJ / Hsp40 family, the crucial partners for Hsp70 chaperones. *Cellular and molecular life sciences* **63**, 2560-2570.

**Racaniello VR** (2001). *Picornaviridae: The viruses and their replication*. In: Fields Virology, Fourth edition, edited by Knipe DM, Howley PM, Griffin DE, Lamb RA, Martin MA, Roizman B & Straus SE. Philadelphia, USA: Lippincott Williams and Wilkins Publishers, pp 685-722.

**Ramsey AJ, Russell LC, Whitt SR & Chinkers M** (2000) Overlapping sites of tetratricopeptide repeat protein binding and chaperone activity in heat shock protein 90. *Journal of biological chemistry* **275**, 17857–17862.

**Reece RJ & Maxwell A** (1991) DNA gyrase: structure and function. *Critical reviews in biochemistry and molecular biology* **26**, 335–375.

**Reyes-Del Valle J, Chavez-Salinas S, Medina F & Del Angel RM** (2005) Heat shock protein 90 and heat shock protein 70 are components of dengue virus receptor complex in human cells. *Journal of virology* **79**, 4557–4567.

**Roe SM, Prodromou C, O'Brien R, Ladbury JE, Piper PW & Pearl LH** (1999) Structural basis for inhibition of the hsp90 molecular chaperone by the antitumor antibiotics radicicol and geldanamycin. *Journal of medicinal chemistry* **42**, 260–266.

**Rohll JB, Moon DH, Evans DJ & Almond JW** (1995) The 3' untranslated region of picornavirus RNA features required for efficient genome replication. *Journal of virology* **69**, 7835-7844.

**Roivainen M, Hypia T, Pilrainen L, Rikonen T & Heino J** (1994) Entry of coxsackie virus A9 into host cell: Specific interactions with ( $\alpha\beta$ )<sub>3</sub> integrin, the vitronectin receptor. *Journal of virology* **203**, 354-354.

**Rosser MFN & Cyr DM** (2007) *Do Hsp40s act as chaperones or co-chaperones?* In: Networking of Chaperones by Co-Chaperones, edited by Blatch GL. Springer Biosciences and Media, LCC and Landes Bioscience, pp. 38–51.

**Ryan MD, King AM & Thomas GP** (1991) Cleavage of foot-and-mouth disease virus polyprotein is mediated by residues located within a 19 amino acid sequence. *Journal of general virology* **72** (11), 2727-2732.

**Sainis I, Angelidis C, Pagoulatos GN & Lazaridis I** (1994) The hsc70 gene which is slightly induced by heat is the main virus inducible member of the hsp70 gene family. *FEBS letters*. **355**(3), 282-286.

**Sali A, Potterton L, Yuan F, van Vlijmen H, & Karplus M** (1995) Evaluation of comparative protein modeling by MODELLER. *Proteins* **23**, 318-326.

**Saphire AC, Guan T, Schirmer EC, Nemerow GR & Gerace L** (2000) Nuclear import of adenovirus DNA in vitro involves the nuclear protein import pathway and Hsc70. *Journal of biological chemistry* **275**, 4298-4304.

**Sato N, Yamamoto T, Sekine Y, Yumioka T, Junicho A, Fuse H & Matsuda T** (2003) Involvement of heat-shock protein 90 in the interleukin-6-mediated signaling pathway through STAT3. *Biochemical and biophysical research communications* **300**, 847-852.

**Scheufler C, Brinker A, Bourenkov G, Pegoraro S, Moroder L, Bartunik H, Hartl FU & Moarefi I** (2000) Structure of TPR domain-peptide complexes: critical in the assembly of the Hsp70/Hsp90 multichaperone machine. *Cell* **101**, 199-210.

**Schultz J, Milpetz F, Bork P & Ponting C** (1997) SMART, simple molecular architecture research tool: identification of signalling domains. *Proceedings of the national academy of sciences of the United States of America* **95**, 5857-5864.

**Smith DF, Whitesell L, Nair SC, Chen S, Prapapanich V and Rimerman RA** (1995) Progesterone receptor structure and function altered by geldanamycin, an Hsp90 binding agent. *Molecular and cell biology*, **15**, 6804–6812.

**Smith DR, McCarthy S, Chrovian A, Olinger G, Stossel A, Geisbert TW, Hensley LE & Connor JH** (2010) Inhibition of heat-shock protein 90 reduces Ebola virus replication. *Antiviral research* **87**, 187-194.

**Snoeckx LH, Cornelussen RN, Van Nieuwenhoven Fa, Reneman RS & Van Der Vusse GJ** (2001) Heat shock proteins and cardiovascular pathophysiology. *Physiological reviews* **81**, 1461-1497.

**Sohn S, Kim J, Baek K, Ryu W & Ahn B** (2006a) Turnover of hepatitis B virus X protein is facilitated by Hdj1, a human Hsp40/DnaJ protein. *Biochemical and biophysical research communications* **347**, 764-768.

**Sohn S, Kim S, Kim J & Ahn B** (2006b) Negative regulation of hepatitis B virus replication by cellular Hsp40/DnaJ proteins through destabilization of viral core and X proteins. *Journal of general virology* **87**, 1883-1891.

**Soltys BJ & Gupta RS** (1996) Immunoelectron microscopic localization of the 60-kDa heat shock chaperonin protein (Hsp60) in mammalian cells. *Experimental cell research* **222**, 16–27.

**Sóti C, Rácz A & Csermely P** (2002) A nucleotide-dependent molecular switch controls ATP binding at the C- terminal domain of Hsp90: N-terminal nucleotide binding unmask a C-terminal binding pocket. *Journal of biological chemistry* **277**, 7066–7075.

**Stahl M, Retzlaff M, Nassal M & Beck J** (2007) Chaperone activation of the hepadnaviral reverse transcriptase for template RNA binding is established by the Hsp70 and stimulated by the Hsp90 system. *Nucleic acids research* **35**, 6124-6136.

**Stebbins CE, Russo AA, Schneider C, Rosen N, Hartl FU & Pavletich NP** (1997) Crystal Structure of an Hsp90 – Geldanamycin Complex: Targeting of a Protein Chaperone by an Antitumor Agent. *Cell* **89**, 239-250.

**Stewart SR & Semler BL** (1997) RNA determinants of picornavirus cap-independent translation initiation. *Seminars in virology* **8**, 242-255.

**Suh DA, Giddings Jr TH & Kirkegaard K** (2000) Remodelling the endoplasmic reticulum by poliovirus infection and by individual viral proteins: an autophagic-like origin for virus-induced vesicles. *Journal of virology* **74**, 8953-8965.

**Sullivan CS & Pipas JM** (2001) The virus-chaperone connection. *Virology* **287**, 1-8.

**Sullivan W, Stensgard B, Caucutt G, Bartha B, McMahon N, Alnemri ES, Litwack G & Toft D** (1997) Nucleotides and two functional states of hsp90. *Journal of biological chemistry* **272**, 8007-8012.

**Sullivan WP, Owen BA & Toft DO** (2002) The influence of ATP and p23 on the conformation of hsp90. *Journal of biological chemistry* **277**, 45942-45948.

**Sumiyoshi Y, Takuto N, Watanabe T & Kano K** (1983) Inhibition of retrovirus RNA-dependent DNA polymerase by novobiocin and nalidixic acid. *Journal of general virology* **64**, 2329-2333.

**Suzuki H** (1996) A hypothesis about the mechanism of assembly of double-shelled rotavirus particles. *Archives of virology* **12**, 79-85.

**Szabo A, Korszun R, Hartl FU & Flanagan JB** (1994) A zinc finger like domain of the molecular chaperone DnaJ is involved in binding to denatured protein substrates. *EMBO Journal* **15**, 408-417.

**Takata Y, Imamura T, Iwata M, Usui I, Haruta T, Nandachi N, Ishiki M, Sasaoka T & Kobayashi M** (1997) Functional importance of heat shock protein 90 associated with insulin receptor on insulin-stimulated mitogenesis. *Biochemical and biophysical research communications* **237**, 345-347.

**Teterina NL, Bienz K, Egger D, Gorbalenya AE & Ehrenfeld E** (1997) Induction of Intracellular Membrane Rearrangements by HAV Proteins 2C and 2BC. *Proteins* **77**, 66-77.

**Theiler M** (1937) Spontaneous encephalomyelitis of mice, a new virus disease. *Journal of experimental medicine* **65**, 705–719.

**Theiler M & Gard S** (1940) Encephalomyelitis of mice. 1. Characteristics and pathogenesis of the virus. *Journal of experimental medicine* **72**, 49-67.

**Theysen H, Schuster HP, Packschies L, Bukau B & Reinstein J** (1996) The second step of ATP binding to DnaK induces peptide release. *Journal of molecular biology* **263**, 657-670.

**Thompson JD, Higgins DG & Gibson TJ** (1994) CLUSTAL W: improving sequence weighting positions, specific gap penalties and weight matrix position. *Nucleic acid research*.

**Thompson D, Muriel P, Russell D, Osborne P, Bromley A, Rowland M, Creigh-Tyte S & Brown C** (2002) Economic costs of the Foot and mouth disease outbreak in the United Kingdom in 2001. *Review of science and technology* **21**, 675-687.

**Tomita Y, Mizuno T, Díez J, Naito S & Ahlquist P** (2003) Mutation of Host dnaJ Homolog Inhibits Brome Mosaic Virus Negative-Strand RNA Synthesis. *Journal of virology* **77**, 2990-2997.

**Triantafilou K, Fradelizi D, Wilson K & Triantafilou M** (2002) GRP78, a coreceptor for coxsackievirus A9, interacts with major histocompatibility complex class I molecules which mediate virus internalization. *Journal of virology* **76**, 633–643.

**Triantafilou M, Triantafilou K, Wilson KM, Takada Y, Fernandez N & Stanway G** (1999) Involvement of  $\beta_2$ -microglobulin and integrin  $\alpha V\beta 3$  molecules in the coxsackievirus A9 infectious cycle. *Journal of general virology* **80**, 2591–2600.

**Tsai J & Douglas MG** (1996) A conserved HPD sequence of the J-domain is necessary for YDJ1 stimulation of Hsp70 ATPase activity at a site distinct from substrate binding. *Journal of biological chemistry* **271**, 9347-9354.

**Upla P, Marjomäki V, Kankaanpää P, Ivaska J, Hyypiä T, van der Goot FG & Heino J** (2004) Clustering Induces a Lateral Redistribution of  $\alpha 2\beta 1$  Integrin from Membrane Rafts to

Caveolae and Subsequent Protein Kinase C – dependent Internalization. *Molecular biology of the cell* **15**, 625- 636.

**van Bergen en Henegouwen PM, Berbers G, Linnemans W A & van Wijk R** (1987) Subcellular localization of the 84,000 dalton heat-shock protein in mouse neuroblastoma cells: evidence for a cytoplasmic and nuclear location. *Cell biology* **43**, 469-478.

**van Kuppeveld FJ, Melchers WJ, Willems PH & Gadella TW Jr** (2002) Homomultimerization of the coxsackievirus 2B protein in living cells visualized by fluorescence resonance energy transfer microscopy. *Journal of virology* **76**, 9446-56.

**van Pesch V, van Eyll O & Michiels T** (2001) The Leader Protein of Theiler ' s Virus Inhibits Immediate-Early Alpha / Beta Interferon Production. *Journal of virology* **75**, 7811-7817.

**Wada Y, Pierce ML & Fujinami RS** (1994) Importance of Amino acid 101 within Capsid Protein VP1 for Modulation of Theiler's Virus-Induced Disease. *Journal of virology* **68**, 1219-1223.

**Wall D, Zylitz M & Georgopoulos C** (1994) The NH<sub>2</sub>-terminal of 108 amino acid of the Escherichia coli DnaJ protein stimulates the ATPase activity of DnaK and are sufficient for lambda replication. *Journal of biological chemistry* **269**, 5446-5451.

**Walsh P, Bursać D, Law YC, Cyr D & Lithgow T** (2004) The J-protein family: modulating protein assembly, disassembly and translocation. *EMBO reports* **5**, 567-571.

**Waxman L, Whitney M, Pollok BA, Kuo LC & Darke PL** (2001) Host cell factor requirement for hepatitis C virus enzyme maturation. *Proceedings of the national academy of sciences of the United States of America* **98**, 13931–13935.

**Weeks SA, Shield WP, Sahi C, Craig EA, Rospert S & Miller DJ** (2008) The heat shock protein 70 co-chaperone YDJ1 is required for efficient membrane-specific Flock House virus RNA replication complex assembly and function in *Saccharomyces cerevisiae*. *Journal of virology* **82**, 2004-2012.

**Weeks SA, Shield WP, Sahi C, Craig EA, Rospert S & Miller DJ** (2010) A targeted analysis of cellular chaperones reveals contrasting roles for heat shock protein 70 in flock house virus RNA replication. *Journal of virology* **84**, 330-339.

**Whitesell L & Cook P** (1996). Stable and specific binding of heat shock protein 90 by geldanamycin disrupts glucocorticoid receptor function in intact cells. *Molecular endocrinology* **10**, 705–712.

**Whitesell L & Lindquist SL** (2005). HSP90 and the chaperoning of cancer. *Nature review of Cancer*. **5**,761–772.

**Whitesell L, Mimnaugh EG, De Costa B, Myers CE & Neckers LM** (1994). Inhibition of heat shock protein HSP90–pp60v-src heteroprotein complex formation by benzoquinone ansamycins: essential role for stress proteins in oncogenic transformation. *Proceedings of the national academy of sciences of the United States of America* **91**, 8324–8328.

**Wurzer WJ, Planz O, Ehrhardt C, Giner M, Silberzahn T, Pleschka S & Ludwig S** (2003) Caspase 3 activation is essential for efficient influenza virus propagation. *EMBO Journal* **22**, 2717–2728.

**Xiao A, Wong J & Luo H** (2010) Viral interaction with molecular chaperones: role in regulating viral infection. *Archives of virology* **155**, 1021-1031

**Xing L, Huhtala M, Pietia V, Ka J, Heino J, Johnson MS, Hyypia T & Cheng RH** (2004) Structural and Functional Analysis of Integrin  $\alpha_2$ I Domain Interaction with Echovirus 1. *Biochemistry* **279**, 11632-11638.

**Xu Q** (2002) Role of Heat Shock Proteins in Atherosclerosis. *Arteriosclerosis, thrombosis, and vascular biology* **22**, 1547-1559.

**Yamane M, Hattori H, Sugito K, Hayashi Y, Tohnai I, Ueda M, Nishizawa K & Ohtsuka K** (1995) Cotranslocation and colocalization of hsp40 (DnaJ) with hsp70 (DnaK) in mammalian cells. *Cell structure and function* **20**, 157- 166.

**Young JC, Agashe VR, Siegers K & Hartl FU** (2004) Pathways of chaperone mediated protein folding in the cytosol. *Nature reviews molecular cell biology* **5**, 781-791.

**Yun B, Huang W, Leach N, Hartson SD & Matts RL** (2004) Novobiocin induces a distinct conformation of Hsp90 and alters Hsp90-co-chaperone-client interactions. *Biochemistry* **43**, 8217-8229.

**Zarate S, Cuadras MA, Espinosa R, Romero P, Juarez KO, Camacho-Nuez M, Arias CF & Lopez S** (2003) Interaction of rotaviruses with Hsc70 during cell entry is mediated by VP5. *Journal of virology* **77**, 7254–7260.

**Zhu X, Zhao Z, Burkholder WF, Gragerov A, Ogata CM, Gottesman ME & Hendrickson WA** (1996) Structural analysis of substrate binding by the molecular chaperone DnaK. *Science* **272**, 1606-1614.

**Zhu XD, Li CL, Lang ZW, Gao GF & Tien P** (2004) Significant correlation between expression level of HSP gp96 and progression of hepatitis B virus induced diseases. *Journal of gastroenterology* **10**, 1141–1145.

**Zoll J, Erkens Hulshof S, Lanke K, Verduyn Lunel F, Melchers WJ, Schoondermark-van de Ven E, Roivainen M, Galama JM & van Kuppeveld FJ** (2009) Saffold virus, a human Theiler's-like cardiovirus, is ubiquitous and causes infection early in life. *Pathogens* **5**, e1000416.

**Zylicz M & Georgopoulos C** (1984) Purification and properties of the Escherichia coli dnaK replication protein. *Journal of biological chemistry* **259**(14), 8820–8825.

**Zylicz M, Ang D & Georgopoulos C** (1987) The grpE protein of Escherichia coli. Purification and properties. *Journal of biological chemistry* **262**(36), 17437–17442.

**Zylicz M, Ang D, Liberek K & Georgopoulos C** (1989) Initiation of lambda DNA replication with purified host- and bacteriophage-encoded proteins: the role of the dnaK, dnaJ and grpE heat shock proteins. *EMBO Journal* **8**, 1601-1608.

**Zylicz M, Yamamoto T, McKittrick N, Sell S & Georgopoulos C** (1985) Purification and properties of the dnaJ replication protein of Escherichia coli. *Journal of biological chemistry* **260** (12), 7591–7598.

Internet:

ICTV (2009) <http://www.ictvonline.org/virusTaxonomy.asp>. Accessed: 11/11/10